DYNAMIC RESPONSE OF SANDWICH AND LAMINATED COMPOSITES WITH IMPERFECT INTERFACE AND DELAMINATION

By

JIAMIN BAI

A DISSERTATION PRESENTED TO THE GRADUATE SCHOOL
OF THE UNIVERSITY OF FLORIDA IN PARTIAL FULFILLMENT
OF THE REQUIREMENT FOR THE DEGREE
OF DOCTOR OF PHILOSOPHY

UNIVERSITY OF FLORIDA

1994

ACKNOWLEDGEMENTS

The author would like to express his deepest gratitude to his committee chairman, Professor Chang-Tsan Sun, for his guidance, friendship and the freedom to discover, fail and succeed. The author also sincerely appreciates Dr. Sun's genuine care for his students.

The author is also grateful to his committee members, Dr. Deborah Weissman-Berman and Dr. Bhavani V. Sankar, for their guidance and encouragement. Gratitude is also extended to Dr. Ibrahim K. Ebcioglu, Dr. Sharma Chakravarthy and Dr. Clifford O. Hays for serving on the committee and for their constant support.

TABLE OF CONTENTS

ACKNOWLEDGEMENTS ii

ABSTRACT v

CHAPTERS

1 INTRODUCTION 1
  1.1 Background 1
  1.2 Literature Survey 5
    1.2.1 Sandwich Vibration Theories 5
    1.2.2 Interface Effects of Sandwich Panels 8
    1.2.3 Laminated Structure Vibration Theories 9
  1.3 Objective and Outline of Present Study 14

2 A REFINED VIBRATION THEORY OF SANDWICH BEAMS 17
  2.1 Basic Assumptions 18
  2.2 Governing Equations of Motion 22
  2.3 Solution of Forced Harmonic Motion 29
  2.4 Verification Problems 33
  2.5 Parametric Study 39

3 EFFECTS OF VISCOELASTIC INTERFACE OF SANDWICH BEAMS 46
  3.1 Viscoelastic Interface Model 47
  3.2 Governing Equations of Motion 49
  3.3 Calculation of Loss Factors 56
    3.3.1 Complex Eigenvalue Approach 58
    3.3.2 Direct Frequency Response Approach 61
    3.3.3 Modal Strain Energy Approach 64
  3.4 Numerical Examples 65

4 A REFINED VIBRATION THEORY OF SANDWICH PLATES . . . 73
  4.1 Basic Formulations 73
  4.2 Equations of Motion 81
  4.3 Solution and Discussion 86

5 VIBRATION OF DELAMINATED SANDWICH BEAM-PLATES ... 91
5.1 A Beam-Plate Model ... 91
5.2 Deformation Mode Modeling ... 94
5.3 Analytical Formulation and Discussion ... 96
5.3.1 The Free Mode Model ... 97
5.3.2 The Constrained Mode Model ... 103
5.4 Example Problems ... 106
5.4.1 The Free Mode Model ... 106
5.4.2 The Constrained Mode Model ... 110

6 VIBRATION OF LAMINATED BEAMS WITH DELAMINATIONS 116
6.1 The Layer-Wise Finite Element Model ... 116
6.2 Parallel Algorithm Design for Finite Element Analysis ... 121
6.2.1 Domain Decomposition ... 123
6.2.2 Optimal Mapping of Irregular Finite Element Domains .. 126
6.3 Example Problems ... 129

7 CONCLUSIONS AND FUTURE WORK ... 132
7.1 Conclusions ... 132
7.2 Future Study of Related Research ... 134

APPENDICES

A EQUATIONS OF MOTION OF A SANDWICH BEAM ... 135

B EQUATIONS OF MOTION WITH INTERFACE EFFECTS ... 150

REFERENCES ... 166

BIOGRAPHICAL SKETCH ... 175

Abstract of Dissertation Presented to the Graduate School
of the University of Florida in Partial Fulfillment of the
Requirement for the Degree of Doctor of Philosophy

DYNAMIC RESPONSE OF SANDWICH AND LAMINATED COMPOSITES WITH IMPERFECT INTERFACE AND DELAMINATION

By

JIAMIN BAI

December 1994

Chairman: Dr. Chang-Tsan Sun
Major Department: Aerospace Engineering, Mechanics and Engineering Science

Analyses of free vibrations, forced vibrations and structural damping characteristics of sandwich and laminated composites with imperfect interface and delaminations are presented. A refined high-order theory for the vibration of sandwich beams and plates to specifically deal with a transversely flexible core has been introduced. The effect of imperfect viscoelastic interface on the structural damping of a sandwich beam is studied. Analytical models of vibrations of sandwich and laminated plates with delaminations are developed.

The refined vibration theory embodies a general systematic approach to the analysis of sandwich beam and plate having high-order effects owing to the non-linear pattern of the longitudinal and transverse deformation of the thick core. Inertia effects due to all the displacements are taken into account. As such it improves on the available classical and shear deformation theories. It is used to corporate the imperfect interface model and vibration damping approach to exam the interface layer effect on the structural damping of the sandwich beam. Results show that the imperfect interface affects vibration damping significantly.

Based on this theory the free vibration behavior of a sandwich plate with a through-width delamination is examined. The shear deformation effect and compressive in-plane force effect have been taken into account in the analysis. Two analytical models of different deformation modes are discussed. Fundamental frequencies and vibration mode shapes are calculated and the physical admissible model is identified. It is found that delamination length, delamination location and core thickness have significant effect on vibration characteristics.

Finally, vibration analysis of laminated composite beams with delaminations based on a layer-wise finite element model is presented. Parallel algorithm design for the finite element analysis is discussed and efficient approximation algorithms are developed. The fundamental natural frequencies of laminated composites with delamination are examined for the effects of delamination length and compressive in-plane loading.

CHAPTER 1
INTRODUCTION

1.1 Background

Sandwich construction has been used in aeronautical applications for more than 40 years, since it has many advantages, for example, high bending stiffness, good weight saving, good surface finish, good fatigue properties, good thermal and acoustical insulation, etc.[1]. Today, there is a renewed interest in using sandwich structures due to the introduction of new materials such as laminated composites for the face materials and various nonmetallic honeycomb and plastic foam core materials. However, these new materials also induce some new problems that need to be solved. Delamination is one of the most frequently encountered problems. To use new materials efficiently, a good understanding of their structural dynamic behaviors under various loads is needed.

Advanced fiber-reinforced composite materials such as graphite-epoxy laminates offer several advantages for structures which require a combination of high strength and stiffness with low weight. With their capability of being tailored for a specific application, composite materials have been widely used in aeronautical industries to replace metals. However, these materials are, in general, more brittle than their metallic counterparts. Also, in contrast to their in-plane properties, transverse tensile and interlaminar shear strengths of composite laminates are quite low. As a consequence, advanced composite laminates are susceptible to delamination from a wide variety of sources.

Delamination, also referred to as interface cracking or debonding where adjacent laminae become unattached from one another, is a unique failure mode in sandwich and laminated composites. For composite sandwich panels, an interface bond between the face and the core is relatively thicker and may be weaker than that in laminated composites. In many sandwich structures, the bond is not of the perfect kind that can be modeled by continuity of tractions and displacements across a discrete face-core interface. Instead, the bond is effected across a thin interfacial zone, which has its own mechanical properties. Poorly bonded areas are probable locations for delaminations to occur, and these regions of imperfect bonding might be attributed to foreign matter or nonuniform distribution of the adhesive material. Clearly, such an interface may significantly affect the integral dynamic properties of the sandwich structures.

Delamination may occur as a consequence of the imperfections in the production process such as fabrication stresses, or the effects of external factors during the operational life such as environmental cycling, handling damage, and foreign object impact damage. During manufacturing, for example, air pockets may arise from layers not being compressed against one another before curing process. Once fabricated, delaminations may develop from an impact as minor as a dropped screwdriver or other tools. Hence, the delamination can be located in various places in the sandwich and laminate structures. Regardless of its location, delamination may reduce the overall stiffness, lower the load-carrying capacity of the composite panels and, thereby, alter the static and dynamic characteristics of the structural system [2, 3]. Sandwich and laminate structures are usually being used in situations which require them to withstand vibrational forces. The resonant frequency shift and degradation of dynamic stiffness due to the delamination may lead to global structural failure at loads below the design load.

The presence of delamination has also been of major concern in the marine industry, where sandwich composites have attracted considerable attention. For example, highly advanced racing boats employ carbon/epoxy laminates in the hull faces over low-density PVC foam core to reduce weight [4]. Their technology is based on wet lay-up processes and room temperature cure resins other than using autoclaves and specialized prepregs to achieve satisfactory face-core bonds. Although the success has been tremendous, the marine industry is recognizing that delamination between the core and faces due to wave slamming on critical regions of the hull may present a problem [5]. Cyclic water-generated loading or transient wave-slamming loading of high magnitude and short duration may cause initiation and growth of face-core debonding that may be disastrous for the load bearing capability of the structure. The tendency for this failure mode is expected to be greatly enhanced by the presence of flaws or partial debonding that are likely to exist between the core and face sheets. Considerable vibration within the plate components of the structure can be set up under working conditions and there may have a severe effect upon the plate stability. It is, therefore, necessary to undertake vibration and dynamic stability analyses and to design the system accordingly.

Since dynamic response is governed by stiffness, mass, and damping, the effects of damage such as delamination and crack on these properties are of interest. The use of dynamic testing to detect and quantify the effects of internal damage on modal parameters has been studied on a continuous but limited basis over the last twenty years. In recent years several studies have been concerned with damage-induced changes in stiffness as found from observed changes in resonant frequencies of composite specimen [6, 7]. Other studies have shown that, for a variety of structures and loading conditions, damping is generally far more sensitive to damage than stiffness [8, 9]. More recently, the amount of research in this area has increased due primarily to the availability of inexpensive multi-channel Fourier analyzers. Shifts in natural frequencies have been used to identify damage generated by static loading [10, 11], fatigue loading [12, 13], mechanical damage such as saw cuts and local cracks [14, 15], foreign object impact [16-18], and prescribed delamination [19-21]. Although these work show that system dynamic property measurements can be used qualitatively detect damage, there are still some major problems remaining and much more effort will be needed to devote to this area. A better understanding of vibration and damping characteristics of sandwich and laminated structures with delamination will certainly help achieve more effective means of detecting the various delamination damage using dynamic testing.

1.2 Literature Survey

A significant amount of research has been conducted on the vibration and stability analyses of sandwich and laminated beams and plates. Both analytical (closed form, Galerkin, Rayleigh-Ritz method) and numerical methods have been used. A recent report by Leissa [22] contains over 400 references relative to the research work in this area on sandwich and laminated plates and shells. A review of the technical literature on dynamic behavior of laminated composites was given by Bert [23] and on the application of the finite-element method to study the vibration response of composite plates by Reddy [24, 25].

1.2.1 Sandwich Vibration Theories

Most of the literature on the vibration of sandwich panels can be separated into two areas. The first is to deal with undamped sandwich beams, plates and shells without considering highly damped core effects on vibration response. Those work are most concerned about the calculation of vibration mode shape and the evaluation of the critical buckling loads for various types of instabilities including the combination and interaction with face wrinkling for sandwich panels [26]. The second aspect is to investigate the vibration response of viscoelastically damped sandwich structures including beams, plates, rings and shells. Most of the research done in this area is to find an effective analytical model of predicting system loss factors and damped resonance frequencies under forced vibration.

Sandwich panels with traditional honeycombed cores were studied by many researchers. The basic approach used in sandwich static and dynamic problems is based on the assumption of an anti-plane core, i.e., the core with shear rigidity only, its plane of section remains plan after deformation and the height of the core is kept unchanged [27, 28]. The Hexcel designer manual [29] outlines design procedures for such sandwich beams. Ojavo [30] assumed different deflections to the two faces, but ignored the peeling stresses. Ogorkiewicz [31] dealt with a foam core by replacing it with an ordinary beam with equivalent properties. Weissman-Berman [32] developed an elastic foundation model to improve the sandwich beam theory with simply supported boundary conditions.

Vibration problems of sandwich panels using the anti-plane assumption were solved either by finite element method [33] or analytical approaches [34, 35]. In recent years, various vibration theories of undamped sandwich beams have been developed by Ko [36], Lu and Libove [37] and Bai and Sun [38] in the similar basis. A high-order theory used by Reddy [39, 40] may be applied to such panels to overcome the deficiencies encountered in the classical theories. These two theories, however, assume that the core is incompressible in the transverse direction, and the boundary conditions at the same section are identical for the two faces. These assumption are unrealistic whenever a sandwich panel with a soft compressible core is considered, particularly with concentrated mechanical impedance or partially distributed loads. Those characteristics must be addressed by a refined high-order theory.

The damping effect has not taken into account in the above studies, and only free vibration has been considered. However, the damping capacity of the composite sandwiches is much greater due to the highly damped core materials and their shear deformations. Flexural vibration of viscoelastic sandwich beams has long been of interests since 1960's. In a very fundamental paper, Ross, Ungar and Kerwin [41] treated the problem by assuming perfect interface, the same amount of transverse displacement in each layer, damping only from the shearing of the viscoelastic core, and simply supported boundary conditions. DiTaranto [42] extended this analysis to freely vibrating beams having any type of boundary conditions. Based on DiTaranto's work sixth-order differential equations of motion were derived in terms of transverse displacement by Mead and Markus [43], and this theory was correlated with experimental data by Lu and Douglas [44]. Yan and Dowell [45] used the principle of virtual work to obtain a set of five differential governing equations. A more accurate theory including the inertia effects of transverse, longitudinal and rotary motions was carried out by Rao and Nakra [46].

Although there are some published papers dealing with the delamination problems of sandwich panels, to the author's best knowledge, none of them consider the dynamic response. The buckling and postbuckling of a delaminated sandwich beam with laminated faces and honeycomb core were studied by Hwu and Hu [47]. Debonding failure of sandwich composite materials has been investigated analytically and experimentally by Carlsson, Sendlein and Merry [48]. They employed laminated beam shear deformation theory to calculate effective bending properties of delamination region and fracture toughness. The study presented here is trying to conduct some basic vibration analyses of delaminated sandwich beams and plates with various core and face materials.

1.2.2 Interface Effects of Sandwich Panels

Existing theories of vibration damping of sandwich structures have invariably assumed perfect bonding between faces and core as well as constant transverse displacement through the thickness of the beams. Subsequently the plane of sections remains plane and the transverse normal (peeling) stresses are neglected. On the other hand, the assumption of negligible normal stress of the core (or constant transverse displacement through the core) is not applicable when the core is made of low strength materials such as foams and aramid honeycomb. In reality, however, for flexible core materials a more complex state exists between faces and core. The assumptions of equal amount of transverse displacement and perfect bonding may not be suitable to describe the problem accurately.

The existence of an interface layer or adhesive layer between the face and the core on the physical behavior of the sandwich composite materials has been recognized during recent years. The interface has been described as either a layer of specified thickness and of elastic constants different from those of the face and the core, or a very thin interfacial zone of unspecified thickness where tractions are continuous but the displacements may not. Advanced racing boats, for example, employ carbon/epoxy laminates in the hull skin over low density PVC foam where interfacial layers are considered to be effective in energy absorption [49]. Fazio, Hussein and Ha [50] introduced a nonrigid bonding effect into the elasticity solutions for sandwich beam-columns under transverse static loading. Imperfect interface conditions have been quantitatively defined as linear relations between interface displacement discontinuities and associated traction components. Hussein [51] presented analytical solutions of sandwich plates assembled with nonrigid adhesive layers. Their results have shown that the bonding stiffness, up to a certain level, has a strong effect on the deflections and stresses of beam-columns and plates. Such adhesive layer effects on buckling load was also extended to consider the case of viscoelastic interface between viscoelastic cross-ply composite faces and the elastic core by Kim and Hong [52]. In the present study, we will examine the effect of viscoelastic interface on the structural damping of sandwich beams.

1.2.3 Laminated Structure Vibration Theories

Kapania and Raciti [53, 54] have given a more recent survey on vibration response of symmetric and unsymmetric laminated beams and plates. We hereby give some representative research work in this field. Reddy and Kuppusamy [55] performed a vibration analysis of laminated plates using a three-dimensional solution. Bhimaraddi and Stephens [56] presented results of vibrations of thick laminated plates using a high-order theory. The effect of transverse shear on the cylindrical bending, vibration, and buckling of laminated plates was presented by Stein and Jegley [57]. Effects of delamination on vibration and stability characteristics of laminated composites have not been considered until recent years.

The effect of delamination on buckling load, postbuckling deformation and delamination growth with various geometrical parameters, loading conditions, material properties and boundary conditions have been studied extensively. Most studies on the subject of delamination buckling and growth were based on the static postbuckling solutions of homogeneous or laminated plates [58, 59]. The energy release rate is used in the analysis and the Griffith-type fracture criterion with a constant specific fracture energy is assumed in these studies. These include the differentiation of the total strain energy with respect to the delamination length by Chai et al. [60] and Chow and Ngan [61], a finite element method to compute the crack closure integral by Whitcomb [62], and the path independent J integral by Yin and Wang [63]. Dynamic analysis of the growth for a thin, homogeneous, strip delamination in a thick, axially loaded base plate was studied recently [64-66].

A more general theory for modeling of delamination in composite laminates, based on a layer-wise displacement field, was presented by Barbero and Readdy [67]. They suggested that the same displacement distributions in individual layer is capable of representing displacement discontinuity conditions at interfaces between layers. It demonstrated that the layer-wise laminate theory provides an adequate framework for the delamination analysis of laminated composites. It must be noted, however, that the computational cost of the analysis makes it unattractive for prediction of delamination buckling behavior in engineering practice when the number of layer is large. Based on a 1-D layer-wise theory, a finite element model was developed by Lee et al. [68] to examine the buckling of axially loaded composite beams with multiple through-width delaminations. A parallel study by Suemasu [69, 70] shows common numerical trends that are similar to those observed by Lee et al. Kutlu and Chang [71] also studied the compression failure of laminated composites containing multiple through-width delaminations. The effect of elliptical delamination of composite plates on elastic and buckling behavior was investigated by Peck and Springer [72]. However, only a few investigations of delamination effects on vibration characteristics have been conducted.

Kulkarni and Frederick [73] were among the first to study the vibration characteristics of laminated structures with delaminations. They considered the particular case of a circular cylindrical shell with a circumferentially symmetric delamination crack of small length at the middle surface. In their study, the effect of the delamination was taken into account as a reduced bending rigidity of the shell over the delamination zone, obtained by replacing the moment of inertia of the delaminated layers. However, as show in some later studies, such a modeling grossly overestimates the reduction in the bending stiffness caused by the delamination. Using a similar model, Ramkumar et al. [74] formulated the vibration of a delaminated beam based on the Timoshenko beam theory. The coupling effect of the oscillatory axial forces in the upper and lower delaminated layers was not taken into account in the analysis which results in consistently much lower natural frequencies as compared to the experimental data. This consistency exists even for cases with short delamination. Wang et al. [75] then studied the vibration of isotropic beams with a through-width delamination, analyzing the flawed beam as four different Euler beams that are joined together, with appropriate boundary and matching conditions imposed to obtain the response of the beam as whole. The coupling effect of axial forces in split layers was considered in the analysis. Their analysis examined various delamination length and locations, and their effects on the beam natural frequencies and mode shapes. It was found that for the delaminated beam with a short and close-to-midplane delamination, the calculated fundamental frequency is close to the experimental results. Their analysis, however, leads to modes of deformation of the delaminated beam which are not physically admissible in the case of off-midplane delaminations because the sublaminates above and below the plane of delamination were implicitly assumed to be free to deflect and thus have different transverse displacements in the formulation.

For vibration relative to the natural (unloaded) referential state in which there is no opening between the upper and lower delaminated layers, geometric incompatibility (i.e. overlap between upper and lower sublaminates) will occur if the mode shapes of the upper and lower sublaminates are different. A constraint of identical transverse displacements of upper and lower sublaminates have been imposed by Mujumdar and Suryanarayan [76] in their proposed analytical model. Their analysis is based on a one-dimensional Euler beam analysis in such a "constrained mode" can take into account delaminations located at an arbitrary position in both the spanwise and thicknesswise directions. Numerical results for frequencies were obtained by using this "constrained mode" for various boundary conditions and mode numbers for a certain range of values of the delamination size, spanwise location and thicknesswise location of the delamination.

Vibration response of delaminated composite beam-plates relative to the postbuckling state has also been studied. Yin and Jane [77] considered the vibration behavior of a compressed clamped-clamped beam-plate with a symmetrically located delamination in the buckled states. The natural frequencies of the delaminated plate at postbuckled states were compared to the natural frequencies of a perfect plate for various delamination sizes and depths. The effect of delamination in a cantilevered composite beam on natural frequencies and mode shapes is evaluated both analytically and experimentally by Shen and Grady [78] recently. For vibrations relative to the postbuckling state, the constraint of identical transverse displacements of upper and lower sublaminates is not necessary because there is an opening between the upper and lower sublaminates. A free mode formulation as used in Wang's work [75] is appropriate. Chen and Goggin [79] used shear deformation theory to determine the transverse shear effect on natural frequencies and mode shapes in compressed delaminated plates at the postbuckled state.

It can be seen that most of the research on the vibration response of laminated composites with delaminations is restricted to the symmetric delaminated cases. Symmetric delaminated laminates are simpler to analyze since they do not exhibit bending-extension coupling that is characteristic of unsymmetric laminates. When symmetric laminates are delaminated during manufacturing or operation, unsymmetric laminates are usually formed. As a result, the coupling effect may be important on the vibration characteristics of delaminated plate. Besides there are some other reasons for designing structural elements with such coupling effects. As suggested by Minich and Chamis [80], for example, it would be possible to select coupling effects that will provide built-in self-damping mechanisms when subjected to dynamic responses. Also the coupling effects are used in aeroelastic tailoring to control mode shapes and frequencies of high-aspect-ratio lifting surfaces [81, 82]. In the present study, the bending-extension coupling effects on the vibration response of delaminated laminates will be included.

1.3 Objective and Outline of Present Study

Accurate knowledge of dynamic behavior of sandwich and laminated composites is essential for reliable and lightweight structural design, particularly in the high-speed transportation industries. The presence of imperfect interface and delamination not only affect the strength and integrity of the structure by contributing to the final failure, but also cause a reduction in the stiffness, thus affecting its vibration and stability characteristics. As was discussed in the previous section, there have been very few research work in the subject of vibration characteristics of laminated structures with delaminations, and no study toward the vibration of sandwich panels with delaminations has been conducted to date. In the research area of sandwich constructions, the viscoelastic face-core interface effect has also not been examined in the dynamic response region.

The main objective of this research is to develop analytical models for the analysis of dynamic responses of sandwich and laminated composites with imperfect interface and delamination. Emphasis is placed on developing refined beam and plate vibration theories which is specially suitable for the sandwich construction with compressible and flexible core materials. Another problem of interest is to examine viscoelasic interface effects on structural damping of sandwich panels and free vibration behavior of delaminated sandwich and laminated composites. A finite element model based on layer-wise theory is also implemented in conjunction with parallel algorithm design for finite element analysis.

In the present study, refined beam and plate theories of sandwich vibration damping are derived via variation of the Hamilton principle. The nonlinear displacement field of the core in both longitudinal and vertical directions through the thickness are assumed based on the elasticity solution. The face layers are considered as the ordinary beams, acting longitudinally only and interconnected with the core through equilibrium and compatibility at the interface layers. The boundary conditions are given at each face layers and core respectively, accomplished by either prescribing the stress resultants or the corresponding time derivatives of the displacement components. Imperfect interface between face and core of a sandwich panel is quantitatively defined as the longitudinal displacements discontinuities at the interface layers being proportional to the associated shear stresses. Vibration analysis of delaminated sandwich panels is performed using this refined theory.

The organization of the dissertation is as follows: in the next chapter we derive a refined vibration theory of sandwich beam using Hamilton principle and perform the verification and parametric studies. An interface model is introduced and viscoelastic face-core interface effects on vibration damping of sandwich beams are examined in Chapter 3. Chapter 4 extends the refined vibration beam theory into a plate theory. In Chapter 5 vibration of delaminated sandwich plates is studied based on the refined theory. Vibration analysis of laminate beams is carried out in Chapter 6 using a finite element model based on the layer-wise theory with a parallel computation consideration. Finally, conclusions drawn from this study and recommendations for future research are presented in Chapter 7.

CHAPTER 2
A REFINED VIBRATION THEORY OF SANDWICH BEAMS

The effects of more flexible core materials on the dynamic response and damping properties of sandwich beams are studied by introducing a refined vibration theory of sandwich beams. The theory of the core is based on the elasticity solution of more accurate displacement assumptions, including nonlinear transverse deformation. The face layers are considered as ordinary beams with axial and bending resistance.

With the viscoelastic properties of the core material which is complex and is function of frequency for a given temperature, the linear equations of motion describing the vibration of the sandwich finite beam are derived based on the Hamilton principle. In addition to transverse inertia effects, longitudinal translatory and rotary inertia effects have been included. Consistent boundary conditions are accomplished by either prescribing the stress resultants or the corresponding time derivatives of the displacement components. Typical cases of a simply supported beam under the harmonic excitation are numerically investigated. The numerical results of mechanical impedance examples are well agreed with experimental data in the literature. The effects of core thickness and stiffness on resonance frequencies are studied parametrically.

2.1 Basic Assumptions

Consider a three layer sandwich beam of length l and unit width, subjected to a transverse dynamic load $q(x,t)$. It has face layers of thickness, h_1 and h_2, and a core of thickness h shown in Figure 2.1. The face layers are the elastic material with high Young's moduli of E_1 and E_2. The flexible core is linearly viscoelastic with a Young's modulus E_c and a shear modulus of G_c where E_c and G_c are expressed by complex numbers under the harmonic excitation.

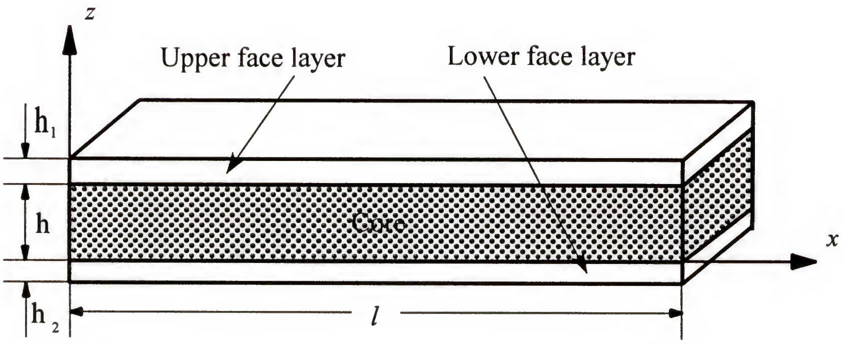

Figure 2.1 Sandwich Beam Construction

The following assumptions underlie the present development:

- The elastic face layers are considered as ordinary beams with axial and bending resistance.
- The viscoelastic core carries null longitudinal stresses, but takes nonlinear displacement fields in both x and z directions.
- The perfect interface, i.e., displacement continuity is hold at the face-core interface.

Based on the assumptions, the following displacement fields are given at the top and bottom face layers:

$$\begin{aligned} u^{t}(x,z,t) &= u_1(x,t) - z_1 \frac{\partial w_1(x,t)}{\partial x} \\ w^{t}(x,z,t) &= w_1(x,t) \end{aligned} \tag{2.1}$$

$$\begin{aligned} u^{b}(x,z,t) &= u_2(x,t) - z_2 \frac{\partial w_2(x,t)}{\partial x} \\ w^{b}(x,z,t) &= w_2(x,t) \end{aligned} \tag{2.2}$$

For the core:

$$u^c(x,z,t) = u_0(x,t) - z\frac{\partial w_0(x,t)}{\partial x} + ze\psi(x,t) - \frac{z^2}{2}\frac{\partial\phi(x,t)}{\partial x} + \frac{z^3}{6}\frac{\partial^2\psi(x,t)}{\partial x^2} \tag{2.3}$$

$$w^c(x,z,t) = w_0(x,t) + z\,\phi(x,t) - \frac{z^2}{2}\frac{\partial\psi(x,t)}{\partial x}$$

where superscripts t, b and c denote top, bottom face layers and the core, $u_i(x,t)$ and $w_i(x,t)$ (i = 0, 1, 2) are the longitudinal and vertical displacements of the centroid of the core and face layers, $e = E_c/G_c$ is a constant and $z_1 = z - h - h_1/2$, $z_2 = z + h_2/2$ are measured from the centroid of the faces respectively, as shown in Figure 2.2. Deformation pattern and sign convention for stresses, resultants and displacements also appear in Figure 2.2.

The core displacement field is derived from the three-dimensional elasticity solution with only an assumption of null in-plane stress (assumption 2). The assumption used here follows those encountered in the classical small elastic deflection theory of sandwich panels where the core has shear rigidity only and its resistance to in-plane longitudinal stresses is negligible. However, the transverse normal stresses (peeling stresses) are considered in the core as well as in the interface layers. The cross-section plane of the core may distort and its height may change. It can be seen from Eqn (2.3) that the transverse displacement of the core can take parabolic variations with the core thickness.

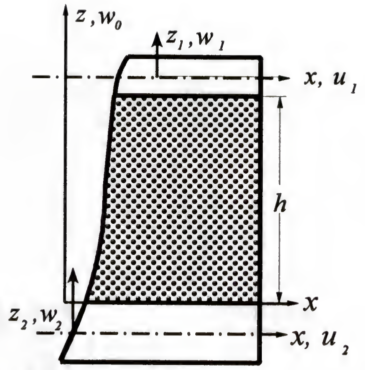

(a) Coordinate System

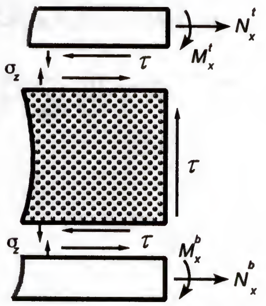

(b) Sign Convention

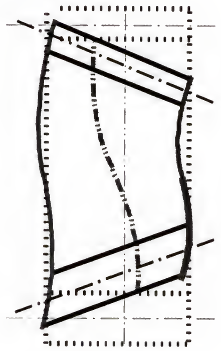

(c) Deformation Pattern

Figure 2.2 Coordinate and Deformation of the Sandwich Beam

2.2 Governing Equations of Motion

The kinematic relations for the face layers, using small deformation theory, can be written as

$$\varepsilon_x^t = \frac{\partial u_1}{\partial x} - z_1 \frac{\partial^2 w_1}{\partial x^2} \qquad (2.4)$$

$$\varepsilon_x^b = \frac{\partial u_2}{\partial x} - z_2 \frac{\partial^2 w_2}{\partial x^2} \qquad (2.5)$$

The kinematic relations for the core are:

$$\begin{aligned} \varepsilon_z^c &= \phi(x,t) - z \frac{\partial \psi(x,t)}{\partial x} \\ \gamma_{xz}^c &= e\, \psi(x,t) \end{aligned} \qquad (2.6)$$

The compatibility conditions of deformations between the faces and the core are described by continuity of displacements across a face-core interface.

At $z=h$ (upper interface), we have

$$u^c = u^t \qquad (2.7)$$

$$w^c = w^t \qquad (2.8)$$

and at $z=0$ (lower interface),

$$u^{c} = u^{b} \tag{2.9}$$

$$w^{c} = w^{b} \tag{2.10}$$

Substituting Eqns. (2.1)-(2.3) into above equations, $u_1(x,t)$, $w_1(x,t)$, $u_2(x,t)$ and $w_2(x,t)$ can be expressed in terms of $w_1(x,t)$, $w_2(x,t)$, $u_0(x,t)$ and $\psi(x,t)$,

$$w_2(x,t) = w_0(x,t) \tag{2.11}$$

$$u_2 = u_0 + \frac{h_2}{2}\frac{\partial w_0}{\partial x} \tag{2.12}$$

$$w_1 = w_0 + h\phi - \frac{h^2}{2}\frac{\partial \psi}{\partial x} \tag{2.13}$$

$$\begin{aligned} u_1 = u_0 - \left(h + \frac{h_1}{2}\right)\frac{\partial w_0}{\partial x} + e\,\psi - \frac{h}{2}(h + h_1)\frac{\partial \phi}{\partial x} \\ + \frac{h_2}{2}\left(\frac{h}{3} + \frac{h_1}{2}\right)\frac{\partial^2 \psi}{\partial x^2} \end{aligned} \tag{2.14}$$

A set of force and moment resultants are defined for top and bottom faces separately:

$$N_x^i = \int_{-\frac{h_j}{2}}^{\frac{h_j}{2}} \sigma_x^i \, dz_j$$

$$M_x^i = \int_{-\frac{h_j}{2}}^{\frac{h_j}{2}} \sigma_x^i z_j \, dz_j \tag{2.15}$$

where $i = t, b$ correspond to $j = 1, 2$ respectively.

Then the constitutive relations for the elastic face layers can be written as follows,

$$N_x^t = E_1 A_1 \frac{\partial u_1}{\partial x}$$

$$N_x^b = E_2 A_2 \frac{\partial u_2}{\partial x}$$

$$M_x^t = -E_1 I_1 \frac{\partial^2 w_1}{\partial x^2} \tag{2.16}$$

$$M_x^b = -E_2 I_2 \frac{\partial^2 w_2}{\partial x^2}$$

where $E_i A_i$ and $E_i I_i$ are the axial and the flexural rigidities of the face layers.

For the viscoelastic core, the constitutive equations are in the form,

$$\sigma_z^c = E_c \varepsilon_z^c = E_c(\phi - z\frac{\partial \psi}{\partial x}) \tag{2.17}$$

$$\tau_{xz}^c = \tau^c = G_c \gamma_{xz}^c = G_c e \psi$$

where G_c and E_c are complex constants.

The governing equations of motion and the boundary conditions are derived via variational calculus, the Hamilton principle, which requires:

$$\delta \int_{t_1}^{t_2} [T - U]\, dt = 0 \tag{2.18}$$

where T is the kinetic energy; U is the total potential energy; t_1, t_2 define the time interval.

The total kinetic energy of the sandwich beam can be expressed as:

$$\begin{aligned} T = \frac{1}{2}\int_0^l \Bigg\{ & \rho_1 h_1 [(\dot{u}_1)^2 + \frac{h_1^2}{12}(\frac{\partial \dot{w}_1}{\partial x})^2 + (\dot{w}_1)^2] \\ & + \rho_2 h_2 [(\dot{u}_2)^2 + \frac{h_2^2}{12}(\frac{\partial \dot{w}_2}{\partial x})^2 + (\dot{w}_2)^2] \\ & + \int_0^h \rho [(\dot{u}^c)^2 + (\dot{w}^c)^2]\, dz \Bigg\} dx \end{aligned} \tag{2.19}$$

where ρ_1, ρ_2 and ρ are the density of the upper face, lower face and the core, respectively, and $(\dot{})$ denotes a first derivative with respect to time.

The total potential energy, U, consists of the contributions from both face layers U_1 and U_2, core shear strain U_3, core normal U_4, and the external potential term V due to applied loading.

$$U = U_1 + U_2 + U_3 + U_4 + V \tag{2.20}$$

$$U_1 = \frac{1}{2}\int_0^l E_1 h_1 \left[(\frac{\partial u_1}{\partial x})^2 + \frac{h_1^2}{12}(\frac{\partial^2 w_1}{\partial x^2})^2 \right] dx$$

$$U_2 = \frac{1}{2}\int_0^l E_2 h_2 \left[(\frac{\partial u_2}{\partial x})^2 + \frac{h_2^2}{12}(\frac{\partial^2 w_2}{\partial x^2})^2 \right] dx \tag{2.21}$$

$$U_3 = \frac{1}{2}\int_0^l G_c h (e\psi)^2 \, dx$$

$$U_4 = \frac{1}{2}\int_0^l \frac{E_c}{h} \left[(w_1 - w_2)^2 + \frac{h^4}{12}\left(\frac{\partial \psi}{\partial x} \right)^2 \right] dx$$

$$V = \int_0^l q w_1 \, dx \tag{2.22}$$

where $q = q(x,t)$ is transverse distributed dynamic loading at surface of top face layer.

It is noted that T and U can be further expressed in terms of four basic unknown functions—$w_1(x,t)$, $w_2(x,t)$, $u_0(x,t)$ and $\psi(x,t)$. Taking variation in the Hamilton's equation with respect to w_1, w_2, u_0 and ψ, four equations of motion and consistent boundary conditions are obtained after integration by parts in x and t, and some algebraic manipulations and substitutions. It is noted that homogeneous conditions for the displacement and the velocity at $t = t_1$, t_2 are assumed. The four governing equations can be written in the matrix form:

$$[\partial M]\{\ddot{U}\} + [\partial K]\{U\} = \{F\} \tag{2.23}$$

where

$\{U\} = \{w_1, w_2, u_0, \psi\}^{\mathrm{T}}$

$\{F\} = \{q, 0, 0, 0\}^{\mathrm{T}}$

$[\partial M]$ — the mass matrix differential operators

$[\partial K]$ — the stiffness matrix differential operators

It is noted that $[\partial K]$, $\{U\}$ and $\{\ddot{U}\}$ are complex valued. In appendix A the mass matrix differential operators $[\partial M]$ and stiffness matrix differential operators $[\partial K]$ are given in terms of the four independent variables, w_1, w_2, u_0 and ψ. It can be seen that inertia effects due to all the assumed displacements are taken into account.

The boundary conditions, at the end of the beam, are given,

at the top face layer ($x = 0$ and $x = l$):

$$N_x^t = 0 \qquad \text{or} \qquad u_1 = 0 \tag{2.24}$$

$$M_x^t = 0 \qquad \text{or} \qquad \frac{\partial w_1}{\partial x} = 0 \tag{2.25}$$

$$\begin{aligned} \frac{\partial M_x^t}{\partial x} + \frac{\rho_1 h_1^3}{12}\frac{\partial \ddot{w}_1}{\partial x} - \frac{\rho h^2}{2}\Bigg(\frac{\ddot{u}_0}{3} + \frac{h}{4} e \ddot{\psi} \\ - \frac{h}{10}\frac{\partial \ddot{w}_1}{\partial x} - \frac{3h}{20}\frac{\partial \ddot{w}_2}{\partial x} - \frac{h^3}{45}\frac{\partial^2 \ddot{\psi}}{\partial x^2}\Bigg) = 0 \end{aligned} \tag{2.26}$$

$$\text{or} \qquad w_1 = 0$$

at the bottom face layer ($x = 0$ and $x = l$):

$$N_x^b = 0 \quad \text{or} \quad u_2 = 0 \tag{2.27}$$

$$M_x^b = 0 \quad \text{or} \quad \frac{\partial w_2}{\partial x} = 0 \tag{2.28}$$

$$\frac{\partial M_x^b}{\partial x} + \frac{\rho_2 h_2^3}{12}\frac{\partial \ddot{w}_2}{\partial x} - \rho h^2 \left(\frac{\ddot{u}_0}{3} + \frac{5eh}{24} - \frac{3h}{40}\frac{\partial \ddot{w}_1}{\partial x} - \frac{2h}{15}\frac{\partial \ddot{w}_2}{\partial x} - \frac{13h^3}{720}\frac{\partial^2 \ddot{\psi}}{\partial x^2} \right) = 0 \tag{2.29}$$

$$\text{or} \quad w_2 = 0$$

and at the core ($x = 0$ and $x = l$):

$$\psi = 0$$

or

$$\frac{h}{12}\frac{\partial \psi}{\partial x} - \frac{\rho}{12E_c}\left[\ddot{w}_1 + \ddot{w}_2 + \left(\frac{2}{3} + 7e \right)\frac{h^2}{10}\frac{\partial \ddot{\psi}}{\partial x} \right] + \frac{\rho h}{3E_c}\left(\frac{1}{4}\frac{\partial \ddot{u}_0}{\partial x} - \frac{h}{15}\frac{\partial^2 \ddot{w}_1}{\partial x^2} - \frac{13h}{120}\frac{\partial^2 \ddot{w}_2}{\partial x^2} - \frac{13h^3}{840}\frac{\partial^3 \ddot{\psi}}{\partial x^3} \right) = 0 \tag{2.30}$$

It is noted that the boundary conditions of the core at each end must be satisfied at any point along the height of the core. It can also be observed that boundary conditions that differ from one face layer to the other at the same section are allowed here. In Appendix A all boundary conditions expressed in terms of four independent functions are given.

2.3 Solution of Forced Harmonic Motion

Consider a sandwich beam under the harmonically varying loading,

$$q(x,t) = Q(x)e^{i\omega t} \tag{2.31}$$

where ω is the forcing frequency. In general, as the frequency of $q(x,t)$ varies, both the amplitude and mode of vibration vary. We assumed here that the response due to the applied force is harmonic and vibrating at the excitation frequency.

Let $\{U(x,t)\}$ be

$$\{U(x,t)\} = \begin{Bmatrix} w_1(x) \\ w_2(x) \\ u_0(x) \\ \psi(x) \end{Bmatrix} e^{i\omega t} \tag{2.32}$$

Thus the partial differential operators in Eqn (2.23) change to ordinary differential operators, and the governing equations, Eqn (2.23) becomes:

$$\left(-\omega^2[M] + [K]\right)\{U\} = \{f\} \tag{2.33}$$

where $\{f(x)\} = \{Q(x), 0, 0, 0\}^T$.

The set of simultaneous ordinary differential equations described by Eqn (2.34) can be solved using known procedures from mathematics [85], in conjunction with the boundary conditions as indicated in Eqns (2.24) to (2.31). Since the motion is now harmonic, it is legitimate to admit viscoelastic damping into the core by putting $G_c = G'(1 + i\eta_G)$ and $E_c = E'(1 + i\eta_E)$. The manner in which the loss factor, η_G and η_E, and the real part of the shear modulus, G' and E' vary with temperature and frequency is quite different for various viscoelastic materials.

It should be pointed out that due to the introduction of viscoelastic damping material in the system, all physical quantities of the system are, in general, complex. Although the purely real solutions for the displacements, for example, are not a general possibility, there are nonetheless exceptions [43].

Since one of the primary objectives of employing the damping composite structures is to attenuate the vibratory responses at the resonant conditions, to find the resonance frequencies of such a system is of great importance. However, the usual procedure used in vibration analysis to find the frequencies can hardly be followed for such a composite system because the characteristic equation for each mode is difficult to obtain. In addition, due to the linear superposition application and the nature of the frequency-dependent material properties, to obtain the resonance frequencies for such a damped system is not easy. It is believed that using the forced vibration analysis is probably the most straightforward procedure to determine the resonance frequencies. The frequencies can be located when the slopes of responses between two frequencies change signs in the neighborhood of resonant conditions. Nonetheless, a method of determining resonance frequencies of damped beams will be presented in the following when the refined vibration theory is used.

Consider a three-layered damped sandwich beam with simply supported boundary conditions. In this case, all boundary conditions are satisfied and the series form solution may be expressed as:

$$\{U(x,t)\} = \sum_{n=0}^{\infty} \begin{Bmatrix} w_{1n} \sin \dfrac{n\pi x}{l} \\ w_{2n} \sin \dfrac{n\pi x}{l} \\ u_{0n} \cos \dfrac{n\pi x}{l} \\ \psi_n \cos \dfrac{n\pi x}{l} \end{Bmatrix} e^{i\omega t} \qquad (2.34)$$

where constants w_{1n}, w_{2n}, u_{0n}, ψ_n ($n = 1, 2, \ldots$) are the amplitude coefficients and n is the wave number.

Substituting Eqn (2-34) into Eqn (2-23), after some manipulation, and utilizing the orthogonality relations of the sine and cosine functions, four linear frequency dependent algebraic equations governing the displacement components w_{1n}, w_{2n}, u_{0n}, and ψ_n can be found. Then, the transverse displacement component of the upper face may yield,

$$w_{1n} = \frac{N(\omega)}{D(\omega)} \qquad (2.35)$$

The resonance frequencies can be obtained by solving the characteristic equation

$$D(\omega) = 0 \qquad (2.36)$$

The solution of this equation yields four frequencies for a given mode. Each of the eigenvalues in general is expected to be complex because the coefficients of Eqn (2.36) are complex. Three family modes of vibration are predominantly flexural, extensional and thickness shear types. For each mode number, the resonance frequency and modal damping (modal loss factor) can be calculated.

For the damped system, Eqn (2.35) can be reduced to such a form that the real and imaginary quantities are present only in the denominator. Following the usual procedure in vibration analysis for small damping, the resonance frequencies for each mode can be determined by solving the polynomial of the denominator with the imaginary part neglected. However, for the case in which there is a considerable amount of damping in the system, the aforementioned procedure to locate the resonance frequencies may not be applied because the resonance frequencies may not be close to the solutions obtained based on the small damping assumption of vibration analysis. For generality, a procedure is proposed to find the frequencies based on the definition of the resonant condition for damped systems.

The resonant condition for the damped system is defined as the frequency for which the response is maximum. For each mode, the resonance frequency may be obtained by differentiating the amplitude of Eqn (2.35) with respect to the frequency parameter and setting it equal to zero. Thus

$$\frac{d}{d\omega}|w_{1n}| = 0$$

or (2.37)

$$\sum_{i=0}^{15} a_i \omega^i = 0$$

This frequency equation turns out to be a 15th-order polynomial with real coefficients. Because of lengthy expression, the explicit form of this polynomial is not given here. Solving this polynomial, the resonance frequency for each mode can be determined.

2.4 Verification Problems

To verify the new refined vibration theory of damped sandwich beams, a free-free damped sandwich beam subjected to a concentrated time harmonic load with circular frequency of excitation ω at the mid-span was examined to correlate both experimental data and analytical solutions published by Lu and Douglas [44]. In their experiment, two damped three-layer laminates were constructed to compare with the analytical solutions given by Mead and Markus [43].

Specimen 1 incorporated a thin 0.004-inch (0.01 cm) acrylic base viscoelastic material, with mass density 1.03×10^{-4} lb-s^2/in^4 (1.124×10^{-3} g-s^2/cm^4), sandwiched between two identical steel machined flats, 1/4-inch thick (0.635 cm), 1-inch wide (2.54 cm), and 24 3/16-inches long (61.456 cm). The machined flats helped ensure a uniform cross section for the thin damping core. The viscoelastic material used is a 3M Company product, two-sided adhesive tape designated as

SJ2015X. The shear storage modulus and shear loss modulus of the viscoelastic layer were obtained for the frequency region of 50 Hz to 1000 Hz from measurements made by the manufacturer on a Melabs rheometer, an instrument that sinusoidally excited small rectangular specimens in a low amplitude shear mode. The complex shear modulus at 124° (51°) could be functionally approximated by the expressions

$$\begin{aligned} \ln G' &= 0.579 \ln \frac{\omega}{2\pi} + 1.136 \quad (G' \text{ in psi}) \\ \ln G'' &= 0.601 \ln \frac{\omega}{2\pi} + 1.144 \quad (G'' \text{in psi}) \end{aligned} \tag{2.38}$$

where the shear modulus $G^* = G(1 + i\eta) = G' + iG''$ (1 psi = 6895 Pascal). Examination of the temperature and frequency dependence of the complex shear modulus showed that this material approximated a class A thermorheologically simple material. By using this assumption, the complex shear modulus was extended to 3000 Hz.

Specimen 2 incorporated a 1/4-inch (0.635 cm) thick neoprene rubber damping core with mass density 9.35×10^{-5} lb-s^2/in^4 (1.02×10^{-3} g-s^2/cm^4) sandwiched between two steel faces, each 1/4-inch (0.635 cm) thick, 2 inches (5.108 cm) wide, and 18 1/8-inches (46.038 cm) long. Comparison of the result of specimen 1 with the thicker damping core in this specimen permitted an evaluation of the analytical model over a wide range of elastic layer to viscoelastic layer thickness ratios. With values given in reference [86], the complex shear modulus at 77° (25°) was found to functionally approximate the expressions,

$$\begin{aligned} \ln G' &= 0.026 \ln \frac{\omega}{2\pi} + 4.754 \quad (G' \text{ in psi}) \\ \ln G'' &= 0.170 \ln \frac{\omega}{2\pi} - 2.705 \quad (G'' \text{ in psi}) \end{aligned} \tag{2.39}$$

for the frequency range of 50 Hz to 10000 Hz (1 psi = 6895 Pascal).

The beams were excited by an electromechanical vibration generator wrapped around a mechanical impedance head which was attached to the beam at mid-span by an area-reducing cone to concentrate the dynamic load. The beams were suspended in air by lightweight elastic shock cords which resulted in a system natural frequency well below 5 Hz. The force and acceleration signals were analyzed by 2 Hz bandwidth tracking filters, and the 20 Hz to 3000 Hz spectrum was swept slowly with a sweep oscillator to obtain a continuous spectrum. The acceleration signal was integrated to obtain velocity. The oscillator sweep rate was slow enough to allow the structure and electronics to accurately record impedance. The beams were tested in a temperature controlled chamber after thermal equilibrium was reached.

The analytical solutions of those mechanical impedance examples are obtained for the free-free damped sandwich beams by using the present refined vibration theory. The terminology "mechanical impedance" used here is the ratio of force causing motion to the velocity at a given point in a vibrating system. The concentrated load applied at the mid-span is expressed in terms of infinite series.

The eight free-free boundary conditions, first equation of Eqns (2.24) through (2.31) are used, and the complete solution can be obtained as:

$$\{U(x,t)\} = \sum_{j=1}^{8}\begin{Bmatrix} A_j e^{\alpha_j x} \\ 0 \\ 0 \\ 0 \end{Bmatrix} + \sum_{n=0}^{\infty}\begin{Bmatrix} w_{1n}\sin\frac{n\pi}{2}\sin\frac{n\pi x}{l} \\ w_{2n}\sin\frac{n\pi}{2}\sin\frac{n\pi x}{l} \\ u_{0n}\cos\frac{n\pi}{2}\cos\frac{n\pi x}{l} \\ \psi_n\cos\frac{n\pi}{2}\cos\frac{n\pi x}{l} \end{Bmatrix} e^{i\omega t} \tag{2.40}$$

where the α_j's are the eight roots of the characteristic equation with complex coefficients, the A_j's are the eight unknown complex constants to be determined from boundary conditions. The eight unknown complex constants can be computed by any standard matrix inversion technique, such as the Gauss-Jordan elimination method. Once the transverse displacements, $w_1(x,t)$, is found, the driving point mechanical impedances can be determined. Since the core used here is relatively thin, the results show that $w_1(x,t)$ and $w_2(x,t)$ are almost the same.

Figures 2.3 and 2.4 show the comparison for the mechanical impedance versus frequency between experimental data and present analytical results. These figures are plots of absolute values of the driving point mechanical impedances versus frequency in Hertz. The two specimens selected are in very different conditions. The first has a very thin relatively highly damped viscoelastic core (SJ2015X) measured at 124°F (51°), while the second has a relatively thick low loss tangent viscoelastic core (neoprene rubber) measured at 77° (25°). In both

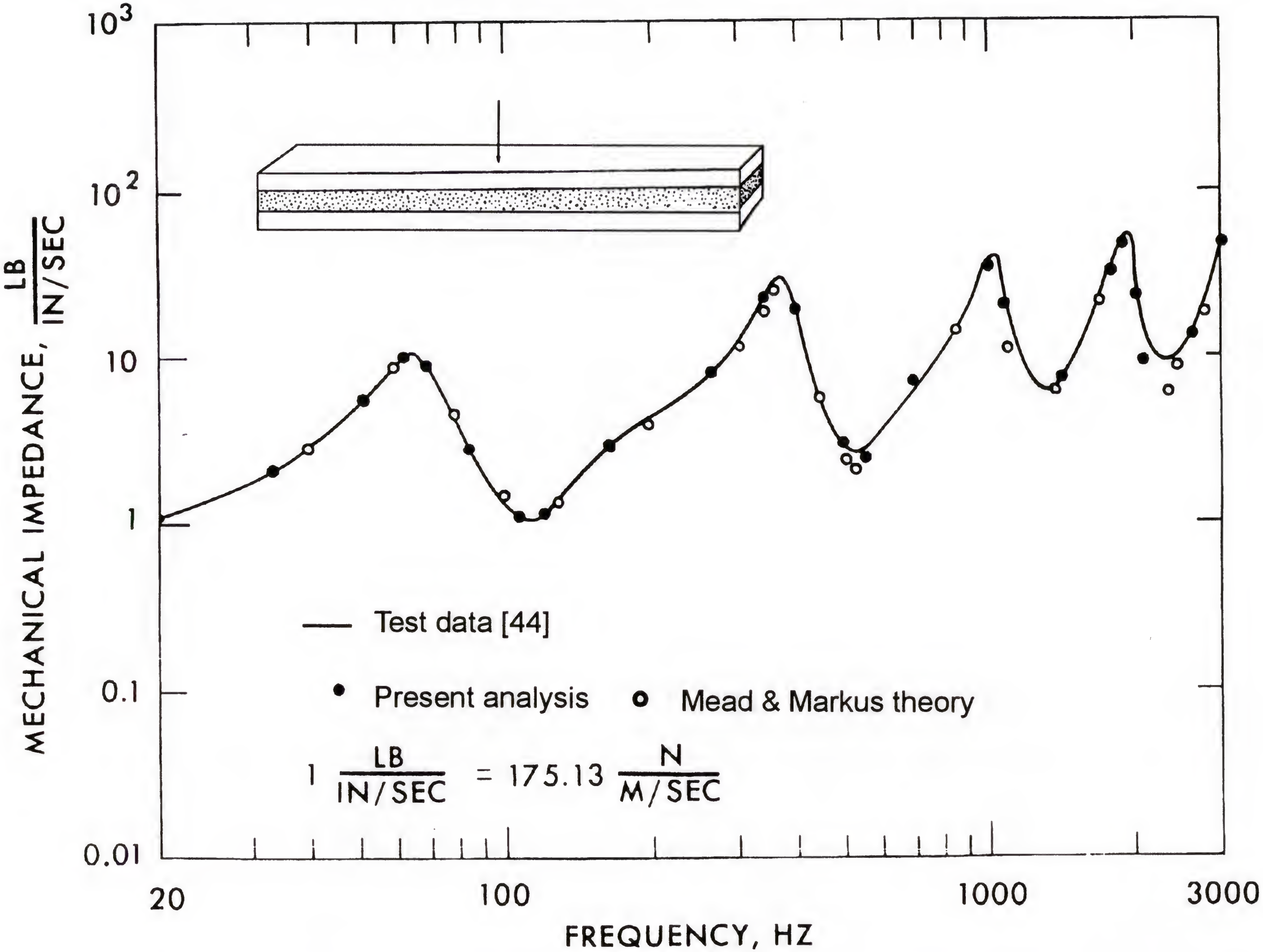

Figure 2.3 Driving Point Mechanical Impedance of a Damped Sandwich Beam (Specimen 1)

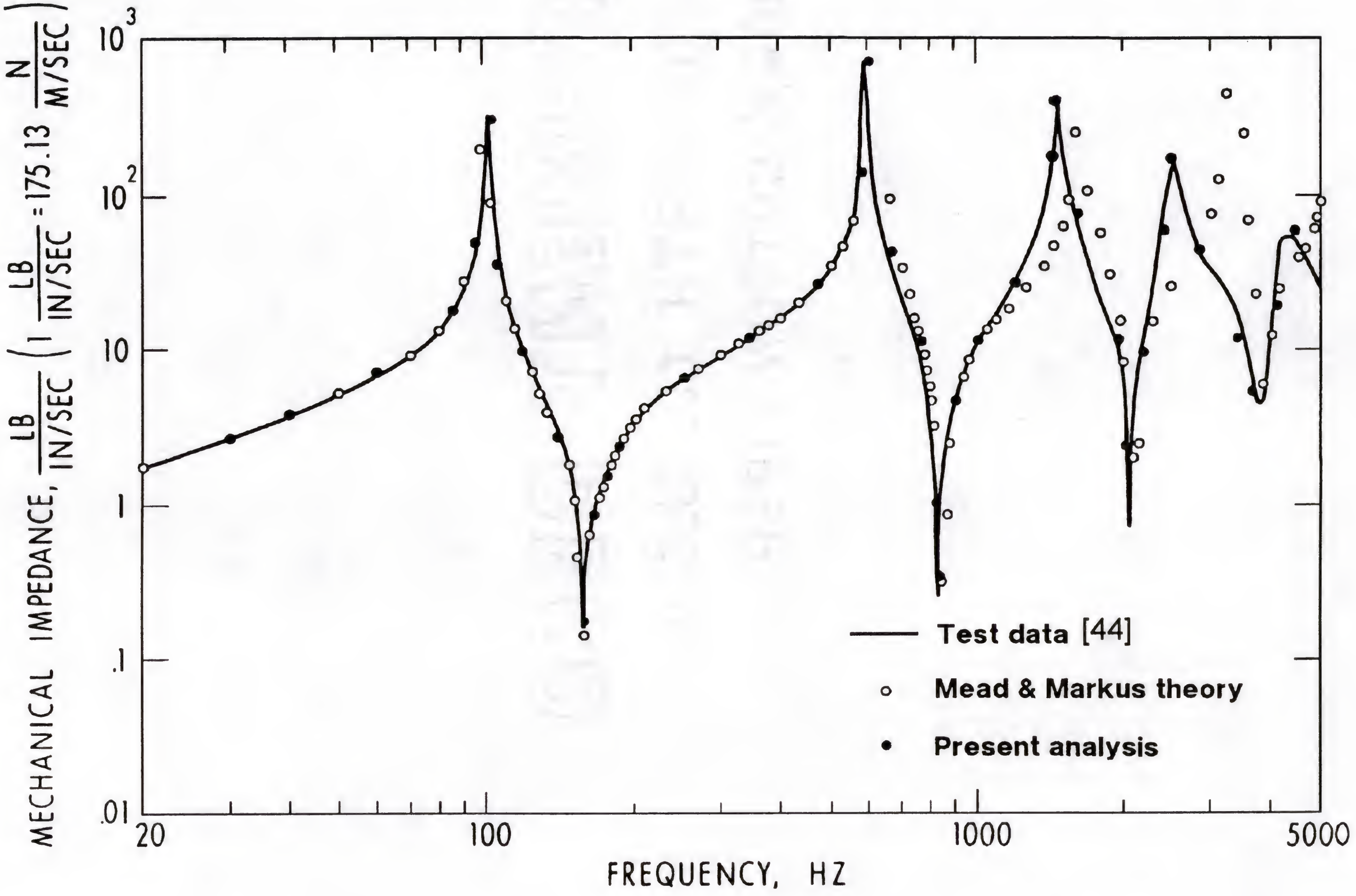

Figure 2.4 Driving Point Mechanical Impedance of a Damped Sandwich Beam (Specimen 2)

cases, not only are the damped resonance frequencies well predicted by the refined theory but also the resonant amplitudes. It is noted that although Mead and Markus theory [43] is well agreed with the experiment data, the present theory improves the high mode results.

2.5 Parametric Study

For a given damped system, it is anticipated that the vibrational behavior is complicated by the involvement of many parameters. It depends on many geometrical and material parameters of the structural system including the modulus, width, length, and thickness of the upper and lower face layer structures; the thickness, shear modulus and loss factor of the damped core material; the half wavelength of the mode which in turn depends on the mode number and the boundary conditions. Moreover, the damping material properties are functions of frequency as well as temperature which has made the design of engineering structures with damping for a specific application even more difficult. Therefore, for an optimized design of any particular damped structural system, a complete parametric study is required.

The resonance frequency behavior of a simply supported sandwich beam is studied parametrically. The results are presented for a symmetric construction which consist of two identical faces and a soft core. The non-dimensional n-th mode frequency parameter Ω_n used in the figures is defined as

$$\Omega_n^2 = \omega_n^2(1 + i\eta_n)\frac{\rho h_1 l^4}{E_1 I_1} \tag{2.41}$$

The fundamental mode resonates at the frequency ω_1 and has a loss factor of η_1. Unless mentioned otherwise, the loss factors of the core are assumed as $\eta_G = 0.2$ and $\eta_E = 0.05$.

The effect of the core thickness on the resonant frequency is presented in Figure 2.5. It can be seen that the resonant frequency decreases with increasing the core thickness, and Mead and Markus theory overestimates the resonant frequency especially for the thicker core.

Figure 2.6 shows the effect of the modulus of elasticity of the core in the vertical direction on the fundamental resonant frequency. In the Mead and Markus theory, $\varepsilon_z^c = 0$, meaning that $E_c = \infty$, so that it overestimates the resonance frequency. Such discrepancy may be greater if the core material is getting softer.

In Figure 2.7, the effect of the modulus of elasticity of the core in the vertical direction on the resonance frequency is examined in the other way in which the frequency is normalized with respect to the ordinary beams. The frequency of a Euler-Bernoulli beam with the same mass and flexural rigidity is denoted by ω_o, and that of a Timoshenko beam which has shear rigidity and rotational inertia is denoted by ω_t. The damping effects are neglected here and first and second mode are considered. It can be seen that shear rigidity and rotational inertia have less effects on the second mode than the first mode. It is noted that an increase in the core modulus E_c is always associated the with an

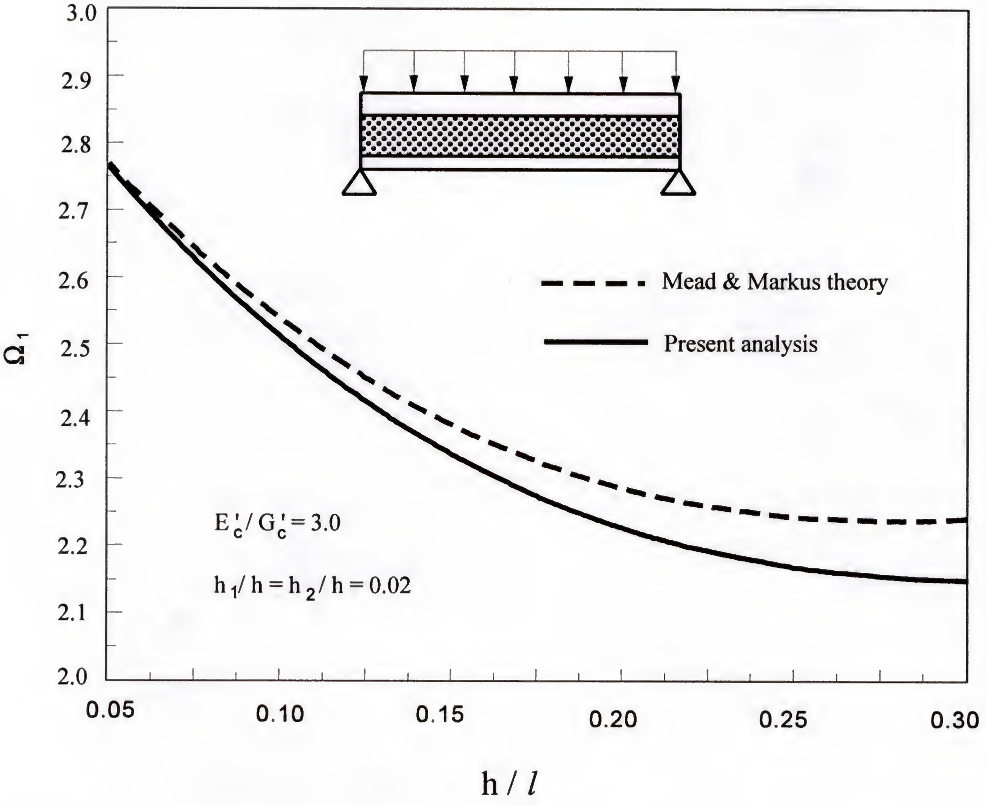

Figure 2.5 Variation of First Resonance Frequency with Core Thickness

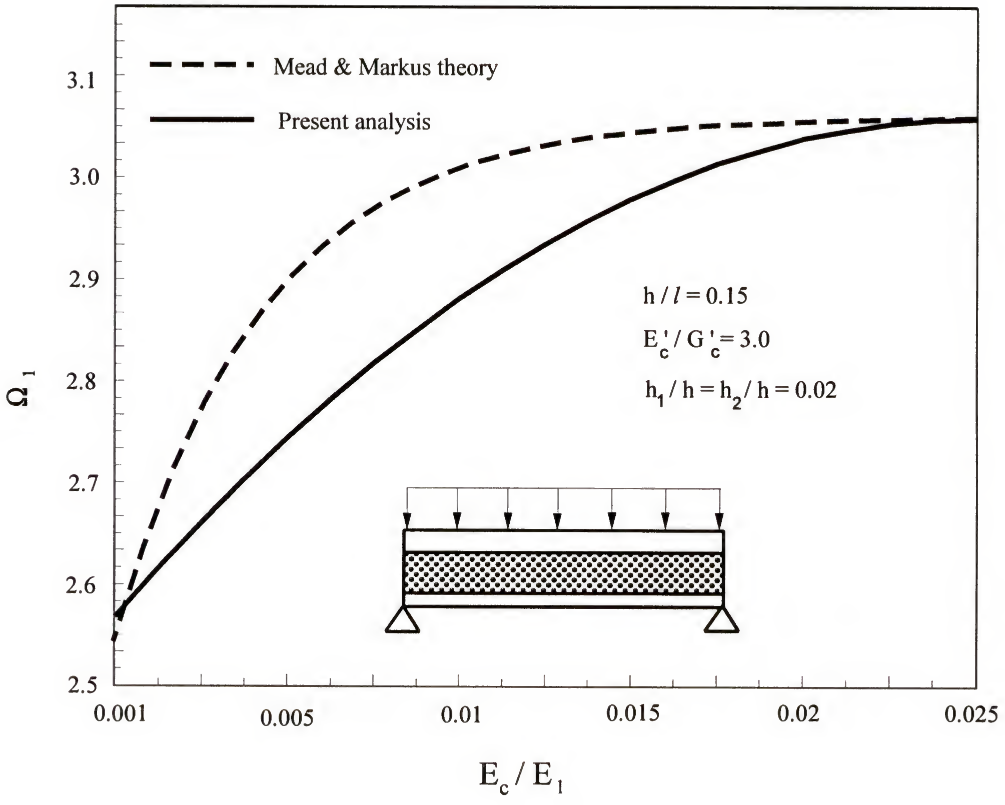

Figure 2.6 Effect of Core Modulus on the Resonance Frequency

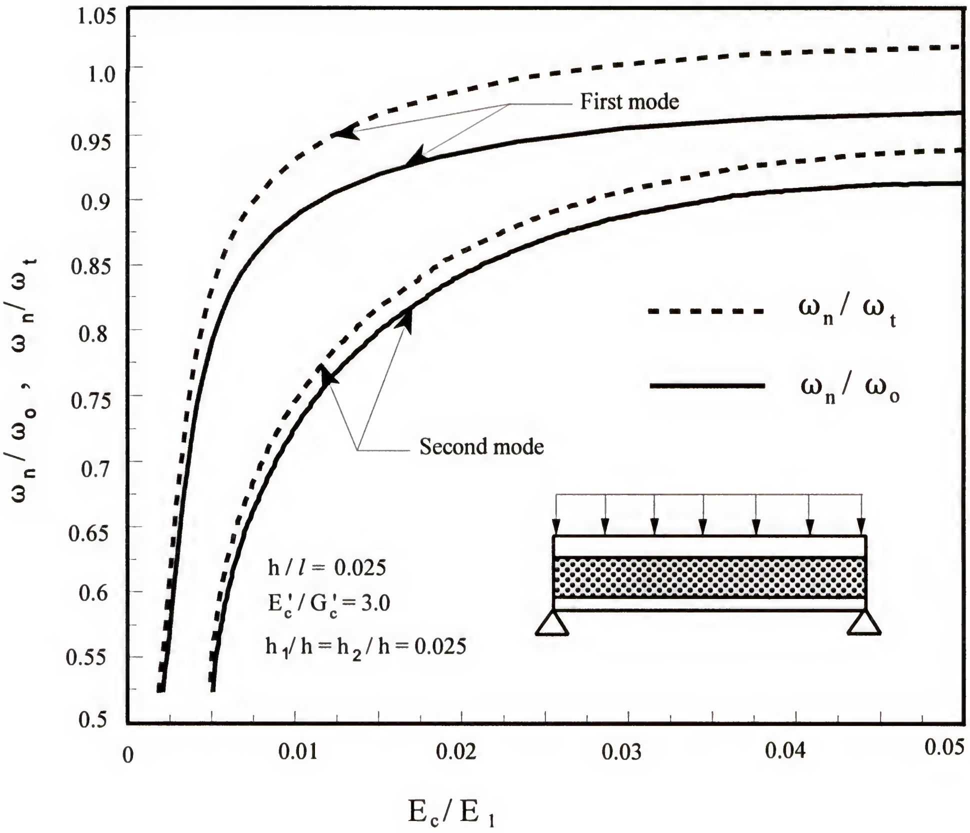

Figure 2.7 Shear and Rotational Effects on Resonance Frequencies

increase the core density for the foam or honeycomb core materials. Thus, the natural frequency will increase with the core modulus. The frequency ratio relative to the homogeneous isotropic beam may offer a help for the design of low density sandwich construction in the dynamic environment.

According to the definition of Mead and Markus [43], the shear parameter is defined as

$$s = \frac{G_c l^2}{h}\left(\frac{1}{E_1 h_1} + \frac{1}{E_2 h_2}\right) \tag{2.42}$$

which is an important parameter to represent the core shear effect. Figure 2.8 examines the variation of fundamental resonance frequency with the shear parameter s in different values of face/core thickness ratio. It can be seen that the resonance frequency, and hence the stiffness of the beam, changes more rapidly with s when the face/core thickness ratio is smaller. This may be significant to the performance of a sandwich beam under changing temperature because of changing s.

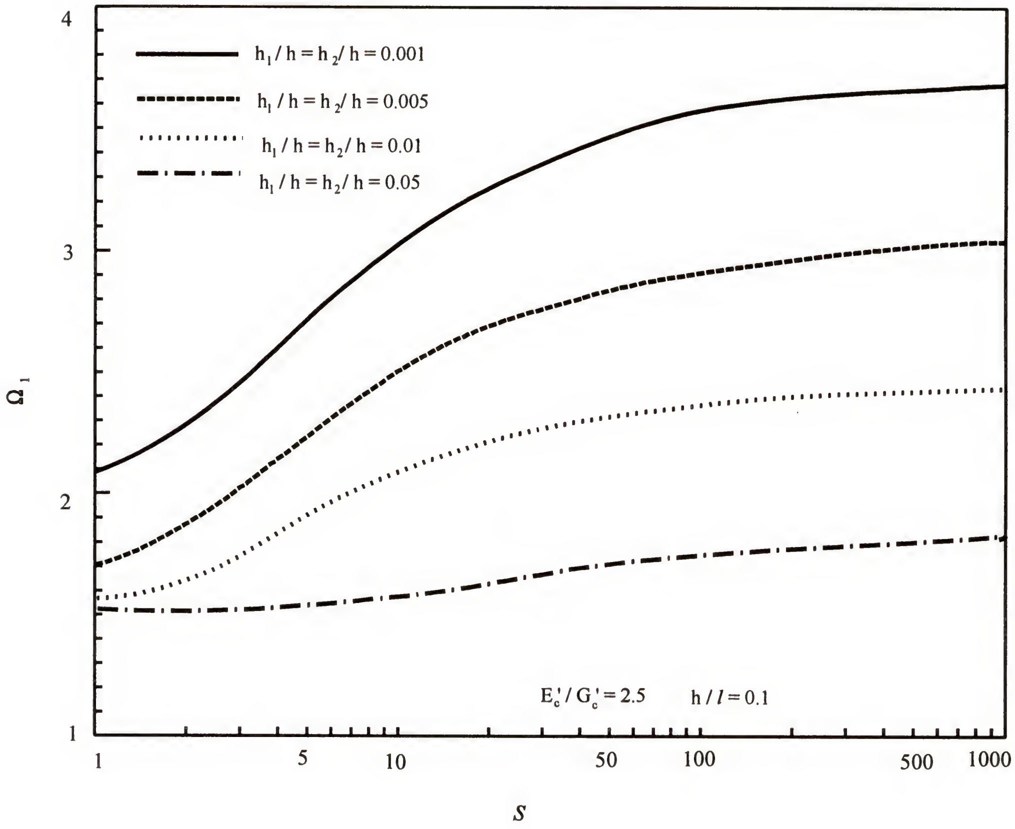

Figure 2.8 Variation of Resonance Frequencies with Shear Parameter

CHAPTER 3
EFFECTS OF VISCOELASTIC INTERFACE OF SANDWICH BEAMS

The effects of viscoelastic interface layer (or adhesive layer) on the dynamic response and structural damping of sandwich structures are studied by employing a refined vibration theory of sandwich beams as discussed in Chapter 2. Imperfect interface conditions between faces and core are defined as linear relations between interface displacements discontinuities and associated shear stresses. With the viscoelastic properties of the interface and the core material which are complex and is function of frequency for a given temperature, the linear equations of motion describing the vibration of the sandwich finite beam are derived based on the Hamilton principle.

Three methods to evaluate system loss factors (structural damping) are discussed. In those methods the overall damping of the structure is calculated from the independent properties of the constituent materials that form the sandwich structure. The effects of storage modulus and loss factor of interface layers on the structural damping and resonance frequencies are numerically investigated for simply supported beams under the harmonic excitation. Results demonstrate that the influence of viscoelastic interface layer on damping is significant and there may exist optimal adhesive bonding stiffness to achieve the maximum sandwich structural damping.

3.1 Viscoelastic Interface Model

Consider a three layer sandwich beam of length l and unit width with two interface layers between upper, lower face layers and core as shown in Figure 3.1. It has face layers of thickness, h_1 and h_2, and a core of thickness h. The face layers are the elastic material with high Young's moduli of E_1 and E_2. The flexible core is linearly viscoelastic with a Young's modulus E_c and a shear modulus of G_c where E_c and G_c are expressed by complex numbers under the harmonic excitation.

The classical compatibility conditions of deformations between the face and core assumed the displacements and associated stress are continuous across the interface layer. This will be referred to as perfect interface conditions and every other kind of interface conditions will be called imperfect. Since most of energy dissipation in the viscoelastic damping mechanism is contributed by the shear deformation, the effect of transverse normal deformation at the interface layer on structural damping is neglected, and the continuity conditions of transverse displacement at the interface layer remain. The imperfect interface conditions are described by the longitudinal displacement discontinuity as described in the following assumption

- The longitudinal displacement discontinuity (slip) is proportional to the shear stress at the face-core interface which is viscoelastic.

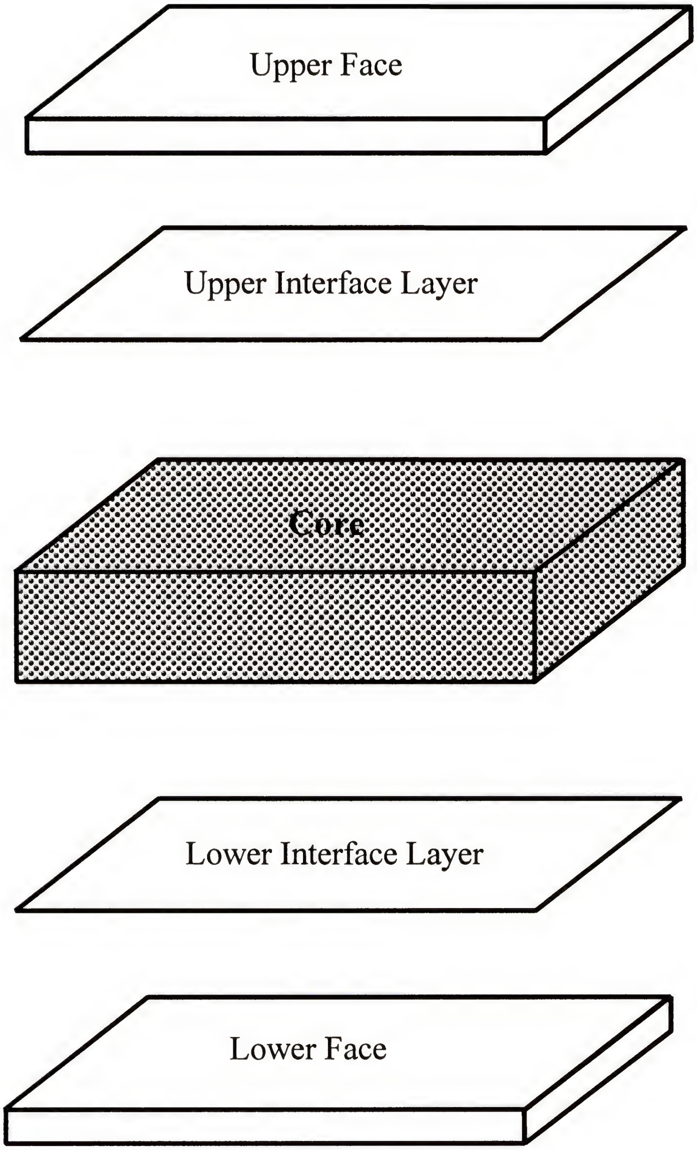

Figure 3.1 A Sandwich Beam with Interface Layers

To study the structural damping problem due to the viscoelastic interface layers and core, the complex modulus approach is used and the compatibility conditions can be written as the following

at $z = h$ (upper interface)

$$\tau_1^i = k^*(u^t - u^c) \tag{3.1}$$

$$w^c = w^t \tag{3.2}$$

at $z = 0$ (lower interface)

$$\tau_2^i = k^*(u^c - u^b) \tag{3.3}$$

$$w^c = w^b \tag{3.4}$$

where τ_1^i and τ_2^i are the shear stress at the upper and lower interface layers respectively, and $k^* = k(\omega)(1 + i\eta_k(\omega))$ is the frequency-dependent complex shear modulus of interface layers. Small values of $k(\omega)$ represent the weak bonding between the faces and the core. When $k \rightarrow \infty$, it approaches perfect bonding interface that is usually assumed in the sandwich theory.

3.2 Governing Equations of Motion

A set of force and moment resultants are defined for top and bottom faces separately:

$$N_x^i = \int_{-\frac{h_j}{2}}^{\frac{h_j}{2}} \sigma_x^i \, dz_j$$

$$M_x^i = \int_{-\frac{h_j}{2}}^{\frac{h_j}{2}} \sigma_x^i z_j \, dz_j \qquad (3.5)$$

where $i = t, b$ correspond to $j = 1, 2$ respectively.

The constitutive relations for the elastic face layers and for the viscoelastic core are exactly the same form as we discussed in Chapter 2, equations (2.16) and (2.17) where frequency-dependent complex shear and Young's modulus of the core, G_c, E_c, are used.

Eliminating $u_0(x,t)$, $w_0(x,t)$, and $\phi(x,t)$ from Eqns (3.1) through (3.4), an independent compatibility equation is obtained:

$$k^{*}\left(u_1 - u_2 + \frac{h_1 + h}{2}\frac{\partial w_1}{\partial x} + \frac{h_2 + h}{2}\frac{\partial w_2}{\partial x}\right) - (k^{*}he + 2E_c)\psi + k^{*}\frac{h^3}{12}\frac{\partial^2 \psi}{\partial x^2} = 0 \qquad (3.6)$$

The governing equations of motion and the boundary conditions are derived via variational calculus, the Hamilton principle, which requires:

$$\delta \int_{t_1}^{t_2} [T - U] \, dt = 0 \qquad (3.7)$$

where T is the kinetic energy; U is the total potential energy; t_1, t_2 define the time interval.

The total kinetic energy of the sandwich beam can be expressed as:

$$T = \frac{1}{2}\int_0^l \left\{ \rho_1 h_1[(\dot{u}_1)^2 + \frac{h_1^2}{12}(\frac{\partial \dot{w}_1}{\partial x})^2 + (\dot{w}_1)^2] \right.$$

$$+ \rho_2 h_2[(\dot{u}_2)^2 + \frac{h_2^2}{12}(\frac{\partial \dot{w}_2}{\partial x})^2 + (\dot{w}_2)^2] \tag{3.8}$$

$$\left. + \int_{-\frac{h}{2}}^{\frac{h}{2}} \rho\,[(\dot{u}^c)^2 + (\dot{w}^c)^2]dz \right\} dx$$

where ρ_1, ρ_2 and ρ are the density of the upper face, lower face and the core, respectively, and the ($\dot{}$) denotes a first derivative with respect to time.

The total potential energy, U, consists of the contributions from both face layers U_1 and U_2, core shear strain U_3, core normal U_4, and potential terms V, due to applied loading. The effects of imperfect bonding, φ is considered by introducing a Lagrange multiplier λ with Eqn (3.6) into the total potential energy contributions. Thus,

$$U = U_1 + U_2 + U_3 + U_4 + \varphi + V \tag{3.9}$$

$$
\begin{aligned}
U_1 &= \frac{1}{2}\int_0^l E_1 h_1 \left[\left(\frac{\partial u_1}{\partial x}\right)^2 + \frac{h_1^2}{12}\left(\frac{\partial^2 w_1}{\partial x^2}\right)^2 \right] dx \\
U_2 &= \frac{1}{2}\int_0^l E_2 h_2 \left[\left(\frac{\partial u_2}{\partial x}\right)^2 + \frac{h_2^2}{12}\left(\frac{\partial^2 w_2}{\partial x^2}\right)^2 \right] dx \\
U_3 &= \frac{1}{2}\int_0^l G_c h \,(e\psi)^2\, dx \\
U_4 &= \frac{1}{2}\int_0^l \frac{E_c}{h} \left[(w_1 - w_2)^2 + \frac{h^4}{12}\left(\frac{\partial \psi}{\partial x}\right)^2 \right] dx
\end{aligned}
\tag{3.10}
$$

$$
\begin{aligned}
\varphi &= \lambda \int_0^l \left[k^{*}\left(u_1 - u_2 + \frac{h_1 + h}{2}\frac{\partial w_1}{\partial x} + \frac{h_2 + h}{2}\frac{\partial w_2}{\partial x}\right) \right. \\
&\qquad \left. - (k^{*} h e + 2E_c)\psi + k^{*}\frac{h^3}{12}\frac{\partial^2 \psi}{\partial x^2} \right] dx
\end{aligned}
\tag{3.11}
$$

$$
V = \int_0^l q\, w_1\, dx
$$

where $q = q(x,t)$ is transverse distributed dynamic loading at surface of top face layer.

It is noted that T and U can be further expressed in terms of five basic unknown functions— $w_1(x,t)$, $w_2(x,t)$, $u_1(x,t)$, $u_2(x,t)$ and $\psi(x,t)$. Taking variation in Hamilton's equation with respect to w_1, w_2, u_1, u_2, ψ and λ, six equations of motion and boundary conditions are obtained after integration by parts in x and t, and some algebraic manipulations and substitutions. It is noted that homogeneous conditions for the displacement and the velocity at $t = t_1$, t_2 are assumed. The physical meaning of Lagrange multiplier λ is the face-core interface shear force.

The number of governing equations is reduced from six to five by eliminating the λ. The governing equations can be written in the matrix form:

$$[\partial M]\{\ddot{U}\} + [\partial K]\{U\} = \{F\} \tag{3.12}$$

where

$\{U\} = \{w_1, w_2, u_1, u_2, \psi\}^{\mathrm{T}}$

$\{F\} = \{q, 0, 0, 0, 0\}^{\mathrm{T}}$

$[\partial M]$ — the mass matrix differential operator

$[\partial K]$ — the stiffness matrix differential operator

It is noted that $[\partial K]$, $\{\ddot{U}\}$ and $\{U\}$ are complex valued.

The boundary conditions, at the end of the beam, are given,

at the top face layer ($x = 0$ and $x = l$):

$$N_x^t = 0 \quad \text{or} \quad u_1 = 0 \tag{3.13}$$

$$M_x^t = 0 \quad \text{or} \quad \frac{\partial w_1}{\partial x} = 0 \tag{3.14}$$

$$\begin{aligned} &\frac{\partial M_x^t}{\partial x} + \frac{h + h_1}{2}\frac{\partial N_x^t}{\partial x} - \rho_1 h_1 \frac{h + h\text{-}1}{2}\ddot{u} + \frac{\rho_1 h_1^3}{12}\frac{\partial \ddot{w}_1}{\partial x} \\ &\quad - \frac{\rho h^2}{2}\left[\frac{\ddot{u}_2}{3} + \left(\frac{E_c}{3k^{*}} + \frac{eh}{4}\right)\ddot{\psi} - \frac{h}{10}\frac{\partial \ddot{w}_1}{\partial x}\right. \\ &\quad \left. - \left(\frac{3h}{20} + \frac{h_2}{6}\right)\frac{\partial \ddot{w}_2}{\partial x} - \frac{h^3}{45}\frac{\partial^2 \ddot{\psi}}{\partial x^2}\right] = 0 \end{aligned} \tag{3.15}$$

$$\text{or} \quad w_1 = 0$$

at the bottom face layer ($x = 0$ and $x = l$):

$$N_x^b = 0 \quad \text{or} \quad u_2 = 0 \tag{3.16}$$

$$M_x^b = 0 \quad \text{or} \quad \frac{\partial w_2}{\partial x} = 0 \tag{3.17}$$

$$\begin{gathered}\frac{\partial M_x^b}{\partial x} + \frac{\rho_2 h_2^3}{12}\frac{\partial \ddot{w}_2}{\partial x} - \rho h\left[\left(\frac{h}{3} + \frac{h_2}{2}\right)\ddot{u}_2\right. \\ + \left(\frac{3h_2 + 2h}{6k}E_c + \frac{2h_2 + h}{8}e h\right)\ddot{\psi} - \left(\frac{h_2}{12} + \frac{3h}{40}\right)\frac{\partial \ddot{w}_1}{\partial x} \\ \left. - \left(\frac{h_2^2}{4} + \frac{hh_2}{3} + \frac{2h^2}{15}\right)\frac{\partial \ddot{w}_2}{\partial x} - \left(\frac{h_2}{48} + \frac{13h}{720}\right)h^3\frac{\partial^2 \ddot{\psi}}{\partial x^2}\right] = 0 \\ \text{or} \quad w_2 = 0\end{gathered} \tag{3.18}$$

and at the core ($x = 0$ and $x = l$):

$$\psi = 0$$

or

$$\begin{gathered}\frac{1}{12}\frac{\partial \psi}{\partial x} + \frac{\rho}{24E_C}\left(\ddot{w}_1 + \ddot{w}_2 + \frac{3h^3}{20}\frac{\partial \ddot{\psi}}{\partial x}\right) \\ - \frac{\rho h}{2E_c}\left[\frac{1}{12}\frac{\partial \ddot{u}_2}{\partial x} + \left(\frac{E_c}{12K^*} + \frac{7eh}{120}\right)\frac{\partial \ddot{\psi}}{\partial x} - \frac{h}{45}\frac{\partial^2 \ddot{w}_1}{\partial x^2}\right. \\ \left. - \left(\frac{13h}{360} + \frac{h_2}{24}\right)\frac{\partial^2 \ddot{w}_2}{\partial x^2} - \frac{13h^3}{3020}\frac{\partial^3 \ddot{\psi}}{\partial x^3}\right] = 0\end{gathered} \tag{3.19}$$

It should be noticed that the boundary conditions of the core at each end must be satisfied at any point along the height of the core. Boundary conditions that differ from one face layer to the other at the same section are allowed here. It is also noted that all boundary conditions, traction type or displacement type, can also be expressed in terms of five basic functions (see Appendix B).

The eight simply supported boundary conditions at each end of the beam will be a combination of these boundary conditions as the following

at the top face layer, ($x = 0$ and $x = l$)

$$N_x^t = 0 \tag{3.20}$$

$$M_x^t = 0 \tag{3.21}$$

$$w_1 = 0 \tag{3.22}$$

at the bottom face layer,

$$N_x^b = 0 \tag{3.23}$$

$$M_x^b = 0 \tag{3.24}$$

$$w_2 = 0 \tag{3.25}$$

at the core,

$$\psi = 0 \quad (\tau_{xz}^c = 0) \tag{3.26}$$

Similarly the fixed end and free end boundary conditions can be obtained in a combination of those boundary conditions given in Eqns (3.13) through (3.19).

3.3 Calculation of Loss Factors

Structural damping refers to a structure's or structural component's capacity for dissipating energy or to its capacity for removing from a structural vibration some of the energy associated with that vibration. This removed energy may be converted directly into heat, transferred to connected structures or ambient media. The mechanism of structural damping is a complicated physical phenomenon. In addition to controlling the amplitude of resonant vibrations, damping also has other effects such as increasing wave attenuation, decreasing sound transmission through structures, reducing structural fatigue, etc.

Usually, a convenient measure of the damping of any dynamical system is its non-dimensional loss factor which can be defined by the energy dissipated per cycle of harmonic motion in a particular mode divided by the maximum potential energy stored in the course of the cycle multiplied by 2π,

$$\eta = \frac{U}{2\pi W} \tag{3.27}$$

where U is the energy dissipated per cycle or the energy that has to be supplied to sustain the steady state vibration, and W is the maximum energy associated with vibration. However, there are many quantitative measures of structural damping ability based on the effect it has on the response of the system. Most of the measures of damping that are used currently, such as resonance bluntness, half-power bandwidth, logarithmic decrement, percentage of critical damping etc, are defined based on linear single degree of freedom systems with frequency independent parameters. Of the many different measures of damping used in resonant analysis, loss factor and quantities closely related to it are still the most generally applicable. On the other hand, all the different measures of damping, under the assumption of low damping, are used interchangeably.

A lot of research work on vibration damping only deal with structural damping, also called hysteretic damping, which was originally postulated as a basis for describing the internal damping properties of solids. It is showed that the structural damping can be considered adequately by using a complex modulus, $E' + iE''$, where the real part is called the storage modulus and the imaginary part the loss modulus. Loss factor, a measure of damping, is the ratio of the imaginary part to the real part. In the case of structural damping, both E' and E'' are constants. Although the complex modulus is only defined for harmonic excitation, the complex modulus approach can also be used for the analysis of a system subjected to arbitrary excitation because any real signal can be represented as a Fourier sum.

However, structural damping is not a physically realizable energy dissipation mechanism in a continuous composite system where it can also be modeled by using complex modulus approach based on the correspondence principle of viscoelasticity [85]. It is known that complex modulus which does not vary with frequency leads to noncausal system response (response anticipates input) [86], and a finite energy dissipation rate at zero frequency. In the case of viscoelastic damping, both E′ and E″ of viscoelastic materials are functions of frequency, instead of constants.

Viscoelastic damping in a continuous composite system can also be analyzed by using the complex modulus approach. According to the elastic-viscoelastic correspondence principle, the elastic constants of the materials are simply replaced by the corresponding frequency-dependent viscoelastic counterparts. In a consequence, the system loss factor can be calculated from the resulting complex valued system of equations in the following three approaches.

3.3.1 Complex Eigenvalue Approach

Consider a sandwich beam under the harmonically varying loading,

$$q(x,t) = Q(x)e^{i\omega t} \tag{3.28}$$

where ω is the forcing frequency. In general, as the frequency of $q(x,t)$ varies, both the amplitude and mode of vibration vary. We assumed here that the response due to the applied force is harmonic and vibrating at the excitation frequency.

Let $\{U(x,t)\}$ be

$$\{U(x,t)\} = \begin{Bmatrix} w_1(x) \\ w_2(x) \\ u_1(x) \\ u_2(x) \\ \psi(x) \end{Bmatrix} e^{i\omega t} \tag{3.29}$$

Thus the partial differential operators change to ordinary differential operators, and the governing equations, Eqn (3.12) becomes:

$$\left(-\omega^2[M] + [K]\right)\{U\} = \{f\} \tag{3.30}$$

where $\{f(x)\} = \{0, Q(x), 0, 0, 0\}^T$.

The eigenvalue problem is then

$$[K][U_n] = \omega_n{}^2[M][U_n] \tag{3.31}$$

where ω_n and $[U_n]$ are the n-th complex eigenvalue and eigenvector.

For a undamped beam, the Raleigh's principle (Raleigh's quotient) can be written as

$$\omega_n^2 = \frac{[U_n]^T[K][U_n]}{[U_n]^T[M][U_n]} \tag{3.32}$$

and for a damped structural system, the complex Raleigh's principle can be extended to

$$([K'] + i[K''])[U_n] = \omega_n^2(1 + i\eta_n)[M][U_n] \tag{3.33}$$

where $[K']$ is the sum of the stiffness matrix of the elastic elements, $[K_e]$, and the real part of the stiffness of the viscoelastic elements, $[K_{Rv}]$. $[K'']$ is the imaginary part of stiffness matrix of the viscoelastic elements which is equal to $\eta[K_{Rv}]$. The modal loss factor of the n-th mode of the structure is denoted by η_n. Then, Eqn (3.33) yields

$$\begin{aligned} \omega_n^2[M][U_n] &= [K'][U_n] \\ \omega_n^2\eta_n[M][U_n] &= [K''][U_n] = \eta[K_{RV}][U_n] \end{aligned} \tag{3.34}$$

where η is the material loss factor of the core. Thus,

$$\begin{aligned} \omega_n^2 &= \frac{[U_n^T][K'][U_n]}{[U_n^T][M][U_n]} \\ \omega_n^2\eta_n &= \frac{[U_n^T][K''][U_n]}{[U_n^T][M][U_n]} = \eta\frac{[U_n^T][K_{RV}][U_n]}{[U_n^T][M][U_n]} \end{aligned} \tag{3.35}$$

Then

$$\eta_n = \frac{\eta[U_n^T][K_{RV}][U_n]}{[U_n^T][K'][U_n]} = \eta\frac{V_n(\mathrm{v})}{V_n} \tag{3.36}$$

where the strain energy of the core associated with a given mode is $V_n(\mathrm{v})$, and the strain energy of the entire elastic system associated with the same mode is V_n.

It should be noted here that the loss factors of the structural system only describe a part of the effectiveness of the damped structure.

In solving the vibration problem, the solutions can be determined in terms of damped normal modes. Both the eigenvalues and the associated eigenvectors will of course be complex in nature. Therefore, the disadvantages of this approach stem from the inherent nature of the involvement of the damping material. Namely, the computational effort is quite expensive, and the properties of real viscoelastic materials are frequency dependent instead of being constant for storage moduli.

3.3.2 Direct Frequency Response Approach

In the direct frequency response method, a forced vibration solving technique is used. The overall damping of the system is calculated from a theoretical response spectrum which is generated over a range of frequencies being considered. Since the complex modulus approach is used, the Eqn (3.30) is complex. For each frequency of excitation, the displacement per unit applied force is calculated by solving the system of complex-valued simultaneous equations, and the response function is thereby generated. Loss factor is calculated from the real part of generated response spectrum as shown in Figure 3.2, or by using the half-power-bandwidth technique. These two methods are used in general purpose finite elemenet analysis package for the layered damped structures, for example, the NASTRAN package. The advantages are that these programs can analyze structures with any complexity and that they are well developed and managed.

The disadvantage is that the computation cost is expensive. But the major difference between these damped systems and other elastic undamped laminated structures analyzed by the finite element direct frequency response method is that the results of these damped problems can be obtained for only one frequency at a time because the shear modulus and the loss factors of the viscoelastic materials are functions of frequency for a given temperature. As a result, NASTRAN's standard normal mode analysis can not be used to determine the resonance frequencies and mode shapes of such systems. The analytical solution is thus necessary and more accurate analysis will be helpful in understanding the structural damping mechanism.

The system loss factor can be obtained more directly by using direct frequency response method. As we discussed in section 2.4 of Chapter 2, the resonance frequencies can be obtained by solving the characteristic equation

$$D(\omega) = 0 \tag{3.37}$$

The solution of normal damped mode can also be calculated. Then loss factor can be calculated by using the energy ratio method. After the resonant frequency and the corresponding displaced shape at resonance have been calculated, the loss factor of the beam system can be calculated from

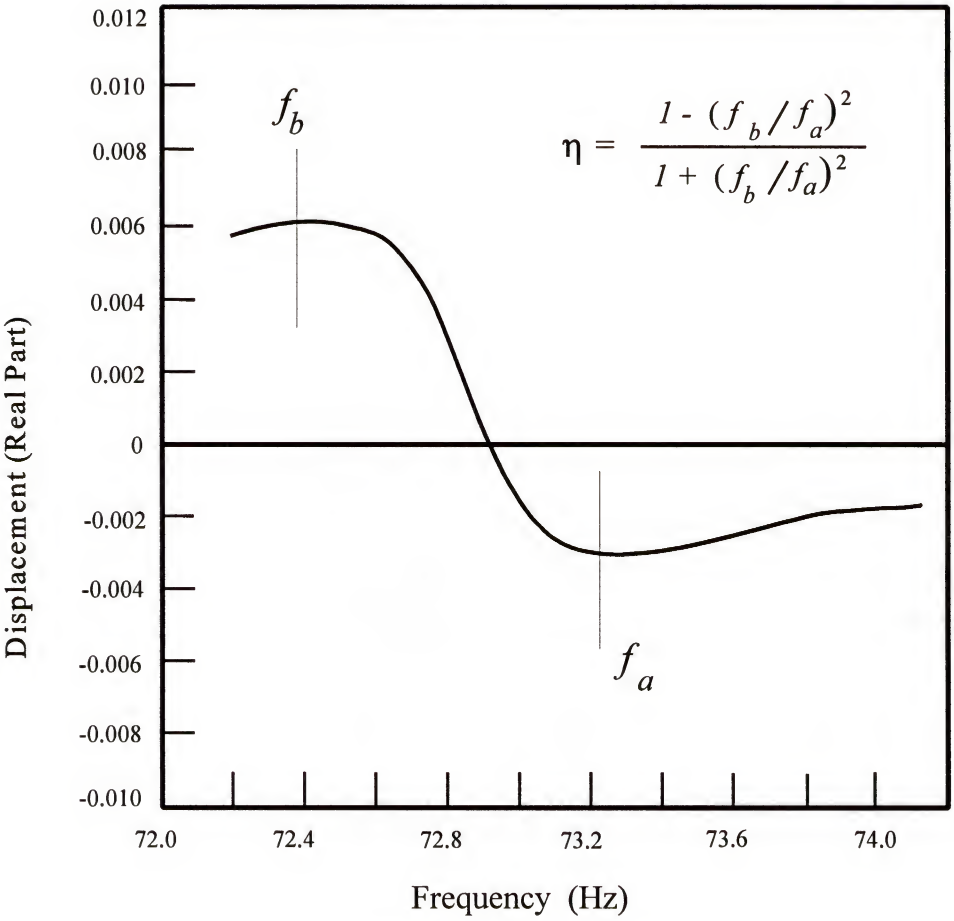

Figure 3.2 Real Part of the Response Spectrum

$$\eta_s = \frac{\{U^{*}\}^T[K'']\{U\}}{\{U^{*}\}^T[K']\{U\}} \tag{3.38}$$

where $\{U^*\}$ is the complex conjugate of $\{U\}$ and

$$[K] = [K'] + i[K''] \tag{3.39}$$

3.3.3 Modal Strain Energy Approach

The concept of modal strain energy approach was formulated from the damping energy and the elastic strain energy of the damped structures. The approach is essentially an extension of Raleigh's principle into the complex domain. An approximate solution for the loss factor, Eqn (3.36), can be calculated by approximating the complex eigenvector $[U_n]$ by the real vector $[U_n']$, which is calculated from purely elastic analysis, i.e., by suppressing the imaginary part of [K″]. It is under this major assumption that the modal loss factors of the damped structural system can be easily determined. Thus, this technique is valid only for systems with relatively small levels of damping where the mode shapes and frequencies of the damped and the undamped structure are similar. Assuming that modal loss factors are a function of the strain energy distributions in undamped eigenmodes (which implies relatively moderate material damping and ignores intermodal coupling effects), a modal loss factor can be defined for a given eigenmode of a damped system.

It was found that loss factor estimates based on weighted ratios of strain energies in the damped and undamped materials, with strain energy terms defined as functions of forced structural deflection shape, agreed with loss factors based on bandwidths of discrete resonant response peaks. This discovery made loss factor estimation possible for a wide range of modes exhibited by finite element idealizations of practical structures, where the stiffness matrix and the corresponding nodal displacements are real since only the real eigenvalue problem is solved. As a result, extensive applications of the modal strain energy numerical method can be easily used for damped structure analysis and particularly for concept evaluations and for design applications. This makes damping design analysis more accessible and economical since undamped eigenmode computation is much less difficult conceptually and much less expensive than the forced damped frequency response computation.

3.4 Numerical Examples

Vibration damping of simply supported sandwich beams is numerically studied. In this case, all boundary conditions are satisfied and the solution is analytical and may be expressed as:

$$\{U(x,t)\} = \sum_{n=0}^{\infty} \begin{Bmatrix} w_{1n}\sin\frac{n\pi x}{l} \\ w_{2n}\sin\frac{n\pi x}{l} \\ u_{1n}\cos\frac{n\pi x}{l} \\ u_{2n}\cos\frac{n\pi x}{l} \\ \psi_n \sin\frac{n\pi x}{l} \end{Bmatrix} e^{i\omega t} \tag{3.40}$$

where w_{1n}, w_{2n}, u_{1n}, u_{2n}, ψ_n are the amplitude coefficients and n is the wave number.

To examine the effects of viscoelastic interfacial bonding, parametric studies are carried out for the variations of non-dimensional resonant frequency and loss factor of the beam system. The effect of the storage shear modulus of the interface layer for a simply supported symmetrical beam on the damping of sandwich structural system, η_s, is presented in Figure 3.3. It can be seen that the interface storage shear modulus (adhesive bonding stiffness) has a strong effect, up to a certain level, on the beam loss factor. Beyond this level, the usual assumption of perfect bonding used in classical theories is quite acceptable. This level to constitute "perfect" interface is given in terms of the ratio of the adhesive stiffness to the core stiffness. There may exist the difference of the level between the static response and dynamic response. On the other hand, there may exist an optimal value of interfacial shear modulus to achieve the maximum structural damping.

Figure 3.4 shows the effect of the loss factor of interface layer on the structural damping. It is shown that the damping of the interface generally enhances the structural damping.

In Figure 3.5, the effect of the core thickness on the system loss factor is examined. It demonstrates that increasing core thickness will generally enhance the sandwich system damping. The variation is also dependent upon the interface shear modulus.

In Figure 3.6, the non-dimensional square resonance frequency of the sandwich beam is plotted against the aspect ratio of the core. It can be seen that the resonance frequency decreases with increasing the core thickness, and the

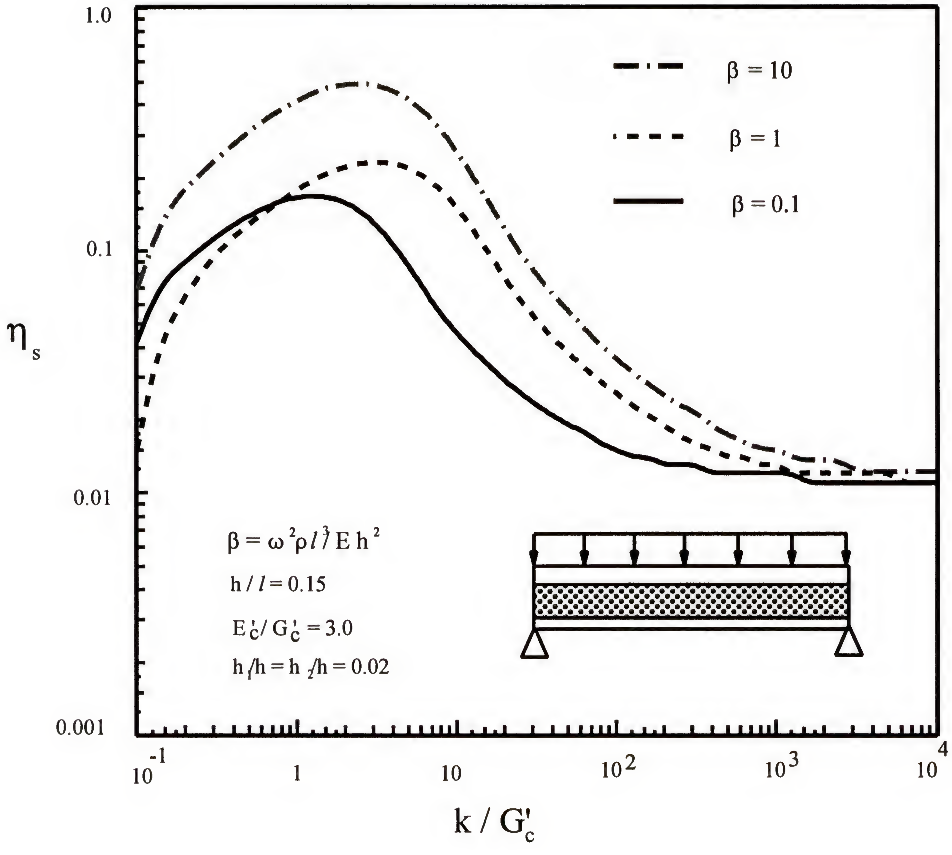

Figure 3.3 Effect of Storage Shear Modulus of Interface On Sandwich Beam Structural Loss Factors

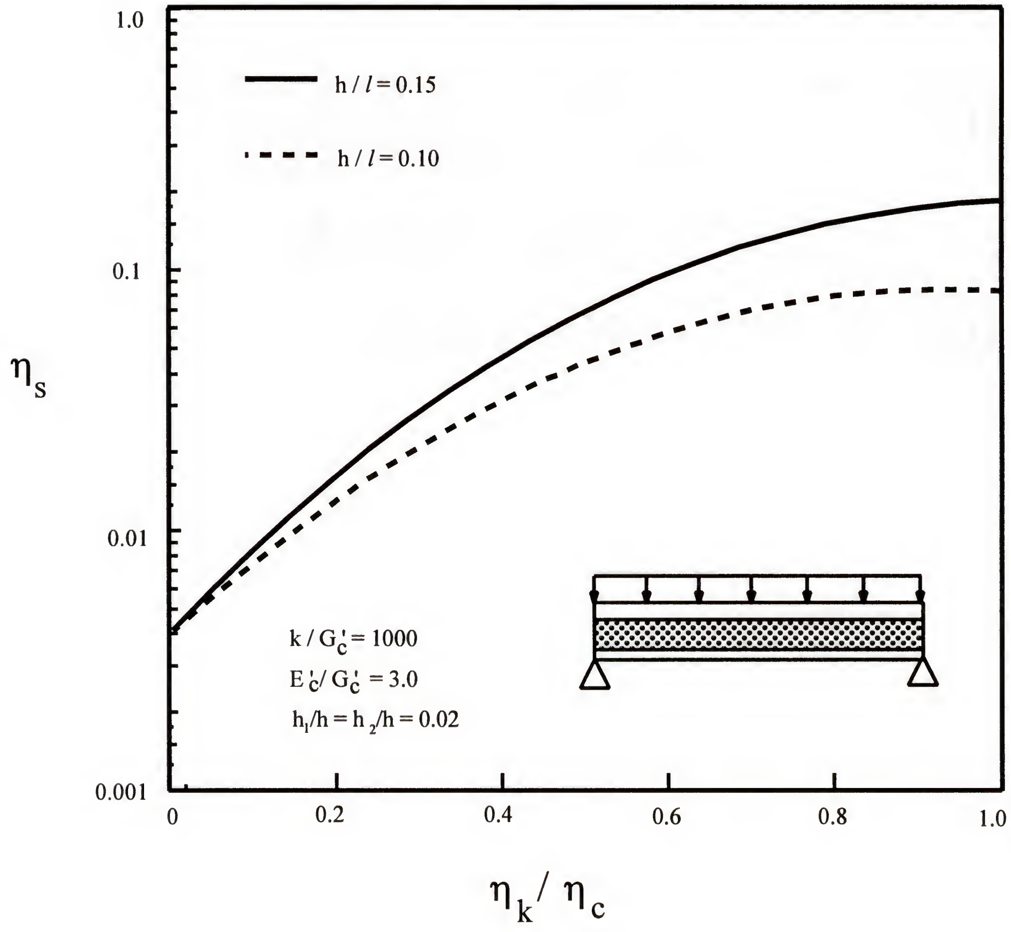

Figure 3.4 Effect of Loss Factor of Interface on Sandwich Beam Structural Loss Factors

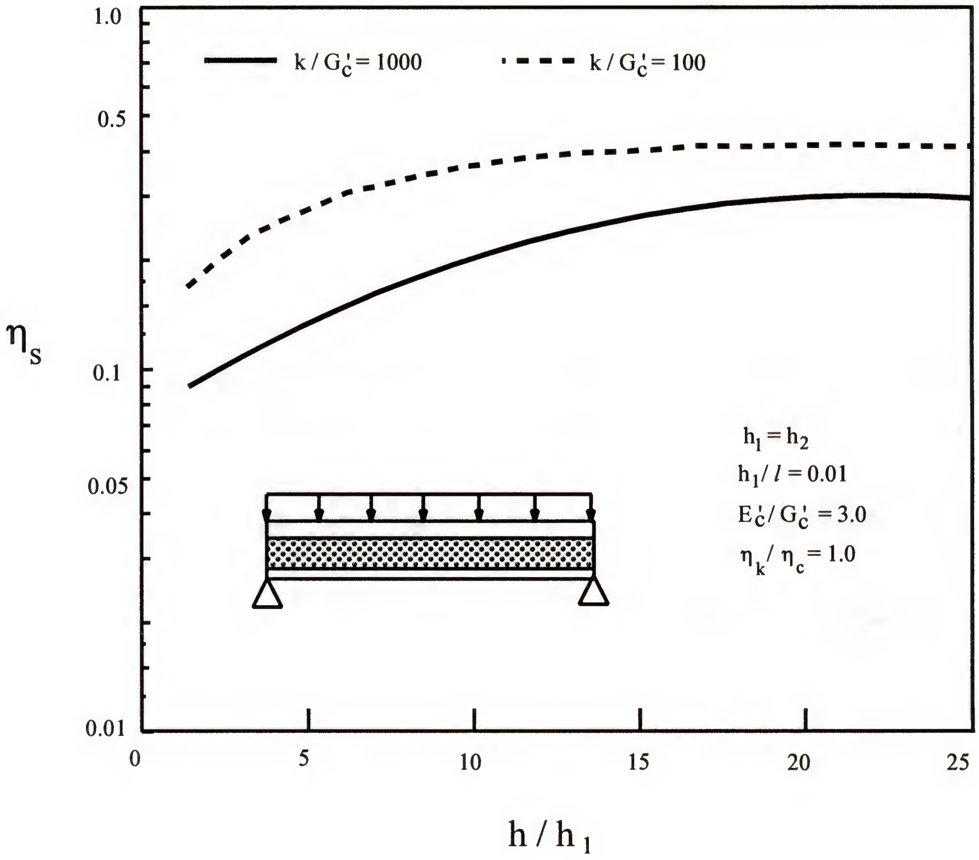

Figure 3.5 Effect of Core Thickness on Sandwich Beam Structural Loss Factors

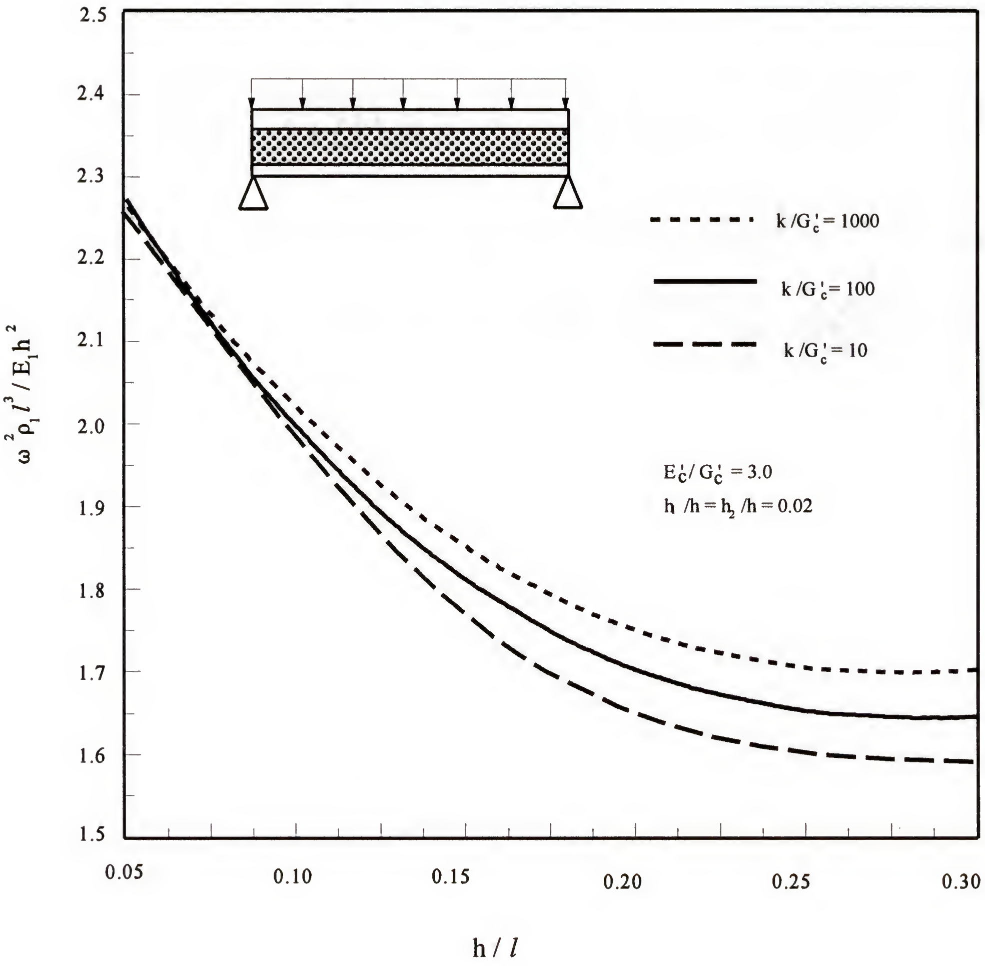

Figure 3.6 Effect of Interface Shear Modulus on First Resonance Frequency

storage shear modulus of the interface layer also has some effects on the resonance frequencies.

It should be mentioned that as damping (loss factor) of the structure is increased, the stiffness of the structure, in general, will be decreased. Therefore, by only improving damping will not reduce the dynamic responses such as displacements, stresses and noise level of the structure. It is a trade-off situation between damping and stiffness. The sandwich dynamic stiffness is observed to increase with increasing the storage modulus of the interface in Figure 3.7. There is also a certain value of the interface modulus to keep the sandwich stiffness close to the "perfect bonding" value. Generally, a proper value of interface shear modulus for the trade-off between enhancement in damping and decrease in stiffness can be obtained in most situations.

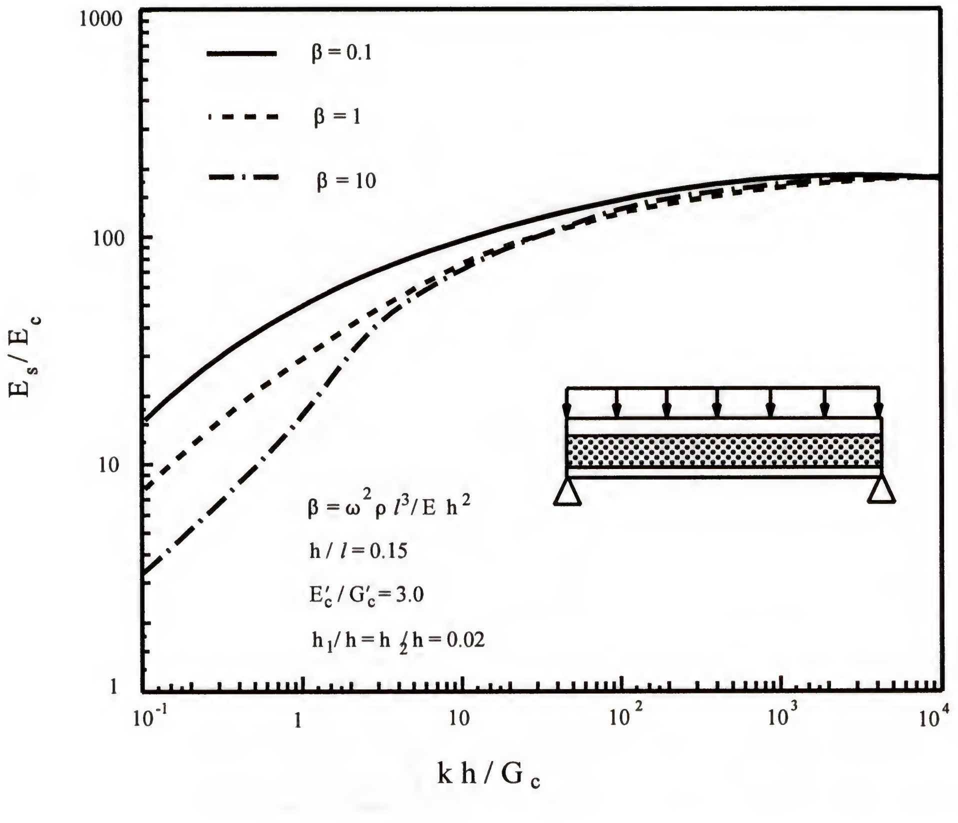

Figure 3.7 Effect of Storage Shear Modulus of Interface on Sandwich Beam Structural Stiffness

CHAPTER 4
A REFINED VIBRATION THEORY OF SANDWICH PLATES

In this chapter, the refined vibration theory of sandwich beams is extended to the sandwich plate theory. By means of variational methods, the basic equations of vibratory bending of sandwich plates with laminated faces and orthotropic core are developed. Taken into consideration are the effects of flexural and membrane energies in the faces, transverse shear and normal strain energies in the core, and rotatory, translator and transverse inertias in both core and faces. These effects are found to be of importance only at very high frequencies for homogeneous beams and plates. These effects are, however, of considerable importance at the lower frequencies for the case of sandwich beams and plates.

4.1 Basic Formulations

Consider a sandwich plate with anisotropic composite laminate faces and an orthotropic honeycomb or an isotropic foam core. The geometry of the sandwich plate considered is shown in Figure 4.1. The thickness of the core is much larger than that of the face, and the transverse modulus of the core normal to the plate is much lower than that of the face. The flexible core is linearly viscoelastic with a Young's modulus E_z in the z direction and a shear modulus of

G_{xz} and G_{yz} where E_z, G_{xz} and G_{yz} are expressed in terms of complex numbers under the harmonic excitation.

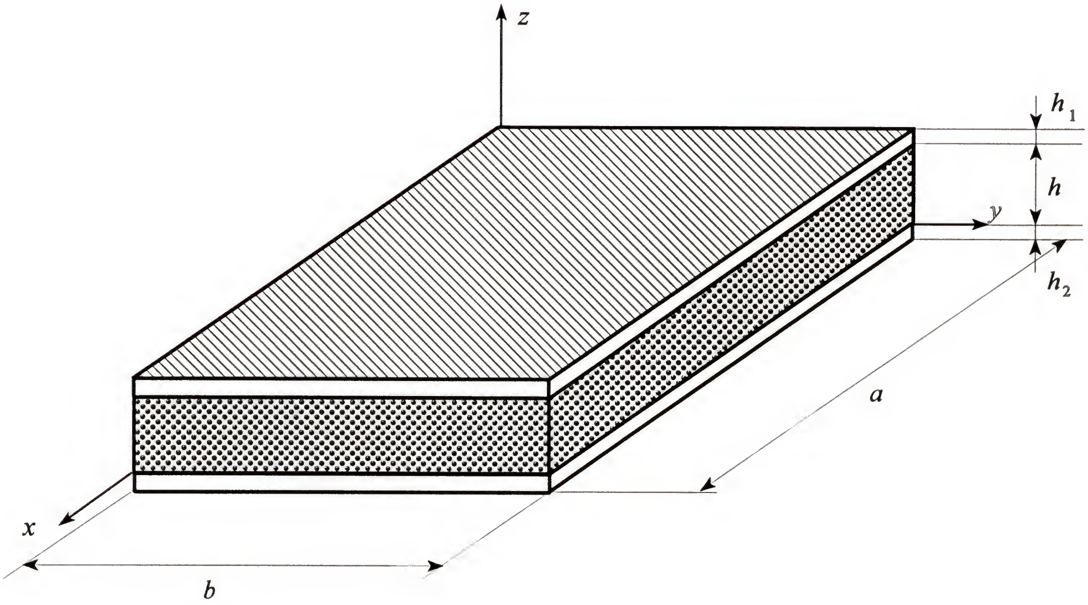

Figure 4.1 Geometry of a Sandwich Plate

In order to determine the response of a sandwich plate due to harmonic excitation, the assumptions are identical to those for sandwich beams, as given in sections 2.1 and 3.1. The classical laminate plate theory is used to deal with the face sheets as the displacement assumption gives in the following.

For the top face layer:

$$\begin{aligned} u^{t}(x,y,z,t) &= u_1(x,y,t) - z_1 \frac{\partial w_1(x,y,t)}{\partial x} \\ v^{t}(x,y,z,t) &= v_1(x,y,t) - z_1 \frac{\partial w_1(x,y,t)}{\partial y} \\ w^{t}(x,y,z,t) &= w_1(x,y,t) \end{aligned} \tag{4.1}$$

For the bottom face layer:

$$\begin{aligned} u^{b}(x,y,z,t) &= u_2(x,y,t) - z_2 \frac{\partial w_2(x,y,t)}{\partial x} \\ v^{b}(x,y,z,t) &= v_2(x,y,t) - z_2 \frac{\partial w_2(x,y,t)}{\partial y} \\ w^{b}(x,y,z,t) &= w_2(x,y,t) \end{aligned} \tag{4.2}$$

where $z_1 = z - h - h_1/2$, $z_2 = z + h_2/2$ are measured from the centroid of the faces respectively, as shown in Figure 4.1. The similar displacement field for the core is assumed as follows:

$$\begin{aligned} u^{c}(x,y,z,t) = u_0 + z\left(c_1 \psi - \frac{\partial w_0}{\partial x} \right) - \frac{z^2}{2}\frac{\partial \phi}{\partial x} \\ + \frac{z^3}{6}\frac{\partial}{\partial x}\left(\frac{\partial \psi}{\partial x} + \frac{\partial \zeta}{\partial y} \right) \end{aligned} \tag{4.3}$$

$$v^{c}(x,y,z,t) = v_0 + z\left(c_2 \zeta - \frac{\partial w_0}{\partial y} \right) - \frac{z^2}{2}\frac{\partial \phi}{\partial y} + \frac{z^3}{6}\frac{\partial}{\partial y}\left(\frac{\partial \psi}{\partial x} + \frac{\partial \zeta}{\partial y} \right) \tag{4.4}$$

$$w^{c}(x,y,z,t) = w_0 + z\,\phi - \frac{z^2}{2}\left(\frac{\partial \psi}{\partial x} + \frac{\partial \zeta}{\partial y} \right) \tag{4.5}$$

where $c_1 = E_z/G_{xz}$ and $c_2 = E_z/G_{yz}$, u_0, v_0, w_0, ψ, ζ and ϕ are functions of x, y and t.

The kinematic relations assuming small linear deformations, take the following form:

$$\varepsilon_x^{j} = \frac{\partial u_k}{\partial x} - z_k \frac{\partial^2 w_k}{\partial x^2} \tag{4.6}$$

$$\varepsilon_y^{j} = \frac{\partial u_k}{\partial x} - z_k \frac{\partial^2 w_k}{\partial x^2} \tag{4.7}$$

$$\gamma_{xy}^{j} = \frac{\partial u_k}{\partial y} + \frac{\partial v_k}{\partial x} - 2 z_k \frac{\partial^2 w_k}{\partial x \partial y} \tag{4.8}$$

where $j = t,\ b$ correspond to $k = 1,\ 2$ respectively.

The kinematic relation for the core is:

$$\gamma_{xz}^{c} = c_1\, \psi(x,y,t)$$

$$\gamma_{yz}^{c} = c_2\, \psi(x,y,t) \tag{4.9}$$

$$\varepsilon_{z}^{c} = \phi(x,y,t) - z\left(\frac{\partial\psi(x,y,t)}{\partial x} + \frac{\partial\zeta(x,y,t)}{\partial y} \right)$$

The compatibility conditions of deformation that the face-core interface shear strain is proportional to the face-core interface shear stress and the continuity conditions may be written in the following:

At the upper interface ($z = h$)

$$\tau_{xz1}^{i} = k^{i}(u^{t} - u^{c})$$

$$\tau_{yz1}^{i} = k^{i}(v^{t} - v^{c}) \tag{4.10}$$

$$w^{c} = w^{t}$$

At the bottom interface ($z = 0$)

$$\tau_{xz2}^{i} = k^{i}(u^{c} - u^{b})$$

$$\tau_{yz2}^{i} = k^{i}(v^{c} - v^{b}) \tag{4.11}$$

$$w^{c} = w^{b}$$

where τ_{xz1}^{i}, τ_{yz1}^{i}, τ_{xz2}^{i} and τ_{yz2}^{i} are the shear stresses at the upper and lower interface layers respectively, and $k^{i} = k(\omega)(1+i\eta_{k}(\omega))$ is the frequency-dependent complex shear modulus of interface layers.

The constitutive relations for the laminated face layers are derived by considering force and moment resultants at the top and bottom faces separately:

$$\left\{N_x^j,\ N_y^j,\ N_{xy}^j,\ M_x^j,\ M_y^j,\ M_{xy}^j\right\} = \int_{-\frac{h_k}{2}}^{\frac{h_k}{2}} \left\{\sigma_x^j,\ \sigma_y^j,\ \tau_{xy}^j,\ \sigma_x^j z_k,\ \sigma_y^j z_k,\ \tau_{xy}^j z_k\right\} dz_k \tag{4.12}$$

where again $j = t, b$ correspond to $k = 1, 2$ respectively. Based on stress-strain relation of plane stress state with respect to the laminate axes oriented at an angle with respect to the ply orthotropic axes in the plane of the laminate

$$\begin{Bmatrix} \sigma_x^j \\ \sigma_y^j \\ \tau_{xy}^j \end{Bmatrix} = \begin{bmatrix} \bar{C}_{11}^j & \bar{C}_{12}^j & \bar{C}_{13}^j \\ & \bar{C}_{22}^j & \bar{C}_{23}^j \\ \text{sym.} & & \bar{C}_{33}^j \end{bmatrix} \begin{Bmatrix} \varepsilon_x^j \\ \varepsilon_y^j \\ \gamma_{xy}^j \end{Bmatrix} \quad (j = t, b) \tag{4.13}$$

the constitutive equations for the face laminates will then be of the form

$$\begin{Bmatrix} N_x^j \\ N_y^j \\ N_{xy}^j \\ M_x^j \\ M_y^j \\ M_{xy}^j \end{Bmatrix} = \begin{bmatrix} A_{11}^j & A_{12}^j & A_{16}^j & B_{11}^j & B_{12}^j & B_{16}^j \\ & A_{22}^j & A_{26}^j & B_{12}^j & B_{22}^j & B_{26}^j \\ & & A_{66}^j & B_{16}^j & B_{26}^j & B_{66}^j \\ & & & D_{11}^j & D_{12}^j & D_{16}^j \\ & & \text{sym.} & & D_{22}^j & D_{26}^j \\ & & & & & D_{66}^j \end{bmatrix} \begin{Bmatrix} \varepsilon_x^j \\ \varepsilon_y^j \\ \gamma_{xy}^j \\ \kappa_x^j \\ \kappa_y^j \\ \kappa_{xy}^j \end{Bmatrix} \quad (j = t, b) \tag{4.14}$$

where the A, B, D matrices can be written as

$$A_{mn}^{j} = \int_{z_k - h_k/2}^{z_k + h_k/2} \bar{C}_{mn}^{j}\, dz_k \qquad (m,n = 1,2,3)$$

$$B_{mn}^{j} = \int_{z_k - h_k/2}^{z_k + h_k/2} \bar{C}_{mn}^{j} z_k\, dz_k \qquad (m,n = 1,2,3) \tag{4.15}$$

$$D_{mn}^{j} = \int_{z_k - h_k/2}^{z_k + h_k/2} \bar{C}_{mn}^{j} z_k^2\, dz_k \qquad (m,n = 1,2,3)$$

and κ_x, κ_y and κ_{xy} are the curvatures of middle surfaces of face layers which can be written as

$$\kappa_x^j = -\frac{\partial^2 w_k}{\partial x^2}$$

$$\kappa_y^j = -\frac{\partial^2 w_k}{\partial y^2} \tag{4.16}$$

$$\kappa_{xy}^j = -2\frac{\partial^2 w_k}{\partial x \partial y}$$

where $j = t, b$ correspond to $k = 1, 2$ respectively.

The stress-strain relations for the core are

$$\sigma_z^c = E_z^c \varepsilon_z^c$$

$$\tau_{xz}^c = G_{xz}^c \gamma_{xz}^c \tag{4.17}$$

$$\tau_{yz}^c = G_{yz}^c \gamma_{xz}^c$$

Using above kinematic relations and constitutive equations, we can eliminate u_0, v_0, w_0 and ϕ from the compatibility equations (Eqns (4.10) and (4.11)) and obtain two independent compatibility equations in the following:

$$\begin{aligned} & u_1 - u_2 + \frac{h_1 + h}{2}\frac{\partial w_1}{\partial x} + \frac{h_2 + h}{2}\frac{\partial w_2}{\partial x} \\ & - \left(2\frac{G_{xz}}{k^i} + h\right) c_1 \psi + \frac{h^3}{12}\frac{\partial}{\partial x}\left(\frac{\partial \psi}{\partial x} + \frac{\partial \zeta}{\partial y}\right) = 0 \end{aligned} \tag{4.18}$$

$$\begin{aligned} & v_1 - v_2 + \frac{h_1 + h}{2}\frac{\partial w_1}{\partial y} + \frac{h_2 + h}{2}\frac{\partial w_2}{\partial y} \\ & - \left(2\frac{G_{yz}}{k^i} + h\right) c_2 \zeta + \frac{h^3}{12}\frac{\partial}{\partial y}\left(\frac{\partial \psi}{\partial x} + \frac{\partial \zeta}{\partial y}\right) = 0 \end{aligned} \tag{4.19}$$

Correspondingly, two Lagrange multipliers λ_x, λ_y with two interfacial effect terms φ_x, φ_y are introduced into the total potential energy equation. The physical meaning of Lagrange multipliers λ_x, λ_y are the face-core interface shear forces in the x, y directions, and φ_x, φ_y can be regarded as the strain energy contribution of the adhesive layer to the total potential energy.

4.2 Equations of Motion

The equations of motion and corresponding boundary conditions can be also derived by using the Hamilton's principle. The total kinetic energy of the sandwich plate can be expressed as in terms of eight basic functions, u_1, u_2, v_1, v_2, w_1, w_2, ψ and ς as follows:

$$T = \frac{1}{2}\int_0^l \left\{ \rho_1 h_1 [(\dot{u}_1)^2 + (\dot{v}_1)^2 + \frac{h_1^2}{12}(\frac{\partial \dot{w}_1}{\partial x})^2 + \frac{h_1^2}{12}(\frac{\partial \dot{w}_1}{\partial y})^2 + (\dot{w}_1)^2] \right.$$

$$+ \rho_2 h_2 [(\dot{u}_2)^2 + (\dot{v}_2)^2 + \frac{h_2^2}{12}(\frac{\partial \dot{w}_2}{\partial x})^2 + \frac{h_2^2}{12}(\frac{\partial \dot{w}_2}{\partial y})^2 + (\dot{w}_2)^2]$$

$$\left. + \int_{-\frac{h}{2}}^{\frac{h}{2}} \rho [(\dot{u}^c)^2 + (\dot{v}^c)^2 + (\dot{w}^c)^2] dz \right\} dx \tag{4.20}$$

where ρ_1, ρ_2 and ρ are the density of the upper face, lower face and the core, respectively, $(\dot{})$ denotes a first derivative with respect to time and $u_c(x,y,z,t)$, $v_c(x,y,z,t)$, $w_c(x,y,z,t)$ are

$$u^c = u_2 + \frac{c_1 G_{xz}}{k^i}\psi - \frac{h_2}{2}\frac{\partial w_2}{\partial x} + z\left(c_1 \psi - \frac{\partial w_2}{\partial x}\right)$$

$$- \frac{z^2}{2}\left[\frac{1}{h}\left(\frac{\partial w_1}{\partial x} - \frac{\partial w_2}{\partial x}\right) + \frac{h}{2}\frac{\partial}{\partial x}\left(\frac{\partial \psi}{\partial x} + \frac{\partial \zeta}{\partial x}\right)\right] \tag{4.21}$$

$$+ \frac{z^3}{6}\frac{\partial}{\partial x}\left(\frac{\partial \psi}{\partial x} + \frac{\partial \zeta}{\partial y}\right)$$

$$v^c = v_2 + \frac{c_2 G_{yz}}{k^i}\zeta - \frac{h_2}{2}\frac{\partial w_2}{\partial y} + z\left(c_2\zeta - \frac{\partial w_2}{\partial y}\right)$$

$$- \frac{z^2}{2}\left[\frac{1}{h}\left(\frac{\partial w_1}{\partial y} - \frac{\partial w_2}{\partial y}\right) + \frac{h}{2}\frac{\partial}{\partial y}\left(\frac{\partial \psi}{\partial x} + \frac{\partial \zeta}{\partial x}\right)\right] \qquad (4.22)$$

$$+ \frac{z^3}{6}\frac{\partial}{\partial y}\left(\frac{\partial \psi}{\partial x} + \frac{\partial \zeta}{\partial y}\right)$$

$$w_c = w_2 + z\left[\frac{w_1 - w_2}{h} + \frac{h}{2}\left(\frac{\partial \psi}{\partial x} + \frac{\partial \zeta}{\partial y}\right)\right] - \frac{z^2}{2}\left(\frac{\partial \psi}{\partial x} + \frac{\partial \zeta}{\partial y}\right) \qquad (4.23)$$

The total potential energy, U, consists of the contributions from both face layers U_1 and U_2, core shear strain U_3, core normal U_4, the external potential term V due to applied loading and the effects of nonrigid adhesive interface layers, φ_x and φ_y

$$U = U_1 + U_2 + U_3 + U_4 + V + \varphi_x + \varphi_y \qquad (4.24)$$

For simplicity, we consider symmetric laminated face layers where $\mathrm{A}^j_{16} = \mathrm{A}^j_{26} = 0$, $\mathrm{B}^j_{m\,n} = 0$ and $\mathrm{D}^j_{16} = \mathrm{D}^j_{26} = 0$ (j = 1, 2; $m = n$ = 1, 2, 6) in Eqn (4.14). The face strain energy contributions then are

$$U_k = \frac{1}{2}\int_0^a\int_0^b \left[A_{11}^j\left(\frac{\partial u_1}{\partial x}\right)^2 + 2A_{12}^j\frac{\partial U_k}{\partial x}\frac{\partial v_k}{\partial y} + A_{22}^j\left(\frac{\partial v_k}{\partial y}\right)^2 \right.$$

$$+ A_{66}^j\left(\frac{\partial u_k}{\partial y} + \frac{\partial v_k}{\partial x}\right) + D_{11}^j\left(\frac{\partial^2 w_k}{\partial x^2}\right)^2 + 2D_{12}^j\frac{\partial^2 w_k}{\partial x^2}\frac{\partial^2 w_k}{\partial y^2} \tag{4.25}$$

$$\left. + D_{22}^j\left(\frac{\partial^2 w_k}{\partial y^2}\right)^2 + 4D_{66}^j\left(\frac{\partial^2 w_k}{\partial x \partial y}\right)^2 \right] dx\, dy$$

in which $j = t,\ b$ when $k = 1,\ 2$. The shear strain contribution of the core is

$$U_3 = \frac{1}{2}\int_0^l h\left[G_{xz}^c(c_1\psi)^2 + G_{yz}^c(c_2\zeta)^2\right]dx \tag{4.26}$$

The transverse normal strain contribution of the core is

$$U_4 = \frac{1}{2}\int_0^a\int_0^b E_c\left[\frac{(w_1 - w_2)^2}{h} + \frac{h^3}{12}\left(\frac{\partial\psi}{\partial x} + \frac{\partial\zeta}{\partial y}\right)^2\right]dx\, dy \tag{4.27}$$

The contribution of face-core compatibilities are,

$$\varphi_x = \lambda_x\int_0^a\int_0^b \left[u_1 - u_2 + \frac{h_1 + h}{2}\frac{\partial w_1}{\partial x} + \frac{h_2 + h}{2}\frac{\partial w_2}{\partial x} \right.$$

$$\left. - \left(2\frac{G_{xz}}{k^i} + h\right)c_1\psi + \frac{h^3}{12}\frac{\partial}{\partial x}\left(\frac{\partial\psi}{\partial x} + \frac{\partial\zeta}{\partial y}\right)\right]dx\, dy \tag{4.28}$$

$$\varphi_y = \lambda_y \int_0^a \int_0^b \left[v_1 - v_2 + \frac{h_1 + h}{2}\frac{\partial w_1}{\partial y} + \frac{h_2 + h}{2}\frac{\partial w_2}{\partial y} \right.$$
$$\left. - \left(2\frac{G_{yz}}{k^i} + h \right) c_2 \zeta + \frac{h^3}{12}\frac{\partial}{\partial y}\left(\frac{\partial \psi}{\partial x} + \frac{\partial \zeta}{\partial y} \right) \right] dx\,dy \tag{4.29}$$

The work done by the external force is

$$V = \int_0^a \int_0^b q\, w_1 \, dxdy \tag{4.30}$$

where $q = q(x,t)$ is transverse distributed dynamic loading at the surface of top face layer.

Taking variation in the Hamilton's equation with respect to u_1, u_2, v_1, v_2, w_1, w_2, ψ, ς, λ_x and λ_y, ten equations of motion and boundary conditions are obtained after integration by parts in x and t, and some algebraic manipulations and substitutions. It is noted that homogeneous conditions for the displacement and the velocity at $t = t_1$, t_2 are assumed. The number of governing equations is reduced from ten to eight by eliminating the λ_x and λ_y. The governing equations can be written in the matrix form:

$$[\partial M]\{\ddot{U}\} + [\partial K]\{U\} = \{F\} \tag{4.31}$$

where

$\{U\} = \{w_1, w_2, u_1, u_2, v_1, v_2, \psi, \varsigma\}^T$

$\{F\} = \{q, 0, 0, 0, 0, 0, 0, 0\}^T$

[∂M] — the mass matrix differential operator

[∂K] — the stiffness matrix differential operator

It is noted that [∂K], {$\ddot{U}$} and {U} are complex valued.

The boundary conditions at the end of the beam can be obtained in a similar way to the beam theory. Hereby only a type of simply supported boundary conditions are given in the following,

at the top face layer, $x = 0$ and $x = a$:

$$N_x^t = v_1 = M_x^t = w_1 = 0 \tag{4.32}$$

$y = 0$ and $y = b$:

$$N_y^t = u_1 = M_y^t = w_1 = 0 \tag{4.33}$$

at the bottom face layer, $x = 0$ and $x = a$:

$$u_2 = N_{xy}^b = M_x^b = w_2 = 0 \tag{4.34}$$

$y = 0$ and $y = b$:

$$v_2 = N_{xy} = M_y^b = w_2 = 0 \tag{4.35}$$

at the core, $x = 0$ and $x = a$:

$$\psi = 0 \quad (\tau_{xz}^c = 0) \tag{4.36}$$

$y = 0$ and $y = b$:

$$\zeta = 0 \quad (\tau_{yz}^c = 0) \tag{4.37}$$

4.3 Solution and Discussion

The solution for a sandwich plate with simply-supported boundary conditions can be assumed as

$$\{U(x,t)\} = \sum_{n=0}^{\infty}\sum_{m=0}^{\infty}\left\{\begin{matrix} w_{1nm}\sin\dfrac{n\pi x}{a}\sin\dfrac{m\pi y}{b} \\ w_{2nm}\sin\dfrac{n\pi x}{a}\sin\dfrac{m\pi y}{b} \\ u_{1nm}\cos\dfrac{n\pi x}{a}\sin\dfrac{m\pi y}{b} \\ u_{2nm}\sin\dfrac{n\pi x}{a}\cos\dfrac{m\pi y}{b} \\ v_{1nm}\sin\dfrac{n\pi x}{a}\cos\dfrac{m\pi y}{b} \\ v_{2nm}\cos\dfrac{n\pi x}{a}\sin\dfrac{m\pi y}{b} \\ \psi_{nm}\sin\dfrac{n\pi x}{a}\sin\dfrac{m\pi y}{b} \\ \zeta_{nm}\sin\dfrac{n\pi x}{a}\sin\dfrac{m\pi y}{b} \end{matrix}\right\} e^{i\omega t} \qquad (4.38)$$

where w_{1nm}, w_{2nm}, u_{1nm}, u_{2nm}, v_{1nm}, v_{2nm}, ψ_{nm} and ς_{nm} are the amplitude coefficients and n is the wave number. This solution fully satisfies the boundary conditions of a plate where faces are simply supported and the vertical deflection of the core through the height is prevented at four edges. The constants w_{1nm}, w_{2nm}, u_{1nm}, u_{2nm}, v_{1nm}, v_{2nm}, ψ_{nm} and ς_{nm} are determined by the solution of the eigenvalue problem.

As an example, a sandwich plate consisting of identical laminated top and bottom face layers with each [0/±45/90] lamination and isotropic core material.

The following material properties are used for the graphite/epoxy lamina,

E_1 = 181 Gpa, E_2 = 10.3 Gpa, G_{12} = 7.17 Gpa

$\nu_{12} = 0.28$, $\rho = 1.58\times10^{-3}$ N-s^2/m^4

The loss factor of the core and interface layer are assumed to be $\eta_c = 0.3$ and $\eta_k = 0.5$, respectively. The effective modulus of face layer is referred to as E_e.

The effect of interface shear modulus on plate structural damping is shown in Figure 4.2. The similar trend to the beam problem can be observed. For the fixed values of faces and core moduli, the interface with some small value of stiffness kh/G_c results in a considerable increase in system damping properties. This can be explained by the fact that the smaller value of k makes E_1/k larger, resulting into larger shear stress concentration and energy dissipation which causes enhancement in damping. Again, a trade-off between damping increase and stiffness decrease must be considered.

In determining the resonance frequency, it is observed that the mode corresponding to the lowest frequency is of predominantly flexural type, the corresponding values of all displacement ratios are small. There are other additional families of modes such as of predominantly extensional type and thickness shear type. In Table 4.1, the resonance frequencies of the predominantly flexural mode are given for comparison of the cases with inertia effects of all assumed displacements and with only transverse inertia effect. The non-dimensional resonance frequency is defined as

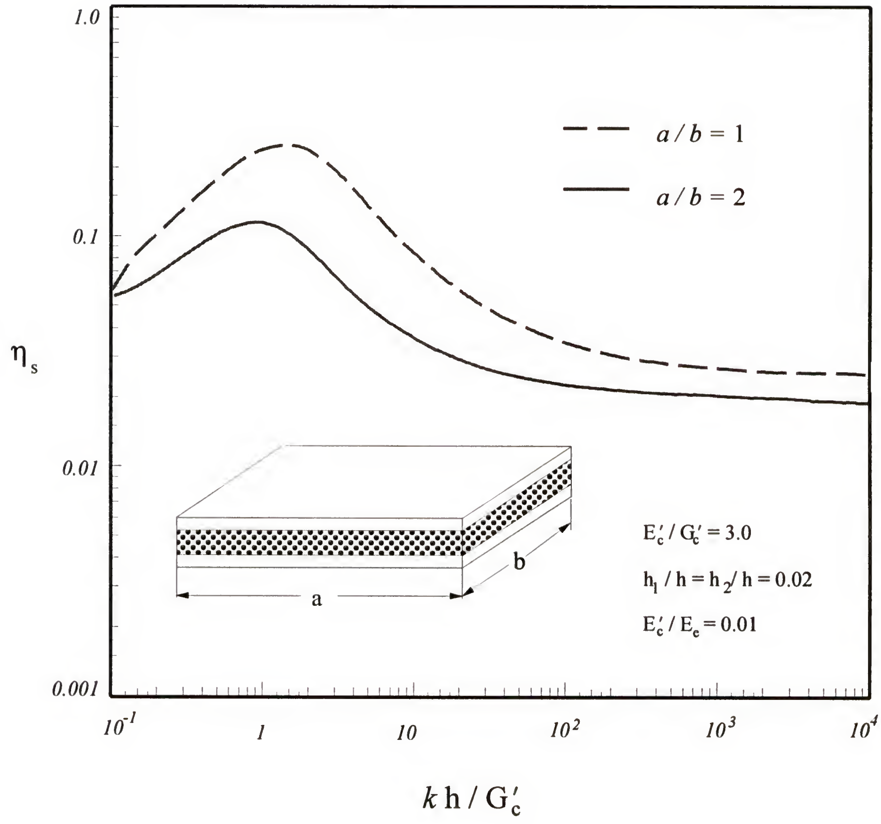

Figure 4.2 Effect of Storage Shear Modulus of Interface on Loss Factor of Sandwich Plate

$$\Omega = \omega h_1 \sqrt{\frac{\rho}{E_e}} \tag{4.39}$$

It can be seen that the transverse inertia effect is the most important effect on the resonance frequencies, and other inertia effects are negligible for this mode.

Table 4.1 Resonance Frequencies of Sandwich Plate

Modal number		Non-dimensional frequency $\Omega \times 10^3$ for predominantly flexural mode	
n	m	Transverse inertia terms	All inertia terms
1	1	1.251	1.248
1	3	11.37	11.31
2	5	69.76	69.59
5	5	145.19	144.91
3	6	232.64	232.14
3	8	294.44	293.67
$a = b$, $h/a = 0.15$, $h_1/h = h_2/h = 0.1$, $G_c'/E_c' = 0.4$, $E_c'/E_e = 0.01$ $\rho/\rho_1 = 0.2$, $kh/G_c' = 1000$.			

Figure 4.3 shows the variation of sandwich plate system loss factor with the ratio of core shear modulus to face effective modulus. It is found that the system loss factor of the lowest frequency first increases with core shear modulus and then decreases, depending on the different aspect ratio of the plate, h_1/a.

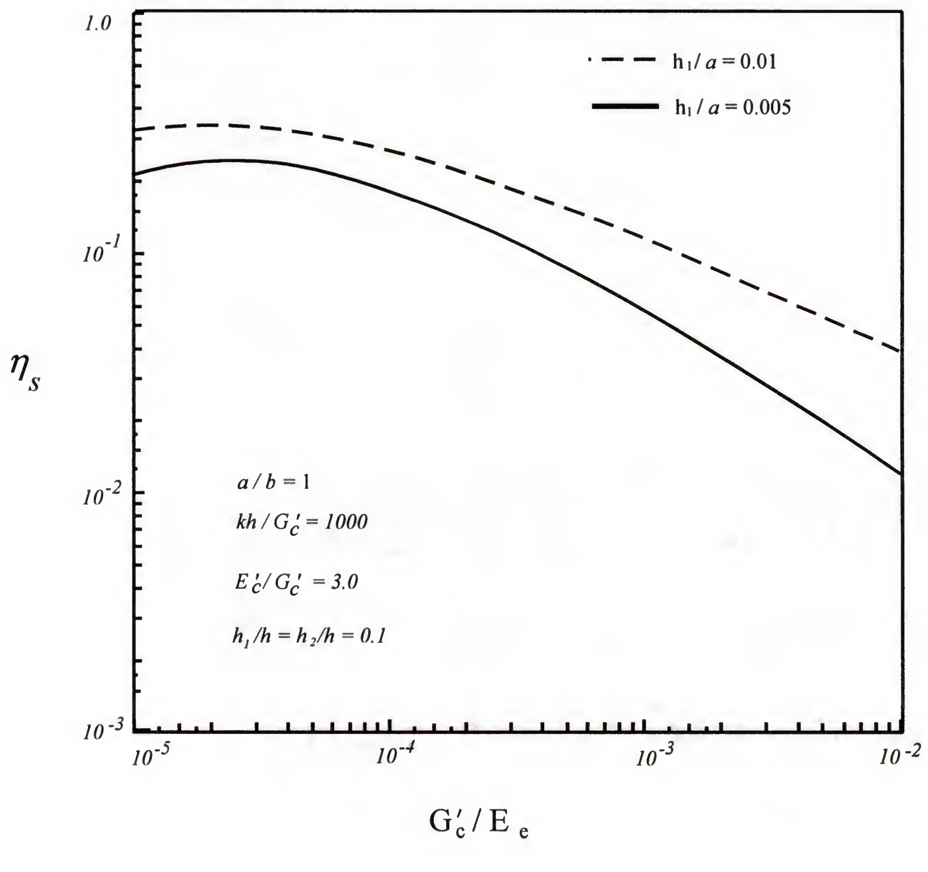

Figure 4.3 Effect of Core Shear Modulus on Loss Factors of Sandwich Plate

CHAPTER 5
VIBRATION OF DELAMINATED SANDWICH BEAM-PLATES

In the Interface model of sandwich beams discussed in Chapter 3, there are two extreme interface conditions, i.e., the case of perfect bond between the face and the core when the interface adhesive stiffness $k^* \rightarrow \infty$, and the case of delamination or interface crack when $k^* \rightarrow 0$. Delaminations are usually formed either due to imperfections in the fabrication processes or under various external conditions or loadings that may occur in the operational life of a composite structure. Delaminations will affect the strength, stiffness and integrity of the composite structure, and may thus cause the change of structural vibration response. In this chapter, a simple beam-plate model is developed for the investigation of the effect of delaminations on the vibration behavior of sandwich composites. The refined vibration theory of sandwich beams presented in Chapter 2 is employed for the analysis. The effects of delamination size and position in determining vibration characteristics are examined.

5.1 A Beam-Plate Model

Consider a typical construction of sandwich plates consisting of two faces, not necessarily identical, metallic or laminated symmetric composites, bonded to the core through interface layers. In modern sandwich structures, plastic foam and non-metallic honeycomb cores are replacing the metallic honeycomb ones, thus achieving weight reduction and flexibility in manufacturing process. In such cases the transverse flexibility of the core affects the overall behavior, the stresses and displacement fields. It is necessary to take this into account by using the refined vibration theory.

A sandwich plate containing an arbitrary located delamination (interface crack) lying between the upper face and the core is shown in Figure 5.1. In the case of a delamination at the lower interface the similar analysis should be used with minor modification. The plate has a constant width between two lateral edges and is subjected to transverse loading q and compressive in-plane force P. A beam-plate model assumes that the delamination extends over an interval $a \leq x \leq b$ and runs across the whole width of the plate as depicted in Figure 5.1. The delamination is assumed to exist before loading and not to grow under it. It is also assumed that the surfaces of delaminated faces and core are free of shear stresses (they may slip one with respect the other) but can accommodate vertical normal compressive stresses when contact between them exists.

For the purpose of analysis, the delaminated sandwich beam-plate has been divided into three spanwise regions as denoted by circle numbers in Figure 5.1, namely, a delamination region and two integral regions one on other side of the delamination region. The delamination region is itself made up of two separate component segment above and below the plane of the delamination, joined at their ends to the integral segments. The beam-plate as a whole are described by equations of motion, continuity requirements at the interface crack tips and boundary conditions at the ends. The governing equations of motion and corresponding boundary conditions for the regions 1 and 3 are the similar one presented in Chapter 2. For the delaminated region 2, the governing equations of motion and the continuity requirements are derived for two different deformation modes by using variational procedures.

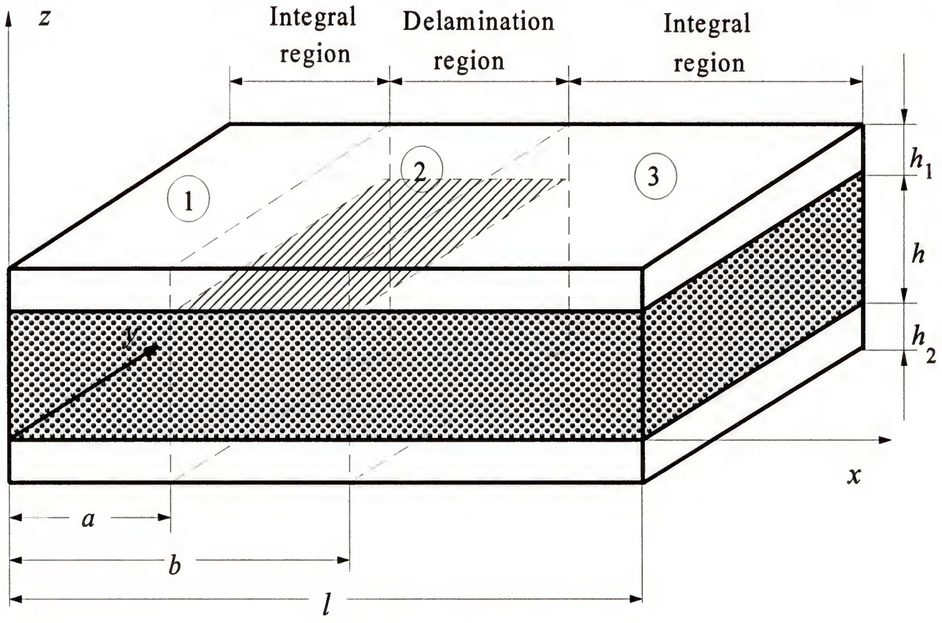

Figure 5.1 Delaminated Composite Sandwich

5.2 Deformation Mode Modeling

As mentioned in Section 1.2.3, there are two different modeling of vibration of the delaminated laminated beam-plate with respect to pre-buckled state and post-buckled state, respectively. Nonetheless, we could not find any research work on vibration analysis of sandwich beam-plate with delaminations. For a delaminated sandwich beam, we can model the delamination region in two different ways: contact or non-contact throughout the entire length of the delaminated region.

In the case of a delamination without contact at the face-core interface of delamination region, the surface are free of stresses any kind. The non-contact assumption implies that each delaminated segment, face or core, above and below the plane of the delamination is free to undergo transverse displacement as per the requirements of equilibrium. The collaboration between the two is a result of the continuity requirements at the ends of the region. The delaminated face and core are thus assumed to be "free" to have different transverse displacements, as shown in Figure 5.2. We refer to such a mode of deformation as the free mode. This mode may also be considered as the vibration relative to the post-buckling state, since there is an opening between the delaminated face and core, as depicted in Figure 5.2.

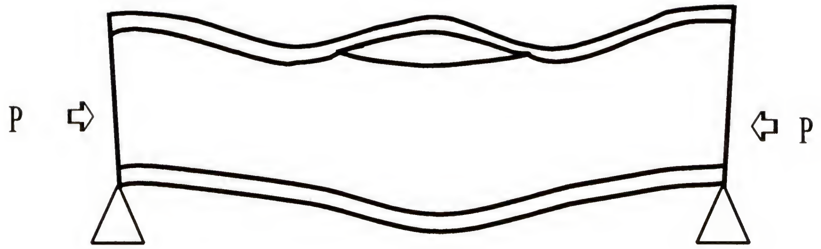

Figure 5.2 The Free Deformation Pattern

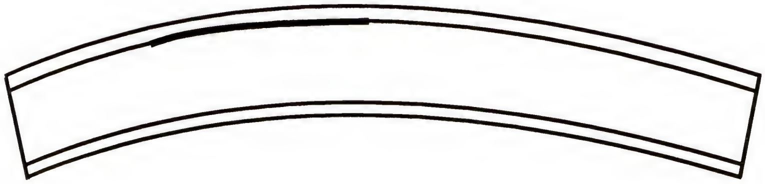

(a)

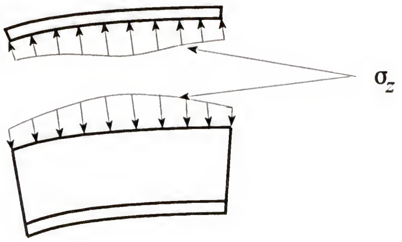

(b)

Figure 5.3 The Constrained Mode (a) Deformation Pattern
(b) Contact Stresses in the Delamination Region

If the vibration is considered relative to the unloaded referential state or pre-buckled state in which there is no opening at the crack interface, it seems necessary to impose the constraint of continuity condition of transverse displacement at the delaminated interface. The crack surfaces of the face and the core are assumed to be free to slide horizontally with respect to one another except at their ends, but remain contact in the thickness direction. Therefore, the delamination interface are subjected to vertical compressive stresses but are free of shear ones, i.e., the contact is assumed to be frictionless. Such a mode of deformation is referred to in this study as the constrained mode. In this model, the assumption of no natural gap between the delaminated face and core must be maintained. When there is a gap existing in the undeformed state, the problem of vibration of delaminated sandwich beams becomes, in general, quite complex and non-linear.

5.3 Analytical Formulation

For the two models of deformation modes, the governing equations of motion and the boundary conditions for the delaminated regions are derived using the Hamilton principle, similar to the procedure described in the Previous chapters. Our primary concern is the delamination with contact, i.e., the constrained mode model because this is a realistic model, whereas the limitation of the free mode model is discussed via some typical results.

5.3.1 The Free Mode Model

In the case of delamination without contact, the stress free conditions at the delaminated interface, i.e., the upper interface, requires

$$\begin{aligned} \sigma_z^c(x, z=h, t) &= 0 \\ \tau_z^c(x, z=h, t) &= 0 \end{aligned} \tag{5.1}$$

Recall the kinematic relations for the core, Eqn (2.6) in Chapter 2, resulting the following equations

$$\begin{aligned} \phi(x,t) &= 0 \\ \psi(x,t) &= 0 \end{aligned} \tag{5.2}$$

The compatibility conditions of deformation at the bounded face-core interface, i.e., the lower interface, yield the same equations as in Chapter 2, at $z = 0$

$$\begin{aligned} u^c &= u^t \\ w^c &= w^t \end{aligned} \tag{5.3}$$

which give the relations between the displacement functions as follows

$$\begin{aligned} w_0(x,t) &= w_2(x,t) \\ u_0(x,t) &= u_2(x,t) - \frac{h_2}{2}\frac{\partial w_2(x,t)}{\partial x} \end{aligned} \tag{5.4}$$

Now the independent displacement functions are $u_1(x,t)$, $w_1(x,t)$, $u_2(x,t)$ and $w_2(x,t)$. Using the Hamilton principle again, the governing equations can be derived via variational calculus. The total kinetic energy of the sandwich segment at the delamination region can be expressed in terms of four independent functions as follows

$$\begin{aligned} T = \frac{1}{2}\int_0^l \Bigg\{ & \rho_1 h_1\left[(\dot{u}_1)^2 + \frac{h_1^2}{12}\left(\frac{\partial \dot{w}_1}{\partial x}\right)^2 + (\dot{w}_1)^2\right] \\ & + \rho_2 h_2\left[(\dot{u}_2)^2 + \frac{h_2^2}{12}\left(\frac{\partial \dot{w}_2}{\partial x}\right)^2 + (\dot{w}_2)^2\right] \\ & + \rho h\left[(\dot{u}_2)^2 - (h + h_2)\dot{u}_2\frac{\partial \dot{w}_2}{\partial x} + \left(\frac{h^2}{3} + \frac{hh_2}{2} + \frac{h_2^2}{4}\right)\left(\frac{\partial \dot{w}_2}{\partial x}\right)^2\right]\Bigg\} dx \end{aligned} \tag{5.5}$$

The total potential energy, U, consisting of the contribution from both faces, and the external potential terms, can be written as

$$\begin{aligned} U = \int_0^l \Bigg\{ & \frac{1}{2}E_1 h_1\left[(\frac{\partial u_1}{\partial x})^2 + \frac{h_1^2}{12}(\frac{\partial^2 w_1}{\partial x^2})^2\right] \\ & \frac{1}{2}E_2 h_2\left[(\frac{\partial u_2}{\partial x})^2 + \frac{h_2^2}{12}(\frac{\partial^2 w_2}{\partial x^2})^2\right] \\ & - q w_1 - (P^t u^t - P^b u^b)\delta_d(x - x_j)\Bigg\} dx \end{aligned} \tag{5.6}$$

where $q = q(x,t)$ is transverse distributed dynamic loading at the surface of the top face layer, and P^t, P^b are longitudinal compressive forces applied at upper and lower faces, respectively.

Taking variation in the Hamilton's equation with respect to w_1, w_2, u_1 and u_2, four equations of motion and consistent boundary conditions are obtained after integration by parts in x and t, and some algebraic manipulations and substitutions. It is noted that homogeneous conditions for the displacement and the velocity at $t = t_1, t_2$ are assumed. The four governing equations can be written in the matrix form:

$$[\partial M]\{\ddot{U}\} + [\partial K]\{U\} = \{F\} \tag{5.7}$$

where

$\{U\} = \{w_1, w_2, u_1, u_2\}^T$

$\{F\} = \{q, 0, 0, 0\}^T$

$[\partial M]$ — the mass matrix differential operators

$[\partial K]$ — the stiffness matrix differential operators

The continuity requirements, at the end of the delamination region, $x=a$ or $x=b$, (see Figure 5.1), consist of six geometrical conditions and six natural conditions.

For the upper face layer, we have

$$\begin{aligned} u_1^{(1)}(x=a,t) &= u_1^{(2)}(x=a,t) \\ u_1^{(2)}(x=b,t) &= u_1^{(3)}(x=b,t) \end{aligned} \tag{5.8}$$

$$\begin{aligned} w_1^{(1)}(x=a,t) &= w_1^{(2)}(x=a,t) \\ w_1^{(2)}(x=b,t) &= w_1^{(3)}(x=b,t) \end{aligned} \tag{5.9}$$

$$\begin{aligned} \frac{\partial w_1^{(1)}(x=a,t)}{\partial x} &= \frac{\partial w_1^{(2)}(x=a,t)}{\partial x} \\ \frac{\partial w_1^{(2)}(x=b,t)}{\partial x} &= \frac{\partial w_1^{(3)}(x=b,t)}{\partial x} \end{aligned} \tag{5.10}$$

$$\begin{aligned} N_x^{t^{(1)}}(x=a,t) &= N_x^{t^{(2)}}(x=a,t) \\ N_x^{t^{(2)}}(x=b,t) &= N_x^{t^{(3)}}(x=b,t) \end{aligned} \tag{5.11}$$

$$\begin{aligned} M_x^{t^{(1)}}(x=a,t) &= M_x^{t^{(2)}}(x=a,t) \\ M_x^{t^{(2)}}(x=b,t) &= M_x^{t^{(3)}}(x=b,t) \end{aligned} \tag{5.12}$$

$$\begin{aligned} \frac{\partial M_x^{t^{(1)}}(x=a,t)}{\partial x} &= \frac{\partial M_x^{t^{(2)}}(x=a,t)}{\partial x} \\ \frac{\partial M_x^{t^{(2)}}(x=b,t)}{\partial x} &= \frac{\partial M_x^{t^{(3)}}(x=b,t)}{\partial x} \end{aligned} \tag{5.13}$$

where the superscripts (1), (2) and (3) represent three regions. It is noted that in the shear force balance conditions at the delamination front, Eqn (5.13), the inertia effects are neglected.

For the lower face layer, we have the similar continuity conditions,

$$
\begin{aligned}
u_2^{(1)}(x=a,t) &= u_2^{(2)}(x=a,t) \\
u_2^{(2)}(x=b,t) &= u_2^{(3)}(x=b,t)
\end{aligned}
\qquad (5.14)
$$

$$
\begin{aligned}
w_2^{(1)}(x=a,t) &= w_2^{(2)}(x=a,t) \\
w_2^{(2)}(x=b,t) &= w_2^{(3)}(x=b,t)
\end{aligned}
\qquad (5.15)
$$

$$
\begin{aligned}
\frac{\partial w_2^{(1)}(x=a,t)}{\partial x} &= \frac{\partial w_2^{(2)}(x=a,t)}{\partial x} \\
\frac{\partial w_2^{(2)}(x=b,t)}{\partial x} &= \frac{\partial w_2^{(3)}(x=b,t)}{\partial x}
\end{aligned}
\qquad (5.16)
$$

$$
\begin{aligned}
N_x^{b^{(1)}}(x=a,t) &= N_x^{b^{(2)}}(x=a,t) \\
N_x^{b^{(2)}}(x=b,t) &= N_x^{b^{(3)}}(x=b,t)
\end{aligned}
\qquad (5.17)
$$

$$
\begin{aligned}
M_x^{b^{(1)}}(x=a,t) &= M_x^{b^{(2)}}(x=a,t) \\
M_x^{b^{(2)}}(x=b,t) &= M_x^{b^{(3)}}(x=b,t)
\end{aligned}
\qquad (5.18)
$$

$$
\begin{aligned}
\frac{\partial M_x^{b^{(1)}}(x=a,t)}{\partial x} &= \frac{\partial M_x^{b^{(2)}}(x=a,t)}{\partial x} \\
\frac{\partial M_x^{b^{(2)}}(x=b,t)}{\partial x} &= \frac{\partial M_x^{b^{(3)}}(x=b,t)}{\partial x}
\end{aligned}
\qquad (5.19)
$$

where N_x^j and M_x^j ($j = t, b$) are the axial forces and the bending moments in the faces, respectively, and the superscripts (i), $i = 1, 2, 3$, denote the three spanwise regions as described in Section 5.1. The constitutive equations relating N_x^j and M_x^j to the corresponding displacements are given in Eqn (2.16).

There is only one continuity condition imposed on the core at each end of delamination region,

$$\begin{aligned} \tau_{xz}^{c(1)}(x=a,t) &= \tau_{xz}^{c(2)}(x=a,t) = 0 \\ \tau_{xz}^{c(2)}(x=b,t) &= \tau_{xz}^{c(3)}(x=b,t) = 0 \end{aligned} \tag{5.20}$$

If the delamination region starts or ends at one of the beam edges, for example, at $x = 0$, the continuity conditions at one end are replaced with boundary conditions which yield,

at the upper face layer ($x = 0$):

$$N_x^t = -P^t \quad \text{or} \quad u_1 = 0 \tag{5.21}$$

$$M_x^t = 0 \quad \text{or} \quad \frac{\partial w_1}{\partial x} = 0 \tag{5.22}$$

$$\begin{gathered} \frac{\partial M_x^t}{\partial x} + \frac{\rho_1 h_1^3}{12}\frac{\partial \ddot{w}_1}{\partial x} - \frac{\rho h^2}{2}\left(\frac{\ddot{u}_0}{3} - \frac{h}{10}\frac{\partial \ddot{w}_1}{\partial x} - \frac{3h}{20}\frac{\partial \ddot{w}_2}{\partial x}\right) = 0 \\ \text{or} \quad w_1 = 0 \end{gathered} \tag{5.23}$$

at the bottom face layer ($x = 0$):

$$N_x^b = -P^b \quad \text{or} \quad u_2 = 0 \tag{5.24}$$

$$M_x^b = 0 \quad \text{or} \quad \frac{\partial w_2}{\partial x} = 0 \tag{5.25}$$

$$\frac{\partial M_x^b}{\partial x} + \frac{\rho_2 h_2^3}{12}\frac{\partial \ddot{w}_2}{\partial x} - \rho h^2\left(\frac{\ddot{u}_0}{3} - \frac{3h}{40}\frac{\partial \ddot{w}_1}{\partial x} - \frac{2h}{15}\frac{\partial \ddot{w}_2}{\partial x}\right) = 0 \tag{5.26}$$

$$\text{or} \quad w_2 = 0$$

and at the core ($x = 0$):

$$\psi = 0 \tag{5.27}$$

5.3.2 The Constrained Mode Model

Consider a delamination region with contact, the crack surfaces remaining in contact vertically but free of shear stresses. Thus, the shear stresses in the core are null, which can be represented as,

$$\psi(x,t) = 0 \tag{5.28}$$

The formulation procedure is identical with that of the free mode model, which leads to similar governing equations of motion and similar continuity and boundary conditions. Some differences, however, exist due to the contact normal stresses at the delaminated surfaces. Such differences are represented by the compatibility condition between the core and the faces at the upper interface in the following:

$$w^t(x, z_1 = -\frac{h_1}{2}, t) = w^c(x, z = h, t) \tag{5.29}$$

The compatibility conditions between the core and the faces at the lower bonded interface are the same as that of the region without contact in Eqn (5.3). Substituting Eqns (5.28), (5.29) and (5.3) into displacement fields, Eqns (2.1), (2.2) and (2.3), the following equations are given,

$$\begin{aligned} u_0 &= u_2 - \frac{h_2}{2}\frac{\partial w_2}{\partial x} \\ w_0 &= w_2 \\ \phi &= \frac{w_1 - w_2}{h} \\ \psi &= 0 \end{aligned} \tag{5.30}$$

which also results in four independent displacement functions, $u_1(x,t)$, $w_1(x,t)$, $u_2(x,t)$ and $w_2(x,t)$, as seen in the free mode model.

The total kinetic energy of the sandwich segment at the delamination region, having different core contribution T_c than the free mode model, can be expressed in the form

$$T = T_1 + T_2 + T_c \tag{5.31}$$

where the kinetic energy contributions from two face layers, T_1 and T_2, are the same as that of the free mode model, and T_c can be written as,

$$\begin{aligned} T_c = \frac{1}{2}\int_0^l \rho h \Bigg\{ (\dot{u}_2)^2 + \left[\frac{h}{3}\frac{\partial \dot{w}_1}{\partial x} - \left(h_2 + \frac{4}{3}h \right) \frac{\partial \dot{w}_2}{\partial x} \right] \dot{u}_2 + \frac{h^2}{20}\left(\frac{\partial \dot{w}_1}{\partial x} \right)^2 \\ + \left(\frac{h_2^2}{4} + \frac{2}{3}hh_2 + \frac{19}{30}h^2 \right)\left(\frac{\partial \dot{w}_2}{\partial x} \right)^2 - \left(\frac{hh_2}{6} + \frac{7h^2}{20} \right) \frac{\partial \dot{w}_1}{\partial x}\frac{\partial \dot{w}_2}{\partial x} \Bigg\} dx \end{aligned} \tag{5.32}$$

It can be seen in Eqn (5.6) that the total potential energy U does not have the contribution from the core in the case of delamination without contact. Since there are contact normal stresses in the constrained model, a potential energy contribution from the core normal stresses must be included in the total potential energy U and it gives,

$$\begin{aligned} U_c &= \frac{1}{2}\int_0^l E_c h \phi^2 \, dx \\ &= \frac{1}{2}\int_0^l \frac{E_c}{h}(w_1 - w_2)^2 \, dx \end{aligned} \tag{5.33}$$

The four governing equations of motion can be derived in a similar way as used in the free mode model. The continuity conditions at the ends of the delamination region will be the same as Eqns (5.8) through (5.20). In the case of the delamination region starting at the beam edge ($x = 0$), the continuity conditions at that end become boundary conditions which are the same as Eqn (5.21) through (5.27). Similarly, the boundary conditions can be obtained if the delamination region ends at the beam edge ($x = l$).

5.4 Example Problems and Discussion

A few numerical example problems are considered for illustrative purpose. To verify the theory and computer program, the first three natural frequencies of two different models were calculated for a delamination length of $0.0001l$ and showed negligible discrepancies from those of a perfect sandwich beam considered in Chapter 2.

5.4.1 The Free Mode Model

The problem of the free vibration ($q = 0$) with simply supported boundary conditions can be solved in the similar way discussed in Chapter 2 and 3 by assuming a harmonic motion. The natural frequencies and mode shapes are calculated for a sandwich beam with a delamination located symmetrically along x direction. Figure 5.4 (a)-(c) show the normalized mode shapes for the case,

$d/l = 0.3$, $h_1/h = 0.1$ and $h_2/h = 0.02$, $h/l = 0.05$

$E_1 = E_2$, $E_c/E_1 = 0.05$, $E_c/G_c = 2.5$

where $d = b - a$ is the delamination length. The transverse displacements w_i (i = 1,2) and coordinates x, z are non-dimensionalized as

$\bar{w}_i = w_i/h$, $(i = 1,2)$, $\bar{x} = x/l$, $\bar{z} = z/(h+h_1+h_2)$

The effect of the delamination length on the natural frequencies has been examined for this case of example problems. The first three natural frequencies of the bending mode are given in Table 5.1. In this table, the non-dimensionalized frequency is defined as

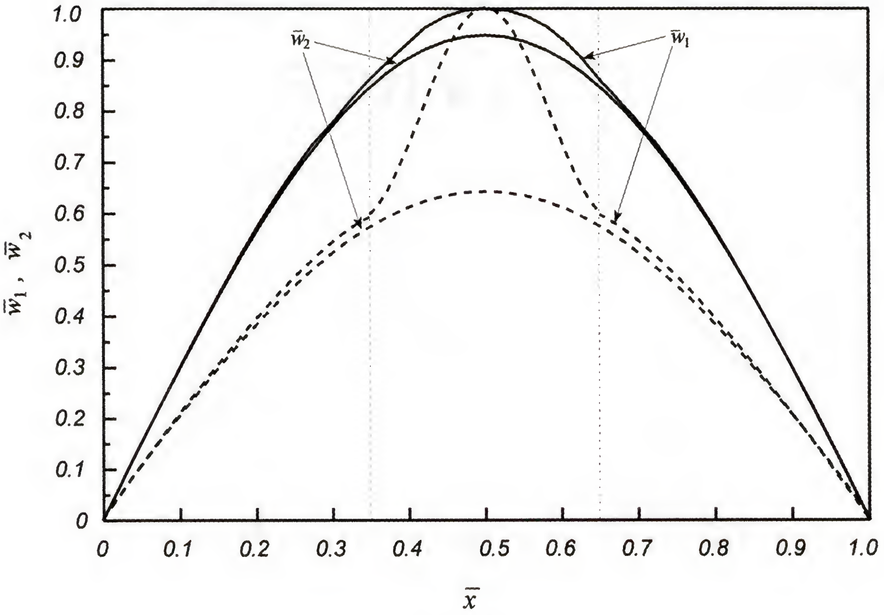

(a) First Mode

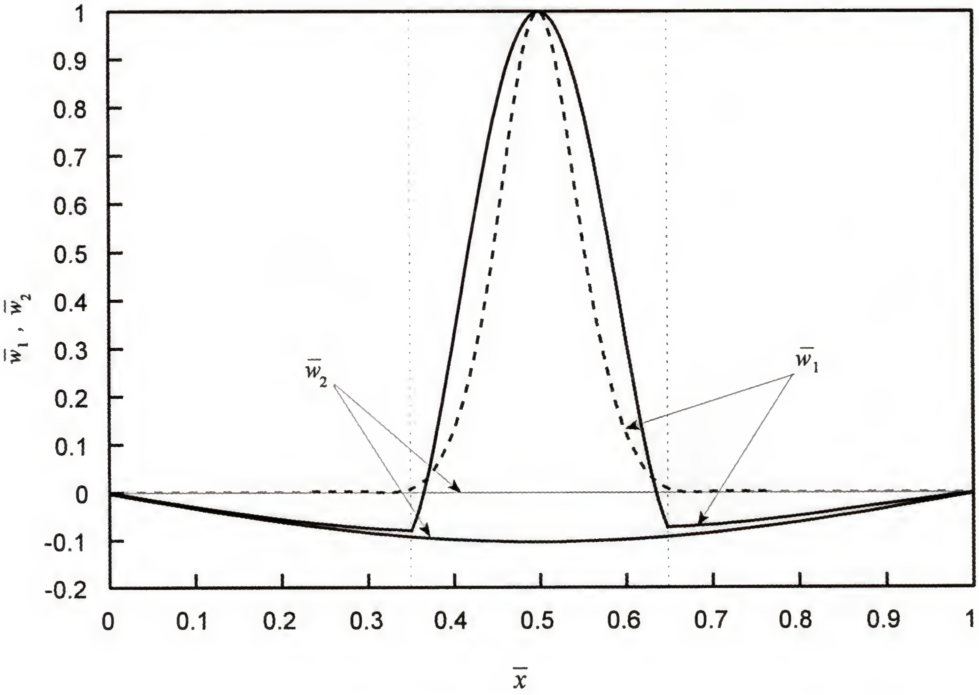

(b) Second Mode

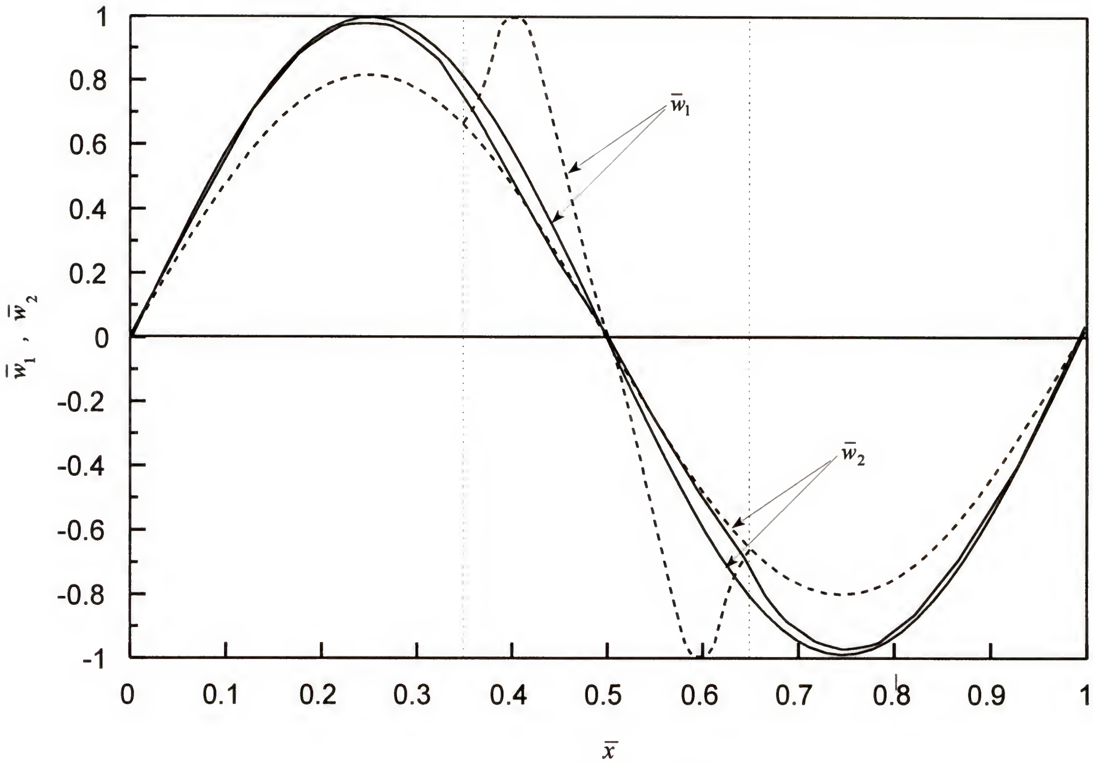

(c) Third Mode

Figure 5.4 Mode Shapes of Vibration of a Sandwich Beam-Plate Based on the Free Mode Model, ———— $h_1/h = 0.1$, ------- $h_1/h = 0.02$

Table 5.1 Natural Frequency Ω_i of Bending Modes

d/l	0.10	0.20	0.30	0.30	0.50	0.70
Ω_1	3.813	3.804	3.781	3.755	3.717	3.627
Ω_2	7.652	7.324	6.701	6.140	5.704	4.651
Ω_3	14.41	13.64	12.25	10.86	9.78	8.26
For a perfect beam, $\Omega_1 = 3.906$, $\Omega_2 = 7.811$, $\Omega_3 = 14.84$						

$$\Omega_i = \omega_i \sqrt{\frac{\rho_1}{E_1 I_1}} \left(\frac{l}{\pi} \right)^2 \tag{5.34}$$

where the subscript of Ω denotes the mode number. It is found that delamination has significant effects on the natural frequencies. All the three frequencies are lower than those of the perfect sandwich beam, and the difference between the second and third natural frequencies is larger than the difference between the first and second ones.

It can be seen that in the case of the first two symmetric modes as shown in Figure 5.4(a) and (b), the mode shapes of the face and core in the delamination region are different and that the transverse displacement of the face is greater than that of the core at all corresponding axial positions. Such a free displacement mode would give rise, in one half of the cycle of motion, to an overlap between the delaminated face and core. This is a downward displacement of the face greater than that of the lower core. In the case of the first antisymmetric mode as shown in Figure 5.4(c), the mode shapes would have an overlap over a half of the delamination region during the complete cycle of motion. It can be shown that similar overlaps will appear at all higher modes in this free mode model. Therefore, the deformation modes given by the free mode model are not physically feasible, although mathematically admissible as equilibrium solutions.

As pointed out earlier, the free mode model may be considered as the vibration relative to the post-buckling state. In this case, the governing equations of motion must therefore account for the geometric stiffness produced by the axial loads. As these loads are themselves functions of the transverse displacements, the terms representing the geometric stiffness in the governing equations of motion are non-linear. These non-linear terms, which are ignored in the analysis of free mode model, may become significant even within the regime of small deformation analysis, depending on the size and location of the delamination. As a result, the governing equations of motion are valid only over a very small portion of the free mode deformation cycle during which it is physically feasible.

5.4.2 The Constrained Mode Model

The above discussions showed that the free mode model gives vibration modes with overlaps of deformation which violate geometric compatibility. In reality, however, the tendency of the delaminated face layers to overlap on the core will be resisted by the development of a contact stress distribution between the face-core interface. Such a contact stress distribution could constrain the transverse deformation of these face and core to be identical and thus ensure the compatibility. This physically admissible mathematical model has been widely used and verified by experiments for vibrations of laminated composites with delaminations [76, 83, 84], where the identical transverse displacements of the delaminated layers were assumed. In the constrained mode model of sandwich beams, the transverse displacements of upper and lower faces may be different, although the compatibility condition at the delaminated interface remains.

In Figure 5.5(a) and (b), the normalized mode shapes of the first two bending modes are shown for a simply supported sandwich beam with the spanwise location of the delamination located at the midpoint. The system parameters are similar to the free mode model as defined in the following:

$h_2/h = 0.02,\ \ h/l = 0.05,\ \ E_1 = E_2,\ \ E_c/E_1 = 0.05,\ \ E_c/G_c = 2.5$

The figure shows that the transverse displacements w_1 and w_2 in the delamination region, comparing to the free mode model, are very close. It is alos noted that the second mode in the free mode model disappears in this case.

Figure 5.6 shows the effect of delamination size on the non-dimensional natural frequencies of the first three bending modes. It can be observed that the reduction in the frequency of the first mode is negligible for small delamination size up to 70%. The weakening effect of the delamination on the second mode and the third mode is much larger than that on the first mode frequency. There is a substantial drop in the frequency values even for the small delamination on the high modes.

Figures 5.7 and 5.8 show the effect of spanwise location of the delamination on the frequencies for the first two bending modes of sandwich beams with simply supported boundary conditions, respectively. It can be seen that the spanwise location of the delaminations has strong effect on the frequency values. Such effects may be explained by the fact that the delamination moves to regions of high shear force or regions of high curvature. In some specific locations the effect of delamination on the frequencies may become a minimum.

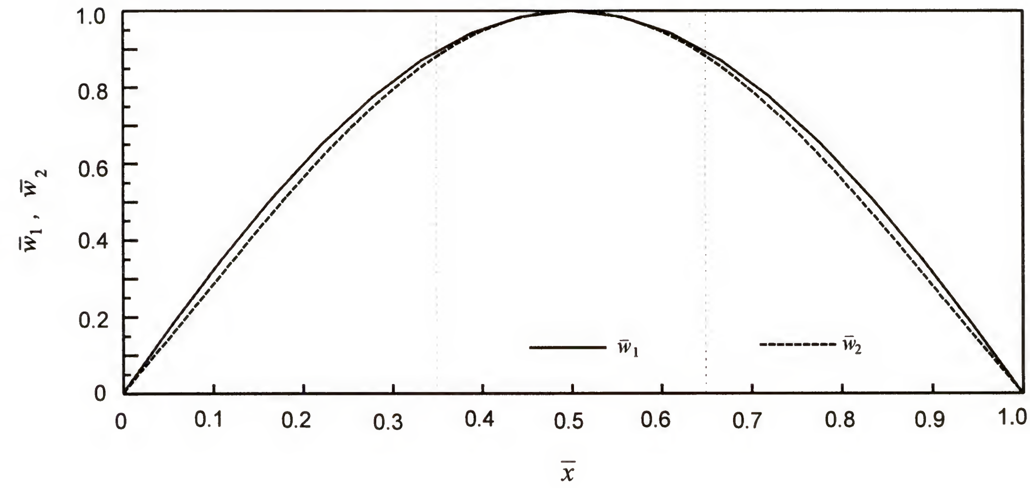

(a) First Mode

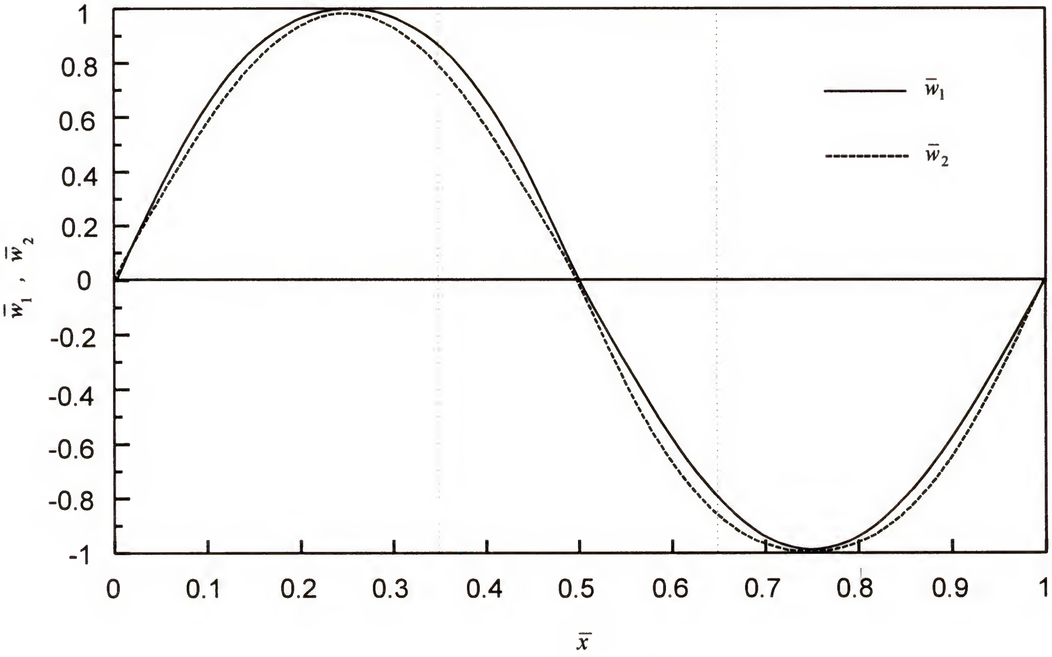

(b) Second Mode

Figure 5.5 Mode Shapes of Vibration of a Sandwich Beam-Plate Based on the Constrained Mode Model, $d/l = 0.3$, $h_1/h = 0.02$, $h/l = 0.05$ $E_1 = E_2$, $E_c/E_1 = 0.05$, $E_c/G_c = 2.5$

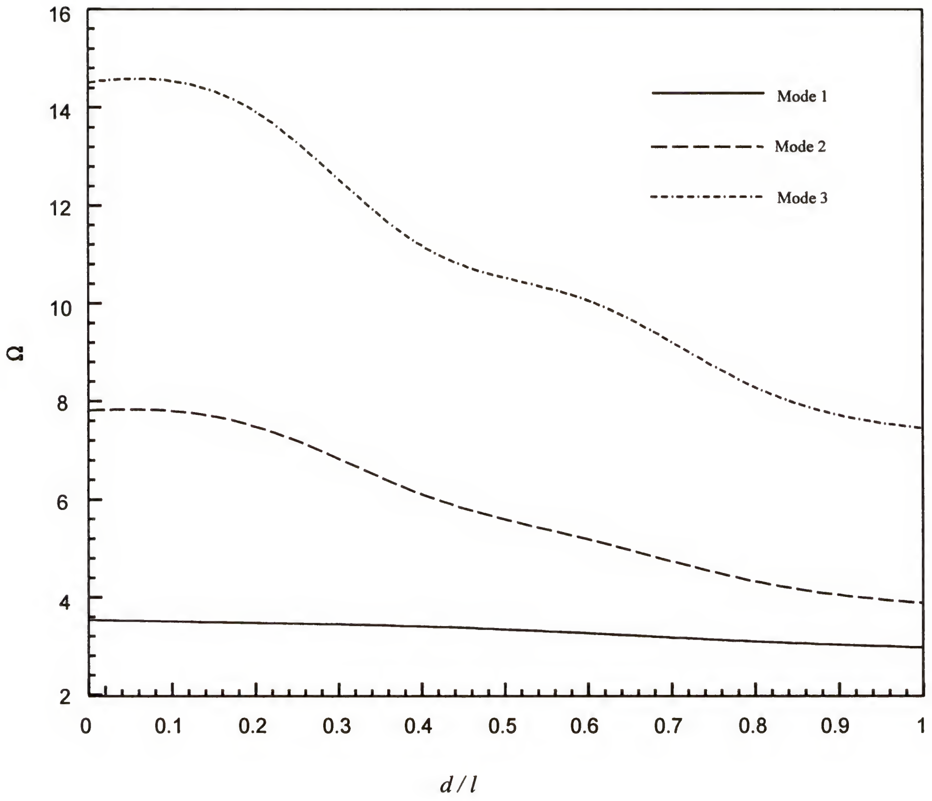

Figure 5.6 Non-dimensional Frequency versus Delamination Size for the First Three Bending Modes

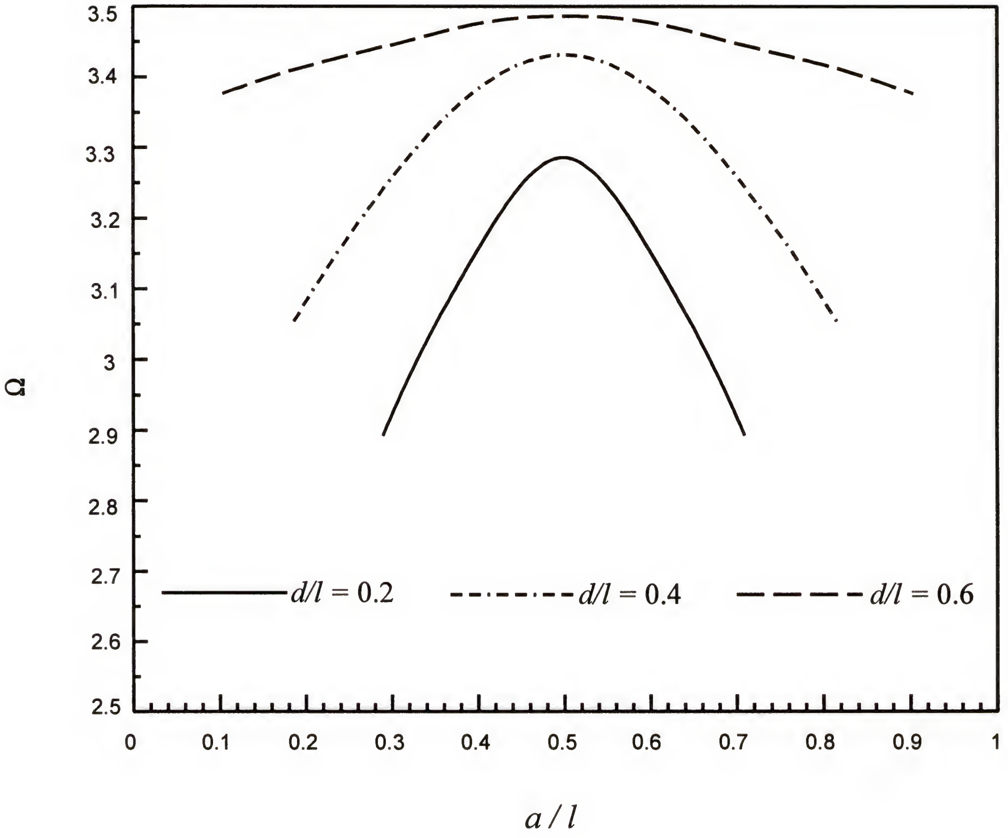

Figure 5.7 Effect of Spanwise Location on the Fundamental Frequency

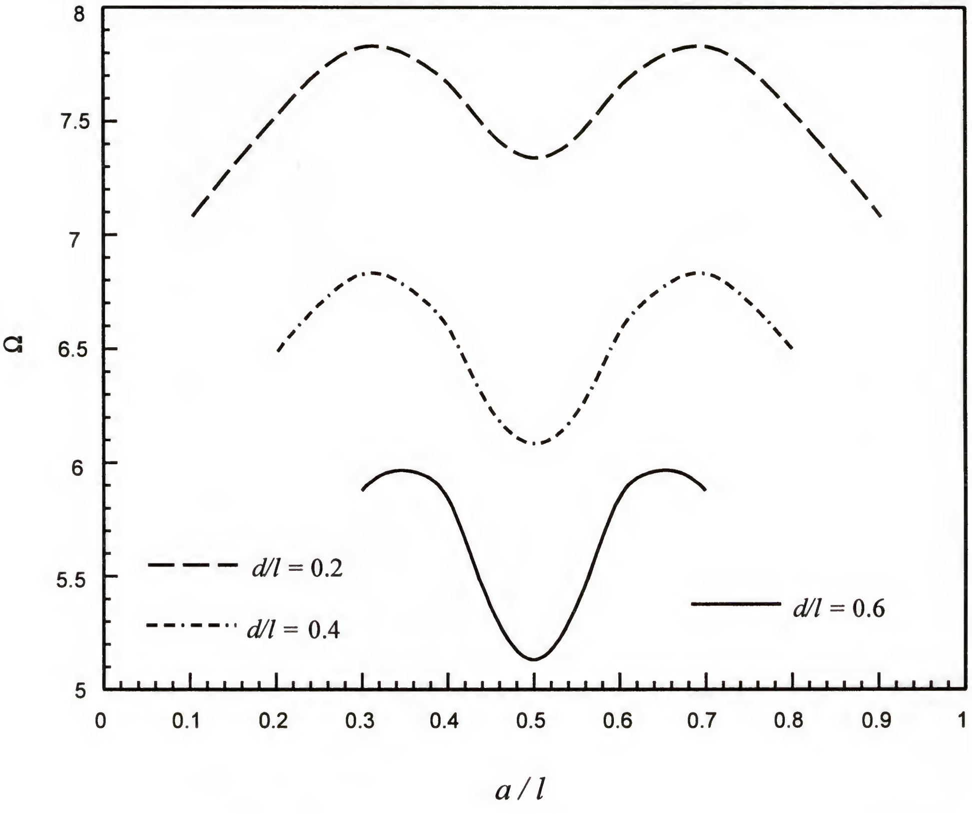

Figure 5.8 Effect of Delamination Spanwise Location on the Frequency of the Second Mode

CHAPTER 6
VIBRATION OF LAMINATED BEAMS WITH DELAMINATIONS

Free vibration of laminated plates with delaminations has been examined by many researchers analytically and experimentally [73-84]. A more general theory for modeling of delamination in composite laminates is based on a layer-wise displacement field. The finite element model of layer-wise theory is not only providing an adequate framework for the delamination analysis of laminated composites, but also capable of dealing with complex geometries of delaminations (e.g., multiple delaminations) and structures. However, the computational cost of the analysis is very expensive, and thus makes it unattractive for delamination analysis in engineering practice when the number of layer is large. We try to implement this layer-wise finite element model in vibration analysis with emphasis on developing parallel algorithms of finite element analysis to minimize both the computational cost and communication cost.

6.1 The Layer-Wise Finite Element Model

In delamination analysis of laminated composites, the layer-wise theory provides a compromise between the 3-D theory and conventional plate theories. Conventional theories based on a single continuous and smooth displacement field through the thickness of a composite laminate give poor estimation of the interlaminar stresses. With layer-wise continuous representation of displacements through the thickness, it predicts the interlaminar stresses very accurately. Moreover, it also has the advantage of all plate theories in the sense that it is a two-dimensional theory, and doesn't suffer from aspect ratio limitations associated with three-dimensional finite element models.

For modeling delamination of laminated composites, the layer-wise theory can be extended to model the kinematics of a layered plate with provision of delamination. It is implied that the same displacement distributions in individual layer is capable of representing displacement discontinuity condition at interfaces between layers. The present study on vibration behavior uses the same approach presented earlier by Barbero and Reddy in the buckling analysis [67]. According to Barbero and Reddy, the in-plane displacements are assumed to have linear through-the-thickness variation within each ply, i.e., the global approximation of the form of in-plane displacements is refined to a layer-by-layer approximation. High order shear deformable theories that allow for quadratic or higher order variations of the in-plane displacements are possible within the context of the layer-wise theory, but the layer-wise first order shear deformable assumption is sufficient for the present study. For simplicity, it is assumed that the delamination extends through the entire width and there are no variations in the y direction, as discussed in the beam-plate model. Furthermore, the location and length of the delaminations are assumed to be known and fixed. As a result, the beam element of the layer-wise finite element model is employed.

Based on these assumptions, the global layer-wise displacement terms, $u(x,z,t)$ and $w(x,z,t)$, which include delaminations can be represented in the following form

$$\begin{aligned} u(x,z,t) &= u_0(x,t) + \sum_{j=1}^{N} \phi^j(z)\, u^j(x,t) + \sum_{i=1}^{D} H^i(z)\, U^i(x,t) \\ w(x,z,t) &= w_0(x,t) + \sum_{i=1}^{D} H^i(z)\, W^i(x,t) \end{aligned} \tag{6.1}$$

where the step functions H^i are computed in terms of the Heaviside step functions H as:

$$\begin{aligned} H^i(z) &= \bar{H}(z - z_i) = 1 \quad \text{for } z \geq z_i \\ H^i(z) &= \bar{H}(z - z_i) = 0 \quad \text{for } z < z_i \end{aligned} \tag{6.2}$$

In Eqn (6.1), the first terms, u_0 and w_0, are the displacement functions of a reference surface; u^j is the layer-wise in-plane displacement function in the x direction; and ϕ^j is a local linear Lagrangian interpolation function. Displacement functions that represent relative in-plane slippage and relative transverse opening displacements across the ith delaminated interface are represented by U^i and W^i, respectively. Using the step functions H^i, we can model any number of delaminations through the thickness; the number of D is equal to the number of delaminations considered. Each ply is assumed to be inextensible in the z direction and the in-plane slippage is assumed to occur across frictionless

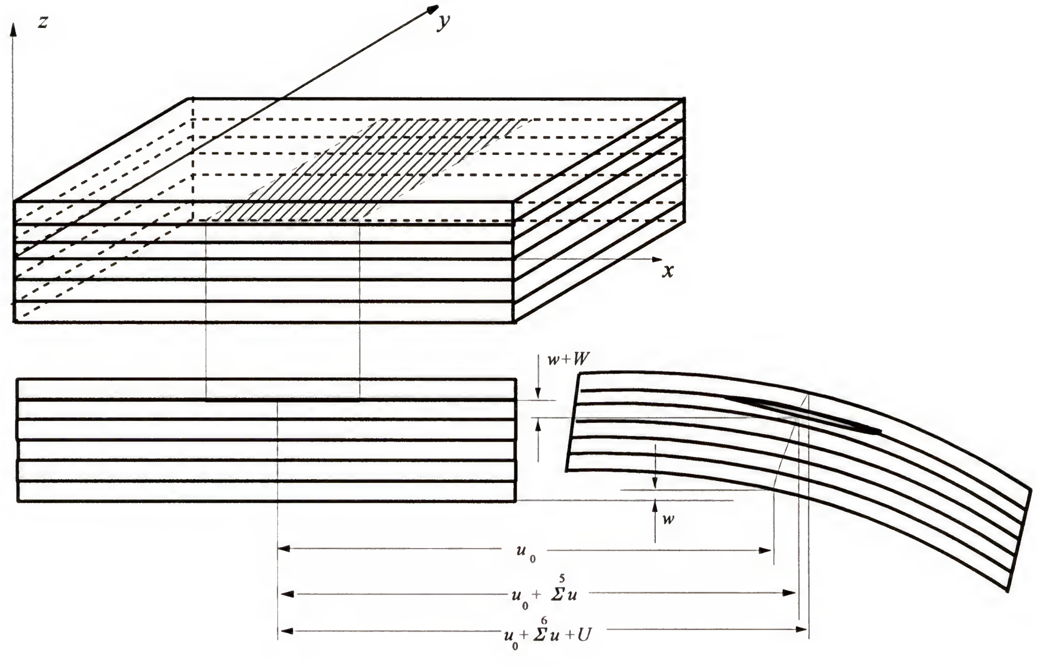
z
y
x
w+W
w
u_0
$u_0 + \overset{5}{\Sigma} u$
$u_0 + \overset{6}{\Sigma} u + U$

Figure 6.1 Laminated Composite with a Delamination

interfaces. The reference surface is taken as the bottom of the laminate, as shown in Figure 6.1.

Following the small deformation theory, the strain-displacement relations and constitutive equations can be obtained for the layer-wise displacement field. By taking the first variation of the total kinetic energy and potential energy or using the principle of virtual work, we can arrive at the governing equations of motion. To develop the corresponding finite element model, the generalized displacements (u_0, w_0, u^j, U^i, W^i) are expressed over each element as a linear combination of the interpolation function ψ_i and the nodal values (u_{0k}, w_{0k}, u_k^j, U_k^i, W_k^i) as follows,

$$\left(u_0, w_0, u^j, U^i, W^i\right) = \sum_{k=1}^{n} \left(u_{0k}, w_{0k}, u_k^j, U_k^i, W_k^j\right)\psi_k \tag{6.3}$$

where n is the number of nodes per element. Then, substituting this model into the governing equations of motion, we obtain the following finite element equations:

$$\begin{bmatrix} m^{11} & m^{12} & \dots & m_N^{12} & m_1^{13} & \dots & m_D^{13} \\ m_1^{21} & m_{11}^{22} & \dots & m_{1N}^{22} & m_{11}^{23} & \dots & m_{1D}^{23} \\ \vdots & \vdots & & \vdots & \vdots & & \vdots \\ m_N^{21} & m_{N1}^{22} & \dots & m_{NN}^{22} & m_{N1}^{23} & \dots & m_{ND}^{23} \\ m_1^{31} & m_{11}^{32} & \dots & m_{1N}^{32} & m_{11}^{33} & \dots & m_{1D}^{33} \\ \vdots & \vdots & & \vdots & \vdots & & \vdots \\ m_D^{31} & m_{D1}^{32} & \dots & m_{DN}^{32} & m_{D1}^{33} & \dots & m_{DD}^{33} \end{bmatrix} \left\{\begin{matrix} \{\ddot{\Delta}\} \\ \{\ddot{\Delta}^1\} \\ \vdots \\ \{\ddot{\Delta}^N\} \\ \{\ddot{\Delta}_d^1\} \\ \vdots \\ \{\ddot{\Delta}_d^D\} \end{matrix}\right\} + \begin{bmatrix} k^{11} & k^{12} & \dots & k_N^{12} & k_1^{13} & \dots & k_D^{13} \\ k_1^{21} & k_{11}^{22} & \dots & k_{1N}^{22} & k_{11}^{23} & \dots & k_{1D}^{23} \\ \vdots & \vdots & & \vdots & \vdots & & \vdots \\ k_N^{21} & k_{N1}^{22} & \dots & k_{NN}^{22} & k_{N1}^{23} & \dots & k_{ND}^{23} \\ k_1^{31} & k_{11}^{32} & \dots & k_{1N}^{32} & k_{11}^{33} & \dots & k_{1D}^{33} \\ \vdots & \vdots & & \vdots & \vdots & & \vdots \\ k_D^{31} & k_{D1}^{32} & \dots & k_{DN}^{32} & k_{D1}^{33} & \dots & k_{DD}^{33} \end{bmatrix} \left\{\begin{matrix} \{\Delta\} \\ \{\Delta^1\} \\ \vdots \\ \{\Delta^N\} \\ \{\Delta_d^1\} \\ \vdots \\ \{\Delta_d^D\} \end{matrix}\right\}$$

$$= \left\{\begin{matrix} \{q\} \\ \{q^1\} \\ \vdots \\ \{q^N\} \\ \{q_d^1\} \\ \vdots \\ \{q_d^D\} \end{matrix}\right\} \tag{6.4}$$

where

$$\{\Delta\}^T = \{u_{01}, w_{01}, \dots, u_{0n}, w_{0n}\}$$

$$\{\Delta^j\}^T = \{u_1^j, u_2^j, \dots, u_n^j\}$$

$$\{\Delta_d^i\}^T = \{U_1^i, W_1^i, \dots, U_n^i, W_n^i\}$$

and the submatrices $[m^{11}]$, $[m_j^{12}]$, $[m_j^{21}]$, $[m_{ji}^{22}]$, $[m_{jr}^{23}]$, $[m_{rj}^{32}]$, $[m_{DD}^{33}]$ and $[k^{11}]$, $[k_j^{12}]$, $[k_j^{21}]$, $[k_{ji}^{22}]$, $[k_{jr}^{23}]$, $[k_{rj}^{32}]$, $[k_{DD}^{33}]$ with $i, j = 1, \dots, N$ and $r, s = 1, \dots, D$ are the mass matrices and stiffness matrices. There are $(2+N+2D)$ displacement variables in each node of the one dimensional finite elements used in representing the 2-D geometry. The load vectors $\{q\}$, $\{q^j\}$, and $\{q_d^i\}$ are similar to the forms of $\{\Delta\}$, $\{\Delta^j\}$ and $\{\Delta_d^i\}$. In the case of free vibration, all load vectors are zero and the following eigenvalue problem can be formulated when the harmonic motion is assumed:

$$\left(-\omega^2[M] + [K]\right)\{\Delta\} = \{0\} \tag{6.5}$$

6.2 Parallel Algorithm Design for Finite Element Analysis

As stated earlier, one of the disadvantages of layer-wise finite element modeling is the expensive computational cost, particularly with large number of layers and/or multiple delaminations. The computational power of the new parallel processing computer system offers an oppotunity to reduce computational times for analysis so that the finite element analysis can be more fruitfully used by the designers.

It is now clear that the analysis and design of practical engineering systems in the future will make extensive use of concurrent processing on computers with multiple processors. Parallel processor computers consisting of multiple processors linked to one another and running subtasks concurrently are becoming widely available for large-scale scientific and engineering computations. These computers are being increasingly used to provide the reduction in effective calculation time (or elapsed time) needed to carry out many real-time applications. A new area of research in computational mechanics is based upon the unique architectural features of parallel processing computers. However, there is still a big gap between well-developed parallel algorithm analysis and their application in the advanced engineering programs. Comparing to the implementation of sequential code, parallel algorithm design in the computational structural mechanics requires a thorough understanding of the nature of the problem and a considerable investment in analyzing the data flow in the solution procedure itself as well as the knowledge of parallel algorithm theory.

In this study, we try to develop approximately optimized parallel algorithms in the layer-wise finite element analysis of delamination problems. Although only such a finite element model has been implemented, it is expected that our approach has the potential of handling various numerical schemes for different purposes of finite element analysis, and to be as much as possible hardware independent. It is noted that efficient non-numerical algorithms such as the concurrent assembly of a mass matrix or a stiffness matrix and fast schemes for the solution of a set of linear equations may be related with specific parallel computers or architectural issues.

A number of special strategies can be used to increase the degree of parallelism in finite element computations. These strategies are applications of "divide and conquer", based on breaking a large (and/or complex) problem into a number of smaller (and/or simpler) subproblems which may be solved independently on distinct processors. The degree of independence of the subproblems is a measure of the effectiveness of the algorithm since it determines the amount and frequency of communication and synchronization.

Two parallel algorithms in finite element analysis are discussed in the following: domain decomposition and optimal mapping.

6.2.1 Domain Decomposition

The basic idea of domain (or spatial) decomposition is to divide the domain into a number of (possibly overlapping) regions. The initial/boundary-value problem is decomposed into one that involves solution of initial/boundary-value problems on subproblems, thereby introducing spatial parallelism. Given a number of available processors N_p, it is attractive to decompose a finite element domain R into the same number of subdomains, because this allows individual subdomain operations to be performed concurrently on separate CPU's. In this way, we are decentralizing the organization of the finite element software system in the sense of data-flow. Each processor p_j is mapped onto a subdomain R_j in which the basic geometrical and physical properties of those elements and some additional control parameters are stored. In stead of seeking a perfect match between the communication structure of the hardware and the communication requirements of subsequent algorithms, we develop an approximate optimal algorithm with generality while we try to maintain a balanced utilization of a given hardware and the software architecture to be designed.

We propose a hardware-independent domain decomposition algorithm to fulfill the requirements of generality in arbitrary discretization, balanced computational loads and minimal communication and/or synchronization. Therefore, it must yield a set of balanced subdomains to make the overall computational load as evenly distributed as possible among the processors, and it must minimize the number of interface nodes to reduce the communication cost.

We define an internal boundary element within a subdomain R_i as an element that is connected to an internal boundary node, which is the same as an interface node of the global domain R. The domain decomposition algorithm will provide the local information on a list of elements, internal boundary nodes and internal boundary elements for each subdomain R_i, and global information on a list of the subdomains that connect to each interface node, the connectivity table (adjacency graph) for the subdomain R_i and the colored graph associated with internal boundary elements. For a distributed multiprocessor computer, as an example, only the node geometry and element properties of subdomain R_j need be stored in the RAM of processor p_j if p_j is assigned to R_j. The algorithm then makes use of a list of elements in each subdomain to load initially each processor with the appropriate data. The communication structure of the problem is established by the subdomain connectivity table. Two subdomains are considered as connected if they share at least one interface node. Then, the list of the subdomains that connect to each interface node, the connectivity table and the list of internal boundary nodes determine the number and content of message to send and/or receive for each processor.

The key here is to properly deal with the internal boundary elements because they constitute a source of inherent serializing computations and potential memory conflict during parallel computations that are carried on at the element level. It can be seen that each of these elements in a subdomain R_i has a corresponding element in some subdomain R_j connected to it through a set of interface nodes. We offer a possible solution to minimize the serializations in these critical regions. We eliminate internal boundary elements, based on the local information, from their original subdomains and treated as a set of elements defining a single subdomain R*. Then, a usual coloring technique is applied to decompose D* into a set of subdomains D_i^* such that each element corresponds to a single color, i.e., no two elements are connected. For each color, because they are mutually disjointed, the elements may be assigned arbitrarily to the N_p processors. This algorithm has been implemented in the vibration analysis of delaminated sandwich beams with a regular finite element mesh. In our practice, this domain decomposition algorithm can improve the computational time at the range of 30% ~ 40% in the case of using 16-processors.

6.2.2 Optimal Mapping of Irregular Finite Element Domains

For the case of irregular finite element domain problems such as structures with delamination and fracture or complex geometry, the good strategy of mapping solution domain into parallel processors is no longer obvious. An arbitrary clustering of elements to form subdomains equal to the number of available processors will undoubtedly result in imbalanced workload distribution among processors. The resources required by each processor depend not only on the computation cost associated with the elements falling within its subdomain, but also on the cost of transferring the subdomain boundary information to other processors containing contiguous subdomains. And even if an equal number of elements are allocated per processor, excessive communication costs may strongly outweigh any parallel processing gains. We use another approximate optimal mapping strategy which guides the process of decomposing complex solution domains into appropriate subdomains so as to balance the workload required by each processor.

First, the cost function C as our criterion for selecting as optimal mapping is defined in the following

$$C = \sum_{i=1}^{N} (w_i)^r + \frac{t_{comm}}{t_{comp}} \sum_{p,q}^{p<q} D_{pq} \tag{6.6}$$

where

w_i = computational workload associated with elements residing in subdomain i, assigned to processor i.

D_{pq} (D_{ij}) = communication distance between two finite elements *p* and *q* residing in two different processors *i* and *j*.

t_{comm}, t_{comp} = typical communication, computation time per element, respectively.

The first term of the cost function serves to equalize the computational workload of various processors. The second term in the cost function represents the communication cost, with the ratio (t_{comm}/t_{comp}) introduced to weigh the relative amount of communication to computation required per element. This ratio depends not only on the nature of the computational problem being modeled, but also on the relative speed of the processors in communicating one floating point number from one processor to its nearest neighbor to its speed in executing one floating point operation on that number. As such, (t_{comm}/t_{comp}) is both problem dependent and machine dependent.

Clearly, the cost function C will assume different values for different decompositions of the solution domain into subdomains. And even if one assumes that the amount of computations associated with each finite element is constant regardless of the nature of domain decomposition and processor assignment, it is important to note that the interelement communication costs will vary. Thus, the total cost of processing each element, and therefore all elements, will depend on the relative allocation of the *n*-elements to the *N*-processors.

It is theoretically possible through enumeration to exactly determine the best assignment policy which will minimize *C*. However, to do this would require one to evaluate and sort *C* as many times as the number of possible ways (combinations) S for clustering n-elements into N-subdomains. The number of these combinations S can be found from the theory of the classical "Occupancy" problem. Unfortunately, this method is practical only for the simple cases when n and N are small (<10).

Instead, we use suboptimal approximation techniques such as simulated annealing heuristic [90]. In anticipation of finding a more global minimum, the simulated annealing heuristic probilistically accepts configurations which temporarily deteriorate the quality of the cost function. The probability of accepting deteriorate the configurations is made highest at the early iterations, but is reduced slowly as the iterations progress, thereby accepting far fewer nonimproving moves near the minimum. As such, a coarse global search evolves into a fine local search near the global minimum, and the probabilistic "jumps" provide an escape from local minima.

Here is the analogy between the annealing simulation and the optimal mapping of finite elements to parallel processors. In Eqn (6.6) where the cost is a function of two conflicting factors (computing costs and communication costs), in the annealing problem the system energy is a function of two conflicting factors: short range repulsive forces and long range attractive forces. The specific assignment of elements to processors governs the total cost function just as the atomic positions determine the body's energy state. In the hypothetical situation in which the attractive forces (communication costs) are assumed absent, the system's energy (cost function) may be minimized by the new dominant repulsive forces (computing costs) requiring that the atoms (elements) be uniformly distributed throughout the body (among processors). Conversely, if the repulsive forces (computing costs) are assumed absent, the minimum of the energy (cost function) will be achieved by placing all atoms as close together as possible (all elements placed in one processor). Of course in reality, both conflicting factors are present and their effect on the global minimum depends on their relative strengths.

6.3 Example Problems

As an example, we consider a finite element representation for the vibrations analysis of a laminated composite beam-plate with delamination. The effects of in-plane loading on the vibration characteristics of $[0_2/90_2]_s$ and $[0/90]_{2s}$ graphite-epoxy composite laminate with fixed-fixed boundary conditions are examined. For simplicity, the delamination is assumed to be located symmetrically along both the spanwise direction and the thickness direction. The ply mechanical properties are given as follows:

$E_1 = 111.2$ GPa, $E_2 = 9.78$ GPa, $G_{12} = 4.82$ GPa, $\nu_{12} = 0.32$

These values are typical of an advanced fiber-reinforced composite materials. Similar to the previous chapters, the natural frequency as well as the in-plane loading are non-dimensionalized in the following

$$\Omega = \sqrt{\frac{m}{D}}\left(\frac{l}{\pi}\right)^2, \quad P^* = \frac{P}{D}\left(\frac{l}{\pi}\right)^2$$

where l is the length of the delaminated plate, m is the mass per unit length and D is the effective bending stiffness of the laminate. The normalized delamination length is defined as a/l where a is the delamination length.

Figure 6.2 shows the variation of the fundamental natural frequency with the compressive load for three different delamination lengths. It can be clearly seen that the fundamental frequency decreases with increasing compressive in-plane load. A substantial drop of the frequency becomes more substantial at the higher compressive load although the effect of the small delamination length is negligible. This shows the effect of long delamination length on the fundamental natural frequency is important. In Figure 6.3, the effect of the compressive in-plane load on the fundamental frequency with two different layups are examined. It shows that the laminate layups also have some effects on the natural frequency in the delamination case.

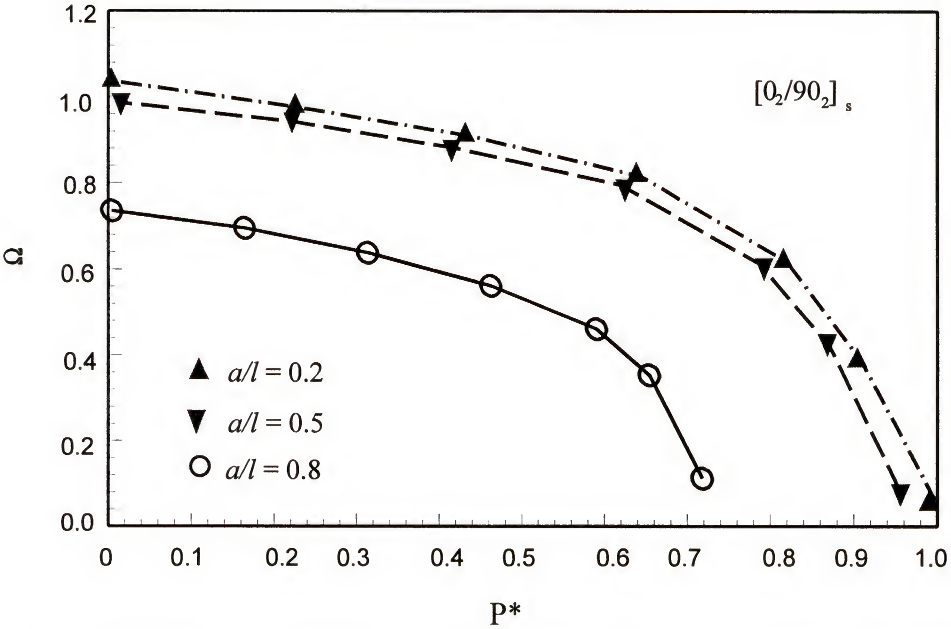

Figure 6.2 Variation of Fundamental Frequency with Compressive In-plane Load for Different Delamination Lengths

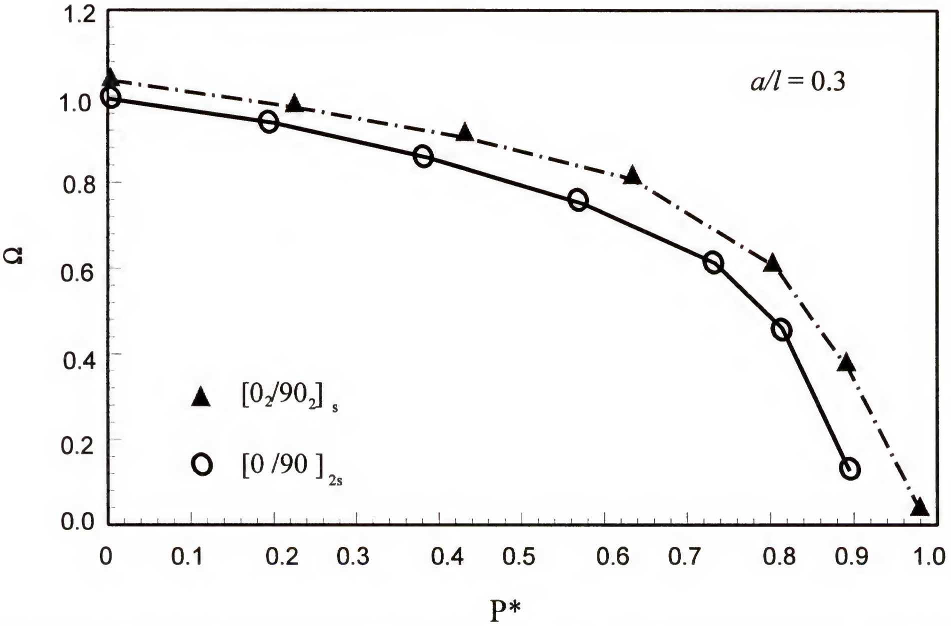

Figure 6.3 Variation of Fundamental Frequency with Compressive In-plane Load for Different Different Layups

CHAPTER 7
CONCLUSIONS AND FUTURE WORK

Refined vibration theories of sandwich beam and plate are proposed to investigate dynamic response characteristics of sandwich construction with newly developed flexible and compressible core materials. The theory is employed to study the vibration damping problems of sandwich beam and plate. The viscoelastic face-core interface effects on structural damping of sandwich beam are examined, and free vibration of delaminated sandwich beam-plate is also analyzed by using the refined theory. Two different deformation modes in vibration of delaminated sandwich beam-plate are discussed and the physically admissible mode is identified. For the vibration of laminated composites with delamination, the layer-wise finite element model is discussed to corporate the parallel algorithm design for the finite element analysis.

7.1 Conclusions

It is shown that the proposed theory enhances the physical insight of the vibration damping behavior of sandwich beams and plates consisting of more flexible cores. Parametric study demonstrates that the shear deformation of the viscoelastic interface layers has a significant contribution to the structural damping. Effects of the storage shear modulus and loss factor of interface layer are important for the structural damping and resonance frequency. Results also demonstrate that the there may exist optimal adhesive bonding stiffness to achieve the maximum sandwich structural damping. This theory is applicable to sandwich beams and plates with any type of construction and flexible core materials.

It should be mentioned that as damping (loss factor) of the structure is increased, the stiffness of the structure, in general, will be decreased. Therefore, by only improving damping will not reduce the dynamic responses such as displacements, stresses and noise level of the structure. It is a trade-off situation between damping and stiffness. Generally, a proper value of interface shear modulus (adhesive stiffness) for the trade-off between enhancement in damping and decrease in stiffness can be obtained in most situations.

An analytical study of the vibration characteristics of sandwich beams with delamination shows that the effect of the delamination on the natural frequencies depends not only on its size but is also very sensitive to its spanwise location and vibration mode. Based on the discussion of the full cycle vibration and linear analysis, it can be seen that the constrained mode model is a physically feasible model for describing the vibration behavior of delaminated sandwich beams whereas the free mode model is not. The layer-wise finite element model for the laminated composites with delamination offers the possibility of dealing with multiple delaminations and complex geometric structural problem, in addition to accurate analysis. Its expensive computational cost brings about the necessity of implementing parallel algorithms for finite element analysis.

7.2 Future Study of Related Research

A logic extension of this study is to investigate the buckling behavior of delaminated sandwich composites by using the proposed displacement field. Since the energy method is used to derive the governing equations of motion in this study, it is a consequence to formulate the energy release rate equations for the fracture analysis of delamination growth problems.

Forced vibration problems need to be considered for the vibration damping of delaminated sandwich beams and plates. The effects of delamination on the loss factors of damped sandwich structures are required to address in the future work, and the correlated experimental study must be performed. It is noted that there exists some controversy on the delamination damage effects on dynamic characteristics of laminated composites, thus more systematic studies in this area are necessary.

For the finite element analysis, we will continue to study the multiple delamination effects of laminated composites. The study can extend to plate element, and more study on parallel algorithm design for finite element analysis are needed to meet the needs of growing computational demand.

APPENDIX A
EQUATIONS OF MOTION OF A SANDWICH BEAM

As we mentioned in Chapter 2, the governing equations of motion and corresponding boundary conditions of a sandwich beam are derived via the variational principles imposed on the total kinetic energy and potential energy in terms of four basic functions, w_1, w_2, u_0 and ψ. The governing equations of motion can be written in the following matrix form:

$$\begin{bmatrix} \partial M_{11} & \partial M_{12} & \partial M_{13} & \partial M_{14} \\ \partial M_{21} & \partial M_{22} & \partial M_{23} & \partial M_{24} \\ \partial M_{31} & \partial M_{32} & \partial M_{33} & \partial M_{34} \\ \partial M_{41} & \partial M_{42} & \partial M_{43} & \partial M_{44} \end{bmatrix} \begin{Bmatrix} \ddot{w}_1 \\ \ddot{w}_2 \\ \ddot{u}_0 \\ \ddot{\psi} \end{Bmatrix} + \begin{bmatrix} \partial K_{11} & \partial M_{12} & \partial K_{13} & \partial K_{14} \\ \partial K_{21} & \partial K_{22} & \partial K_{23} & \partial K_{24} \\ \partial K_{31} & \partial K_{32} & \partial K_{33} & \partial K_{34} \\ \partial K_{41} & \partial K_{42} & \partial K_{43} & \partial K_{44} \end{bmatrix} \begin{Bmatrix} w_1 \\ w_2 \\ u_0 \\ \psi \end{Bmatrix} = \begin{Bmatrix} q_1 \\ 0 \\ 0 \\ 0 \end{Bmatrix} \tag{A.1}$$

where ∂M_{ij} and ∂K_{ij} $(i,\ j = 1, 2, 3, 4)$ are the mass matrix differential operators and stiffness matrix differential operators, respectively. This equation is the same as Eqn (2.23), and the matrix elemenets are

$$\partial M_{11} = \left(\rho_1 h_1 + \rho \frac{h}{6} \right) - \left[\rho_1 \frac{h_1^3}{12} + \rho_1 h_1 \frac{(h_1 + h_2)^2}{4} + \rho \frac{h^3}{20} \right] \frac{\partial^2}{\partial x^2} \tag{A.2}$$

$$\partial M_{12} = \rho \frac{h}{3} - \left[\rho_1 h_1 h \frac{h + h_1}{4} + \frac{3 \rho h^3}{40} \right] \frac{\partial^2}{\partial x^2} \tag{A.3}$$

$$\partial M_{13} = \left[\rho_1 h_1 \frac{h_1 + h}{2} + \rho \frac{h^2}{6}\right]\frac{\partial}{\partial x} \tag{A.4}$$

$$\partial M_{14} = \left[\rho_1 h_1 e h \frac{h + h_1}{2} + \rho \frac{h^3}{8}\left(e + \frac{1}{6}\right)\right]\frac{\partial}{\partial x} + \left[\rho_1 h_1 h^3 \frac{h + h_1}{24} + \frac{\rho h^5}{90}\right]\frac{\partial^3}{\partial x^3} \tag{A.5}$$

$$\partial M_{21} = \partial M_{12} \tag{A.6}$$

$$\partial M_{22} = \rho_2 h_2 + \rho \frac{h}{6} - \left[\rho_2 \frac{h_2^3}{12} + \rho_1 h_1 \frac{h_2^2}{4} + \frac{2\rho h^3}{15}\right]\frac{\partial^2}{\partial x^2} \tag{A.7}$$

$$\partial M_{23} = \left(\rho_1 h_1 \frac{h}{2} - \rho_2 \frac{h_2^2}{2} + \rho \frac{h^2}{3}\right)\frac{\partial}{\partial x} \tag{A.8}$$

$$\partial M_{24} = \left[\rho_1 h^2 e \frac{h_1}{2} + \rho \frac{h^3}{48}(10e + 3)\right]\frac{\partial}{\partial x} - \left(\rho_1 h_1 \frac{h^4}{24} + \frac{13\rho h^5}{720}\right)\frac{\partial^3}{\partial x^3} \tag{A.9}$$

$$\partial M_{31} = -\partial M_{13} \tag{A.10}$$

$$\partial M_{32} = -\partial M_{23} \tag{A.11}$$

$$\partial M_{33} = \rho_1 h_1 + \rho_2 h_2 + \rho h \tag{A.12}$$

$$\partial M_{34} = eh\left(\rho_1 h_1 + \rho\frac{h}{2}\right) - \left(\rho_1 h_1 \frac{h^3}{12} + \rho\frac{h^4}{12}\right)\frac{\partial^2}{\partial x^2} \tag{A.13}$$

$$\begin{aligned}\partial M_{41} = &-\left[\rho_1 h_1 eh\frac{h_1 + h}{2} + \rho\frac{h^3}{8}\left(e + \frac{1}{3}\right)\right]\frac{\partial}{\partial x} \\ &- \left(\rho_1 h_1 h^3\frac{h + h_1}{24} + \frac{\rho h^5}{90}\right)\frac{\partial^3}{\partial x^3}\end{aligned} \tag{A.14}$$

$$\begin{aligned}\partial M_{42} = &-\left[\rho_1 h_1 e\frac{h^2}{2} + \frac{\rho h^3}{24}(5e + 1)\right]\frac{\partial}{\partial x} \\ &- \left(\frac{\rho_1 h_1 h^4}{24} + \frac{13\rho h^5}{720}\right)\frac{\partial^3}{\partial x^3}\end{aligned} \tag{A.15}$$

$$\partial M_{43} = \left(\rho_1 h_1 eh + \rho e\frac{h^2}{2}\right) + \left(\rho_1 h_1\frac{h^3}{12} + \frac{\rho h^4}{24}\right)\frac{\partial^2}{\partial x^2} \tag{A.16}$$

$$\partial M_{44} = \left(\rho_1 h_1 e^2 h^2 + \rho e^2 \frac{h^3}{3} \right) - \frac{\rho h^5}{160} \frac{\partial^2}{\partial x^2}$$

$$- \left(\frac{\rho_1 h^6 h_1}{144} + \frac{13 \rho h^7}{5040} \right) \frac{\partial^4}{\partial x^4} \qquad \text{(A.17)}$$

$$\partial K_{11} = \frac{E_c}{h} + \left(E_1 \frac{h_1^3}{12} + E_1 (h_1 + h)^2 \frac{h_1}{4} \right) \frac{\partial^4}{\partial x^4} \qquad \text{(A.18)}$$

$$\partial K_{12} = -\frac{E_c}{h} + E_1 h_1 h \frac{h_1 + h}{4} \frac{\partial^4}{\partial x^4} \qquad \text{(A.19)}$$

$$\partial K_{13} = -E_1 h_1 \frac{h_1 + h}{2} \frac{\partial^3}{\partial x^3} \qquad \text{(A.20)}$$

$$\partial K_{14} = -E_1 h e (h + h_1) \frac{h}{2} \frac{\partial^3}{\partial x^3} + E_1 h_1 (h_1 + h) \frac{h^3}{24} \frac{\partial^5}{\partial x^5} \qquad \text{(A.21)}$$

$$\partial K_{21} = \partial K_{12} \qquad \text{(A.22)}$$

$$\partial K_{22} = \frac{E_c}{h} + \left(E_1 h_1 \frac{h^2}{4} + \frac{E_2 h_2^3}{3} \right) \frac{\partial^4}{\partial x^4} \qquad \text{(A.23)}$$

$$\partial K_{23} = -\frac{1}{2}\left(E_1 h_1 h - E_2 h_2^2\right)\frac{\partial^3}{\partial x^3} \tag{A.24}$$

$$\partial K_{24} = -E_1 e h_1 \frac{h^2}{2}\frac{\partial^3}{\partial x^3} + E_1 h_1 \frac{h^4}{24}\frac{\partial^5}{\partial x^5} \tag{A.25}$$

$$\partial K_{31} = E_1 (h_1 + h)\frac{h_1}{2}\frac{\partial^3}{\partial x^3} \tag{A.26}$$

$$\partial K_{32} = \frac{1}{2}\left(E_1 h_1 h - E_2 h_2^2\right)\frac{\partial^3}{\partial x^3} \tag{A.27}$$

$$\partial K_{33} = -(E_1 h_1 + E_2 h_2)\frac{\partial^2}{\partial x^2} \tag{A.28}$$

$$\partial K_{34} = -E_1 h_1 e h \frac{\partial^2}{\partial x^2} + E_1 h_1 \frac{h^3}{12}\frac{\partial^4}{\partial x^4} \tag{A.29}$$

$$\begin{aligned}\partial K_{41} = {} & -E_c \frac{h}{2}\frac{\partial}{\partial x} + E_1 h_1 e (h_1 + h)\frac{h}{2}\frac{\partial^3}{\partial x^3} \\ & - E_1 h_1 (h_1 + h)\frac{h^3}{24}\frac{\partial^5}{\partial x^5}\end{aligned} \tag{A.30}$$

$$\partial K_{42} = E_c \frac{h}{2}\frac{\partial}{\partial x} + E_1 h_1 e \frac{h^2}{2}\frac{\partial^3}{\partial x^3} - E_1 h_1 \frac{h^4}{24}\frac{\partial^5}{\partial x^5} \tag{A.31}$$

$$\partial K_{43} = -E_1 h_1 e h \frac{\partial^2}{\partial x^2} + E_1 h_1 \frac{h^3}{12} \frac{\partial^4}{\partial x^4} \tag{A.32}$$

$$\begin{aligned} \partial K_{44} = {} & G_c h e^2 - \left(E_1 h_1 e^2 h^2 + E_c \frac{h^3}{12} \right) \frac{\partial^2}{\partial x^2} \\ & + E_1 h_1 e \frac{h^4}{6} \frac{\partial^4}{\partial x^4} - E_1 h_1 \frac{h^6}{144} \frac{\partial^6}{\partial x^6} \end{aligned} \tag{A.33}$$

The consistent boundary conditions are also derived from the Hamilton principle imposed on total kinetic and potential energy. It is noted that the traction boundary conditions and mixed boundary conditions given in Eqn (2.24) through (2.31) in Chapter 2 can be expressed in term of four basic functions, $w_1(x,t)$, $w_2(x,t)$, $u_0(x,t)$, and $\psi(x,t)$. All boundary conditions at two ends of a sandwich beam are given as follows,

at $x = 0$ and $x = l$,

$$w_1 = 0 \tag{A.34}$$

or

$$\left\{ \partial B_1^1 \;\; \partial B_2^1 \;\; \partial B_3^1 \;\; \partial B_4^1 \right\} \begin{Bmatrix} \ddot{w}_1 \\ \ddot{w}_2 \\ \ddot{u}_0 \\ \ddot{\psi} \end{Bmatrix} + \left\{ \partial C_1^1 \;\; \partial C_2^1 \;\; \partial C_3^1 \;\; \partial C_4^1 \right\} \begin{Bmatrix} w_1 \\ w_2 \\ u_0 \\ \psi \end{Bmatrix} = 0 \tag{A.35}$$

where partial differential operators ∂B_i^1 and ∂C_i^1 $(i = 1, 2, 3, 4)$ are

$$\partial B_1^1 = -\left[\rho_1 h_1\left(\frac{h_1^2}{3} + \frac{h h_1}{2} + \frac{h^2}{4}\right) + \rho\frac{h^3}{20}\right]\frac{\partial}{\partial x} \tag{A.36}$$

$$\partial B_2^1 = -\left(\rho_1 h_1 h\frac{h_1 + h}{4} - \frac{3\rho h^3}{40}\right)\frac{\partial}{\partial x} \tag{A.37}$$

$$\partial B_3^1 = \rho_1 h_1\frac{h_1 + h}{2} + \rho\frac{h^2}{6} \tag{A.38}$$

$$\begin{aligned}\partial B_4^1 = {} & \rho_1 h_1 e h\frac{h_1 + h}{2} + \rho e\frac{h^3}{8} \\ & - \left(\rho_1 h_1 h^3\frac{h + h_1}{24} + \rho\frac{h^5}{90}\right)\frac{\partial^2}{\partial x^2}\end{aligned} \tag{A.39}$$

$$\partial C_1^1 = \frac{E_1 h_1}{12}\left(4h_1^2 + 6h_1 h + 3h^2\right)\frac{\partial^3}{\partial x^3} \tag{A.40}$$

$$\partial C_2^1 = E_1(h_1 + h)h\frac{h_1}{4}\frac{\partial^3}{\partial x^3} \tag{A.41}$$

$$\partial C_3^1 = -E_1(h_1 + h)\frac{h_1}{2}\frac{\partial^2}{\partial x^2} \tag{A.42}$$

$$\partial C_4^1 = -E_1 h_1 e(h_1 + h)\frac{h}{2}\frac{\partial^2}{\partial x^2} + E_1 h_1(h_1 + h)\frac{h^3}{24}\frac{\partial^4}{\partial x^4} \tag{A.43}$$

and

$$\frac{\partial w_1}{\partial x} = 0 \tag{A.44}$$

or

$$\left\{\partial C_1^2 \ \partial C_2^2 \ \partial C_3^2 \ \partial C_4^2\right\}\begin{Bmatrix} w_1 \\ w_2 \\ u_0 \\ \psi \end{Bmatrix} = 0 \tag{A.45}$$

where partial differential operators ∂C_i^2 $(i = 1, 2, 3, 4)$ are

$$\partial C_1^2 = \left[\frac{(h_1 + h)^2}{2} + \frac{h_1^2}{6}\right]\frac{\partial^2}{\partial x^2} \tag{A.46}$$

$$\partial C_2^2 = (h_1 + h)\frac{h}{2}\frac{\partial^2}{\partial x^2} \tag{A.47}$$

$$\partial C_3^2 = -(h_1 + h)\frac{\partial}{\partial x} \tag{A.48}$$

$$\partial C_4^2 = -(h_1 + h)eh\frac{\partial}{\partial x} + (h_1 + h)\frac{h^3}{12}\frac{\partial^3}{\partial x^3} \tag{A.49}$$

and

$$w_2 = 0 \tag{A.50}$$

or

$$\left\{\partial B_1^3 \ \partial B_2^3 \ \partial B_3^3 \ \partial B_4^3\right\}\begin{Bmatrix}\ddot{w}_1\\ \ddot{w}_2\\ \ddot{u}_0\\ \ddot{\psi}\end{Bmatrix} + \left\{\partial C_1^3 \ \partial C_2^3 \ \partial C_3^3 \ \partial C_4^3\right\}\begin{Bmatrix}w_1\\ w_2\\ u_0\\ \psi\end{Bmatrix} = 0 \tag{A.51}$$

where partial differential operators ∂B_i^3 and ∂C_i^3 (i = 1, 2, 3, 4) are

$$\partial B_1^3 = -\left[\rho_1 h_1 h \frac{h_1 + h}{4} + \frac{3\rho h^3}{40}\right]\frac{\partial}{\partial x} \tag{A.52}$$

$$\partial B_2^3 = -\left(\rho_1 h_1 h \frac{h_1 + h}{4} + \rho_2 \frac{h_2^3}{4} + \frac{2\rho h^3}{15}\right)\frac{\partial}{\partial x} \tag{A.53}$$

$$\partial B_3^3 = \rho_1 h_1 \frac{h}{2} - \rho_2 \frac{h_2^2}{2} + \rho \frac{h^2}{3} \tag{A.54}$$

$$\begin{aligned}\partial B_4^3 = {} & \rho_1 h_1 e \frac{h^2}{2} + \frac{5\rho e h^3}{24} \\ & - \left(\rho_1 h_1 \frac{h^4}{24} + \frac{13\rho h^5}{720}\right)\frac{\partial^2}{\partial x^2}\end{aligned} \tag{A.55}$$

$$\partial C_1^3 = E_1(h_1 + h)h\frac{h_1}{4}\frac{\partial^3}{\partial x^3} \tag{A.56}$$

$$\partial C_2^3 = \left(E_1 h_1 \frac{h^2}{4} + E_2\frac{h_2^3}{6}\right)\frac{\partial^3}{\partial x^3} \tag{A.57}$$

$$\partial C_3^3 = -\left(E_1 h_1 \frac{h}{2} + E_2\frac{h_2^2}{2}\right)\frac{\partial^2}{\partial x^2} \tag{A.58}$$

$$\partial C_4^3 = -E_1 h_1 e\frac{h^2}{2}\frac{\partial^2}{\partial x^2} + E_1 h_1\frac{h^4}{24}\frac{\partial^4}{\partial x^4} \tag{A.59}$$

and

$$\frac{\partial w_2}{\partial x} = 0 \tag{A.60}$$

or

$$\left\{\partial C_1^4 \;\; \partial C_2^4 \;\; \partial C_3^4 \;\; \partial C_4^4\right\}\begin{Bmatrix} w_1 \\ w_2 \\ u_0 \\ \psi \end{Bmatrix} = 0 \tag{A.61}$$

where partial differential operators ∂C_i^4 $(i = 1, 2, 3, 4)$ are

$$\partial C_1^4 = E_1 h_1 h \frac{h_1 + h}{4} \frac{\partial^2}{\partial x^2} \tag{A.62}$$

$$\partial C_2^4 = \left(E_1 h_1 \frac{h^2}{4} + E_2 \frac{h_2^3}{3} \right) \frac{\partial^2}{\partial x^2} \tag{A.63}$$

$$\partial C_3^4 = \left(- E_1 h_1 \frac{h}{2} + E_2 \frac{h_2^2}{2} \right) \frac{\partial}{\partial x} \tag{A.64}$$

$$\partial C_4^4 = - E_1 h_1 e \frac{h^2}{2} \frac{\partial}{\partial x} + E_1 h_1 \frac{h^4}{24} \frac{\partial^3}{\partial x^3} \tag{A.65}$$

and

$$u_0 = 0 \tag{A.66}$$

or

$$\left\{ \partial C_1^5 \;\; \partial C_2^5 \;\; \partial C_3^5 \;\; \partial C_4^5 \right\} \begin{Bmatrix} w_1 \\ w_2 \\ u_0 \\ \psi \end{Bmatrix} = 0 \tag{A.67}$$

where partial differential operators ∂C_i^5 $(i = 1, 2, 3, 4)$ are

$$\partial C_1^5 = E_1 h_1 \frac{h_1 + h}{2} \frac{\partial^2}{\partial x^2} \tag{A.68}$$

$$\partial C_2^5 = \left(E_1 h_1 \frac{h}{2} - E_2 h_2 \frac{h}{2} \right) \frac{\partial^2}{\partial x^2} \tag{A.69}$$

$$\partial C_3^5 = -\left(E_1 h_1 + E_2 h_2 \right) \frac{\partial}{\partial x} \tag{A.70}$$

$$\partial C_4^5 = -E_1 h_1 e h \frac{\partial}{\partial x} + E_1 h_1 \frac{h^3}{12} \frac{\partial^3}{\partial x^3} \tag{A.71}$$

and

$$\psi = 0 \tag{A.72}$$

or

$$\left\{ \partial B_1^6 \;\; \partial B_2^6 \;\; \partial B_3^6 \;\; \partial B_4^6 \right\} \begin{Bmatrix} \ddot{w}_1 \\ \ddot{w}_2 \\ \ddot{u}_0 \\ \ddot{\psi} \end{Bmatrix} + \left\{ \partial C_1^6 \;\; \partial C_2^6 \;\; \partial C_3^6 \;\; \partial C_4^6 \right\} \begin{Bmatrix} w_1 \\ w_2 \\ u_0 \\ \psi \end{Bmatrix} = 0 \tag{A.73}$$

where partial differential operators $\partial \mathrm{B}_i^6$ and $\partial \mathrm{C}_i^6$ (i = 1, 2, 3, 4) are

$$\partial B_1^6 = -\frac{\rho h^3}{24} - \left(\rho_1 h_1 h^3 \frac{h_1 + h}{24} + \frac{\rho h^5}{90} \right) \frac{\partial^2}{\partial x^2} \tag{A.74}$$

$$\partial B_2^6 = -\frac{\rho h^3}{24} - \left(\rho_1 h_1 \frac{h^4}{24} + \frac{13 \rho h^5}{720} \right) \frac{\partial^2}{\partial x^2} \tag{A.75}$$

$$\partial B_3^6 = \left(\rho_1 h_1 \frac{h^3}{12} + \rho \frac{h^4}{24} \right) \frac{\partial}{\partial x} \tag{A.76}$$

$$\partial B_4^6 = \frac{1}{12}\left(\rho_1 h_1 e h^4 + \frac{7\rho e h^5}{20} - \frac{3\rho h^5}{40} \right) \frac{\partial}{\partial x} - \frac{1}{12}\left(\frac{\rho_1 h_1 h^6}{12} + \frac{13\rho h^7}{420} \right) \frac{\partial^3}{\partial x^3} \tag{A.77}$$

$$\partial C_1^6 = E_1 (h_1 + h) e h_1 \frac{h}{2} \frac{\partial^2}{\partial x^2} - E_1 (h_1 + h) h_1 \frac{h^3}{2} \frac{\partial^4}{\partial x^4} \tag{A.78}$$

$$\partial C_2^6 = E_1 h_1 e \frac{h^2}{2} \frac{\partial^2}{\partial x^2} - E_1 h_1 \frac{h^4}{24} \frac{\partial^4}{\partial x^4} \tag{A.79}$$

$$\partial C_3^6 = - E_1 h_1 e h \frac{\partial}{\partial x} + E_1 h_1 \frac{h^3}{12} \frac{\partial^3}{\partial x^3} \tag{A.80}$$

$$\partial C_4^6 = - \left(E_c \frac{h^3}{12} + E_1 h_1 e^2 h^2 \right) \frac{\partial}{\partial x} + E_1 h_1 e \frac{h^4}{6} \frac{\partial^3}{\partial x^3} - \frac{E_1 h_1 h^6}{144} \frac{\partial^5}{\partial x^5} \tag{A.81}$$

and

$$\frac{\partial \psi}{\partial x} = 0 \tag{A.82}$$

or

$$\left\{ \partial B_1^7 \;\; \partial B_2^7 \;\; \partial B_3^7 \;\; \partial B_4^7 \right\} \begin{Bmatrix} \ddot{w}_1 \\ \ddot{w}_2 \\ \ddot{u}_0 \\ \ddot{\psi} \end{Bmatrix} + \left\{ \partial C_1^7 \;\; \partial C_2^7 \;\; \partial C_3^7 \;\; \partial C_4^7 \right\} \begin{Bmatrix} w_1 \\ w_2 \\ u_0 \\ \psi \end{Bmatrix} = 0 \tag{A.83}$$

where partial differential operators ∂B_i^7 and ∂C_i^7 (i = 1, 2, 3, 4) are

$$\partial B_1^7 = \left(\rho_1 h_1 h^3 \frac{h_1 + h}{24} + \frac{\rho h^5}{90} \right) \frac{\partial}{\partial x} \tag{A.84}$$

$$\partial B_2^7 = \left(\rho_1 h_1 \frac{h^4}{24} + \frac{13 \rho h^5}{720} \right) \frac{\partial}{\partial x} \tag{A.85}$$

$$\partial B_3^7 = - \left(\rho_1 h_1 \frac{h^3}{12} + \rho \frac{h^4}{24} \right) \tag{A.86}$$

$$\begin{aligned} \partial B_4^7 = & - \frac{1}{12} \left(\rho_1 h_1 e h^4 + \frac{7 \rho e h^5}{20} \right) \\ & + \frac{1}{12} \left(\frac{\rho_1 h_1 h^6}{12} + \frac{13 \rho h^7}{420} \right) \frac{\partial^2}{\partial x^2} \end{aligned} \tag{A.87}$$

$$\partial C_1^7 = E_1 h_1 (h_1 + h) \frac{h^3}{24} \frac{\partial^3}{\partial x^3} \tag{A.88}$$

$$\partial C_2^7 = E_1 h_1 \frac{h^4}{24} \frac{\partial^3}{\partial x^3} \tag{A.89}$$

$$\partial C_3^7 = - E_1 h_1 \frac{h^3}{12} \frac{\partial^2}{\partial x^2} \tag{A.90}$$

$$\partial C_4^7 = -E_1 h_1 e \frac{h^4}{12} \frac{\partial^2}{\partial x^2} + E_1 h_1 \frac{h^6}{144} \frac{\partial^4}{\partial x^4} \tag{A.91}$$

and

$$\frac{\partial^2 \psi}{\partial x^2} = 0 \tag{A.92}$$

or

$$\left\{ \partial C_1^8 \ \partial C_2^8 \ \partial C_3^8 \ \partial C_4^8 \right\} \begin{Bmatrix} w_1 \\ w_2 \\ u_0 \\ \psi \end{Bmatrix} = 0 \tag{A.93}$$

where partial differential operators ∂C_i^8 (i = 1, 2, 3, 4) are

$$\partial C_1^8 = \frac{h_1 + h}{2} \frac{\partial^2}{\partial x^2} \tag{A.94}$$

$$\partial C_2^8 = \frac{h}{2} \frac{\partial^2}{\partial x^2} \tag{A.95}$$

$$\partial C_3^8 = -\frac{\partial}{\partial x} \tag{A.96}$$

$$\partial C_4^8 = -eh \frac{\partial}{\partial x} + \frac{h^3}{12} \frac{\partial^3}{\partial x^3} \tag{A.97}$$

APPENDIX B
EQUATIONS OF MOTION WITH IMPERFECT INTERFACE

Since the imperfect interface conditions were considered in Chapter 3, the Lagrange multiplier has been introduced in deriving the governing equations of motion and corresponding boundary conditions of a sandwich beam based on the variational principles. The five basic functions, $w_1(x,t)$, $w_2(x,t)$, $u_1(x,t)$, $u_2(x,t)$ and $\psi(x,t)$, are used in the governing equations of motion which can be written in the following matrix form:

$$\begin{bmatrix} \partial M_{11} & \partial M_{12} & \partial M_{13} & \partial M_{14} & \partial M_{15} \\ \partial M_{21} & \partial M_{22} & \partial M_{23} & \partial M_{24} & \partial M_{25} \\ \partial M_{31} & \partial M_{32} & \partial M_{33} & \partial M_{34} & \partial M_{35} \\ \partial M_{41} & \partial M_{42} & \partial M_{43} & \partial M_{44} & \partial M_{45} \\ \partial M_{51} & \partial M_{52} & \partial M_{53} & \partial M_{54} & \partial M_{55} \end{bmatrix} \begin{Bmatrix} \ddot{w}_1 \\ \ddot{w}_2 \\ \ddot{u}_1 \\ \ddot{u}_2 \\ \ddot{\psi} \end{Bmatrix} + \begin{bmatrix} \partial K_{11} & \partial M_{12} & \partial K_{13} & \partial K_{14} & \partial K_{15} \\ \partial K_{21} & \partial K_{22} & \partial K_{23} & \partial K_{24} & \partial K_{25} \\ \partial K_{31} & \partial K_{32} & \partial K_{33} & \partial K_{34} & \partial K_{35} \\ \partial K_{41} & \partial K_{42} & \partial K_{43} & \partial K_{44} & \partial K_{45} \\ \partial K_{51} & \partial K_{52} & \partial K_{53} & \partial K_{54} & \partial K_{55} \end{bmatrix} \begin{Bmatrix} w_1 \\ w_2 \\ u_1 \\ u_2 \\ \psi \end{Bmatrix} = \begin{Bmatrix} q_1 \\ 0 \\ 0 \\ 0 \\ 0 \end{Bmatrix} \tag{B.1}$$

where ∂M_{ij} and ∂K_{ij} (i, j = 1, 2...5) are the mass matrix differential operators and stiffness matrix differential operators, respectively. This equation is the same as Eqn (3.12), and the elements in two matrices are

$$\partial M_{11} = \rho_1 h_1 + \rho \frac{h}{6} - \left(\rho_1 \frac{h_1^3}{12} + \rho \frac{h^3}{20} \right) \frac{\partial^2}{\partial x^2} \tag{B.2}$$

$$\partial M_{12} = \rho \frac{h}{3} - \rho \frac{h^2}{4} \left(\frac{h_2}{3} + \frac{3h}{10} \right) \frac{\partial^2}{\partial x^2} \tag{B.3}$$

$$\partial M_{13} = 0 \tag{B.4}$$

$$\partial M_{14} = \rho \frac{h^2}{6} \frac{\partial}{\partial x} \tag{B.5}$$

$$\partial M_{15} = \rho \frac{h^2}{2} \left(\frac{E_c}{3k^*} + \frac{eh}{4} + \frac{h}{24} \right) \frac{\partial}{\partial x} - \rho \frac{h^5}{90} \frac{\partial^3}{\partial x^3} \tag{B.6}$$

$$\partial M_{21} = \partial M_{12} \tag{B.7}$$

$$\partial M_{22} = \rho_2 h_2 + \rho \frac{h}{6} - \left[\rho_2 \frac{h_2^3}{12} + \rho h \left(\frac{h_2^2}{4} + \frac{h_2 h}{3} + \frac{2h^2}{15} \right) \right] \frac{\partial^2}{\partial x^2} \tag{B.8}$$

$$\partial M_{23} = 0 \tag{B.9}$$

$$\partial M_{24} = \rho h \left(\frac{h_2}{2} + \frac{h}{3} \right) \frac{\partial}{\partial x} \tag{B.10}$$

$$\partial M_{25} = \rho\, h\left[\frac{E_c}{k'}\left(\frac{h_2}{2}+\frac{h}{3}\right)+\frac{eh}{4}\left(h_2+\frac{3}{2}h\right)+\frac{h_2}{16}\right]\frac{\partial}{\partial x} - \rho\,\frac{h^4}{18}\left(h_2+\frac{13}{15}h\right)\frac{\partial^3}{\partial x^3} \tag{B.11}$$

$$\partial M_{31} = -\,\rho\,\frac{h^2}{2}\left(\frac{E_c}{3k'}+\frac{eh}{4}+\frac{h}{12}\right)\frac{\partial}{\partial x} - \frac{\rho\, h^5}{90}\frac{\partial^3}{\partial x^3} \tag{B.12}$$

$$\partial M_{32} = -\,\rho\, h\left[\left(\frac{h_1}{2}+\frac{h}{3}\right)\frac{E_c}{k'}+eh\left(\frac{h_2}{4}+\frac{5h}{24}\right)+\frac{h^2}{24}\right]\frac{\partial}{\partial x} - \rho\,\frac{h^4}{2}\left(\frac{h_2}{24}+\frac{13h}{360}\right)\frac{\partial^3}{\partial x^3} \tag{B.13}$$

$$\partial M_{33} = \rho_1 h_1\left(2\frac{E_c}{k'}+e\,h\right) \tag{B.14}$$

$$\partial M_{34} = \rho\, h\left(\frac{E_c}{k'}+\frac{eh}{2}\right)+\frac{\rho h^4}{24}\frac{\partial^2}{\partial x^2} \tag{B.15}$$

$$\partial M_{35} = \rho h\left[\left(\frac{E_c}{k^{\cdot}} + \frac{eh}{2}\right)\frac{E_c}{k^{\cdot}} + \left(\frac{E_c}{k^{\cdot}} + \frac{eh}{3}\right)e\,h\right] - \frac{\rho h^5}{160}\frac{\partial^2}{\partial x^2} - \frac{13\rho h^7}{6040}\frac{\partial^4}{\partial x^4} \tag{B.16}$$

$$\partial M_{41} = -\,\partial M_{14} \tag{B.17}$$

$$\partial M_{42} = -\,\partial M_{24} \tag{B.18}$$

$$\partial M_{43} = \rho_1 h_1 \tag{B.19}$$

$$\partial M_{44} = \rho_2 h_2 + \rho\, h \tag{B.20}$$

$$\partial M_{45} = \rho h\left(\frac{E_c}{k^{\cdot}} + \frac{eh}{2}\right) - \frac{\rho h^4}{24}\frac{\partial^2}{\partial x^2} \tag{B.21}$$

$$\partial M_{51} = 0 \tag{B.22}$$

$$\partial M_{52} = 0 \tag{B.23}$$

$$\partial M_{53} = 0 \tag{B.24}$$

$$\partial M_{54} = 0 \tag{B.25}$$

$$\partial M_{55} = 0 \tag{B.26}$$

$$\partial K_{11} = \frac{E_c}{h} + \frac{E_1 h_1^3}{12}\frac{\partial^4}{\partial x^4} \tag{B.27}$$

$$\partial K_{12} = -\frac{E_c}{h} \tag{B.28}$$

$$\partial K_{13} = 0 \tag{B.29}$$

$$\partial K_{14} = 0 \tag{B.30}$$

$$\partial K_{15} = 0 \tag{B.31}$$

$$\partial K_{21} = \partial K_{12} \tag{B.32}$$

$$\partial K_{22} = \frac{E_c}{h} + \frac{E_2 h_2^3}{3}\frac{\partial^4}{\partial x^4} \tag{B.33}$$

$$\partial K_{23} = 0 \tag{B.34}$$

$$\partial K_{24} = 0 \tag{B.35}$$

$$\partial K_{25} = 0 \tag{B.36}$$

$$\partial K_{31} = 0 \tag{B.37}$$

$$\partial K_{32} = 0 \tag{B.38}$$

$$\partial K_{33} = -E_1 h_1 \left(2\frac{E_c}{k^*} + e\,h \right) \frac{\partial^2}{\partial x^2} \tag{B.39}$$

$$\partial K_{34} = 0 \tag{B.40}$$

$$\partial K_{35} = G_c h e^2 - E_c \frac{h^3}{12} \frac{\partial^2}{\partial x^2} \tag{B.41}$$

$$\partial K_{41} = 0 \tag{B.42}$$

$$\partial K_{42} = 0 \tag{B.43}$$

$$\partial K_{43} = -E_1 h_1 \frac{\partial^2}{\partial x^2} \tag{B.44}$$

$$\partial K_{44} = -E_2 h_2 \frac{\partial^2}{\partial x^2} \tag{B.45}$$

$$\partial K_{45} = 0 \tag{B.46}$$

$$\partial K_{51} = -k^{*}\frac{h+h_1}{2}\frac{\partial}{\partial x} \tag{B.47}$$

$$\partial K_{52} = -k^{*}\frac{h+h_2}{2}\frac{\partial}{\partial x} \tag{B.48}$$

$$\partial K_{53} = -k^{*} \tag{B.49}$$

$$\partial K_{54} = k^{*} \tag{B.50}$$

$$\partial K_{55} = k^{*}eh + 2E_c - k^{*}\frac{h^3}{12}\frac{\partial^2}{\partial x^2} \tag{B.51}$$

The consistent boundary conditions are also derived from the Hamilton principle imposed on total kinetic and potential energy. Both displacement and traction boundary conditions given in Eqns (3.13) through (3-20) can be expressed in term of five basic functions, $w_1(x,t)$, $w_2(x,t)$, $u_1(x,t)$, $u_2(x,t)$ and $\psi(x,t)$, as follows

at $x = 0$ and $x = l$,

$$w_1 = 0 \tag{B.52}$$

or

$$\left\{\partial B_1^1 \;\; \partial B_2^1 \;\; \partial B_3^1 \;\; \partial B_4^1 \;\; B_5^1\right\}\left\{\begin{matrix}\ddot{w}_1\\ \ddot{w}_2\\ \ddot{u}_1\\ \ddot{u}_2\\ \ddot{\psi}\end{matrix}\right\} + \left\{\partial C_1^1 \;\; \partial C_2^1 \;\; \partial C_3^1 \;\; \partial C_4^1 \;\; \partial C_5^1\right\}\left\{\begin{matrix}w_1\\ w_2\\ u_1\\ u_2\\ \psi\end{matrix}\right\} = 0 \quad \text{(B.53)}$$

where partial differential operators ∂B_i^1 and ∂C_i^1 (i = 1, 2,...5) are

$$\partial B_1^1 = -\left(\rho_1 \frac{h_1^3}{12} + \rho \frac{h^3}{20}\right)\frac{\partial}{\partial x} \quad \text{(B.54)}$$

$$\partial B_2^1 = -\rho \frac{h^2}{2}\left(\frac{3h}{20} + \frac{h_2}{6}\right)\frac{\partial}{\partial x} \quad \text{(B.55)}$$

$$\partial B_3^1 = \rho_1 h_1 \frac{h_1 + h}{2} \quad \text{(B.56)}$$

$$\partial B_4^1 = \rho \frac{h^2}{6} \quad \text{(B.57)}$$

$$\partial B_5^1 = \rho \frac{h^2}{2}\left(\frac{E_c}{3k'} + \frac{eh}{4}\right) - \rho \frac{h^5}{90}\frac{\partial^2}{\partial x^2} \quad \text{(B.58)}$$

$$\partial C_1^1 = \frac{E_1 h_1^3}{12}\frac{\partial^3}{\partial x^3} \quad \text{(B.59)}$$

$$\partial C_2^1 = 0 \tag{B.60}$$

$$\partial C_3^1 = -E_1(h_1 + h)\frac{h_1}{2}\frac{\partial^2}{\partial x^2} \tag{B.61}$$

$$\partial C_4^1 = 0 \tag{B.62}$$

$$\partial C_5^1 = 0 \tag{B.63}$$

and

$$\frac{\partial w_1}{\partial x} = 0 \tag{B.64}$$

or

$$\left\{\partial C_1^2 \;\; \partial C_2^2 \;\; \partial C_3^2 \;\; \partial C_4^2\right\}\begin{Bmatrix} w_1 \\ w_2 \\ u_0 \\ \psi \end{Bmatrix} = 0 \tag{B.65}$$

where partial differential operators ∂C_i^2 (i = 1, 2, 3, 4) are

$$\partial C_1^2 = -E_1\frac{h_1^3}{12}\frac{\partial^2}{\partial x^2} \tag{B.66}$$

$$\partial C_2^2 = 0 \tag{B.67}$$

$$\partial C_3^2 = 0 \tag{B.68}$$

$$\partial C_4^2 = 0 \tag{B.69}$$

$$\partial C_5^2 = 0 \tag{B.70}$$

and

$$w_2 = 0 \tag{B.71}$$

or

$$\left\{ \partial B_1^3 \;\; \partial B_2^3 \;\; \partial B_3^3 \;\; \partial B_4^3 \;\; \partial B_5^3 \right\} \left\{ \begin{matrix} \ddot{w}_1 \\ \ddot{w}_2 \\ \ddot{u}_1 \\ \ddot{u}_2 \\ \ddot{\psi} \end{matrix} \right\} + \left\{ \partial C_1^3 \;\; \partial C_2^3 \;\; \partial C_3^3 \;\; \partial C_4^3 \;\; \partial C_5^3 \right\} \left\{ \begin{matrix} w_1 \\ w_2 \\ u_1 \\ u_2 \\ \psi \end{matrix} \right\} = 0 \tag{B.72}$$

where partial differential operators $\partial \mathrm{B}_i^3$ and $\partial \mathrm{C}_i^3$ (i = 1, 2,...5) are

$$\partial B_1^3 = -\rho \frac{h^2}{4} \left(\frac{h_2}{3} + \frac{3h}{10} \right) \frac{\partial}{\partial x} \tag{B.73}$$

$$\partial B_2^3 = -\left[\rho_2 \frac{h_2^3}{12} + \rho h \left(\frac{h_2^2}{4} + \frac{h_2 h}{3} + \frac{2h^2}{15} \right) \right] \frac{\partial}{\partial x} \tag{B.74}$$

$$\partial B_3^3 = 0 \tag{B.75}$$

$$\partial B_4^3 = \rho h \left(\frac{h_2}{2} + \frac{h}{3} \right) \tag{B.76}$$

$$\partial B_5^3 = \rho h \frac{h_2}{2} \left(\frac{E_c}{k^*} + \frac{eh}{2} \right) + \rho h^2 \left(\frac{E_c}{3k^*} + \frac{3eh}{8} \right) - \frac{\rho h^4}{48} \left(h_2 + \frac{h}{15} \right) \frac{\partial^2}{\partial x^2} \tag{B.77}$$

$$\partial C_1^3 = 0 \tag{B.78}$$

$$\partial C_2^3 = E_2 \frac{h_2^3}{12} \tag{B.79}$$

$$\partial C_3^3 = 0 \tag{B.80}$$

$$\partial C_4^3 = 0 \tag{B.81}$$

$$\partial C_5^3 = 0 \tag{B.82}$$

and

$$\frac{\partial w_2}{\partial x} = 0 \tag{B.83}$$

or

$$\left\{ \partial C_1^4 \; \partial C_2^4 \; \partial C_3^4 \; \partial C_4^4 \; \partial C_5^4 \right\} \begin{Bmatrix} w_1 \\ w_2 \\ u_1 \\ u_2 \\ \psi \end{Bmatrix} = 0 \qquad \text{(B.84)}$$

where partial differential operators ∂C_i^4 ($i = 1, 2, ...5$) are

$$\partial C_1^4 = 0 \qquad \text{(B.85)}$$

$$\partial C_2^4 = -E_2 \frac{h_2^3}{12} \frac{\partial^2}{\partial x^2} \qquad \text{(B.86)}$$

$$\partial C_3^4 = 0 \qquad \text{(B.87)}$$

$$\partial C_4^4 = 0 \qquad \text{(B.88)}$$

$$\partial C_5^4 = 0 \qquad \text{(B.89)}$$

and

$$u_1 = 0 \qquad \text{(B.90)}$$

or

$$\left\{ \partial C_1^5 \; \partial C_2^5 \; \partial C_3^5 \; \partial C_4^5 \; \partial C_5^5 \right\} \begin{Bmatrix} w_1 \\ w_2 \\ u_1 \\ u_2 \\ \psi \end{Bmatrix} = 0 \qquad \text{(B.91)}$$

where partial differential operators ∂C_i^5 (i = 1, 2,...5) are

$$\partial C_1^5 = 0 \tag{B.92}$$

$$\partial C_2^5 = 0 \tag{B.93}$$

$$\partial C_3^5 = -E_1 h_1 \frac{\partial}{\partial x} \tag{B.94}$$

$$\partial C_4^5 = 0 \tag{B.95}$$

$$\partial C_5^5 = 0 \tag{B.96}$$

and

$$u_2 = 0 \tag{B.97}$$

or

$$\left\{ \partial C_1^6 \ \partial C_2^6 \ \partial C_3^6 \ \partial C_4^6 \ \partial C_5^6 \right\} \begin{Bmatrix} w_1 \\ w_2 \\ u_1 \\ u_2 \\ \psi \end{Bmatrix} = 0 \tag{B.98}$$

where partial differential operators ∂C_i^6 (i = 1, 2,...5) are

$$\partial C_1^6 = 0 \tag{B.99}$$

$$\partial C_2^6 = 0 \tag{B.100}$$

$$\partial C_3^6 = 0 \tag{B.101}$$

$$\partial C_4^6 = -E_2 h_2 \frac{\partial}{\partial x} \tag{B.102}$$

$$\partial C_5^6 = 0 \tag{B.103}$$

and

$$\psi = 0 \tag{B.104}$$

or

$$\left\{\partial B_1^7 \ \partial B_2^7 \ \partial B_3^7 \ \partial B_4^7 \ \partial B_5^7\right\}\begin{Bmatrix} \ddot{w}_1 \\ \ddot{w}_2 \\ \ddot{u}_1 \\ \ddot{u}_2 \\ \ddot{\psi} \end{Bmatrix} + \left\{\partial C_1^7 \ \partial C_2^7 \ \partial C_3^7 \ \partial C_4^7 \ \partial C_5^7\right\}\begin{Bmatrix} w_1 \\ w_2 \\ u_1 \\ u_2 \\ \psi \end{Bmatrix} = 0 \tag{B.105}$$

where partial differential operators ∂B_i^7 and ∂C_i^7 ($i = 1, 2, \ldots 5$) are

$$\partial B_1^7 = -\frac{\rho h^3}{24} - \frac{\rho h^5}{90}\frac{\partial^2}{\partial x^2} \tag{B.106}$$

$$\partial B_2^7 = -\frac{\rho h^3}{24} - \frac{\rho h^4}{48}\left(h_2 + \frac{13h}{15}\right)\frac{\partial^2}{\partial x^2} \tag{B.107}$$

$$\partial B_3^7 = 0 \tag{B.108}$$

$$\partial B_4^7 = \frac{\rho h^4}{24}\frac{\partial}{\partial x} \tag{B.109}$$

$$\partial B_5^7 = \frac{\rho h^4}{24}\left(\frac{E_c}{k^*} + \frac{7eh}{10} - \frac{3h}{20}\right)\frac{\partial}{\partial x} - \frac{13\rho h^7}{6040}\frac{\partial^3}{\partial x^3} \tag{B.110}$$

$$\partial C_1^7 = 0 \tag{B.111}$$

$$\partial C_2^7 = 0 \tag{B.112}$$

$$\partial C_3^7 = 0 \tag{B.113}$$

$$\partial C_4^7 = 0 \tag{B.114}$$

$$\partial C_5^7 = -E_c\frac{h^3}{12}\frac{\partial}{\partial x} \tag{B.115}$$

and

$$\frac{\partial\psi}{\partial x} = 0 \tag{B.116}$$

or

$$\left\{\partial B_1^8\ \partial B_2^8\ \partial B_3^8\ \partial B_4^8\ \partial B_5^8\right\}\begin{Bmatrix}\ddot{w}_1\\ \ddot{w}_2\\ \ddot{u}_1\\ \ddot{u}_2\\ \ddot{\psi}\end{Bmatrix} + \left\{\partial C_1^8\ \partial C_2^8\ \partial C_3^8\ \partial C_4^8\ \partial C_5^8\right\}\begin{Bmatrix}w_1\\ w_2\\ u_1\\ u_2\\ \psi\end{Bmatrix} = 0 \tag{B.117}$$

where partial differential operators ∂B_i^8 and ∂C_i^8 (i = 1, 2,...5) are

$$\partial B_1^8 = \frac{\rho h^5}{90}\frac{\partial}{\partial x} \tag{B.118}$$

$$\partial B_2^8 = \frac{\rho h^4}{24}\left(h_2 + \frac{13h}{15}\right)\frac{\partial}{\partial x} \tag{B.119}$$

$$\partial B_3^8 = \rho h_1 \frac{h^3}{12} \tag{B.120}$$

$$\partial B_4^8 = -\frac{\rho h^4}{24} \tag{B.121}$$

$$\partial B_5^8 = -\frac{\rho h^4}{24}\left(\frac{E_c}{k^*} + \frac{7eh}{10}\right) + \frac{13\rho h^7}{6040}\frac{\partial^2}{\partial x^2} \tag{B.122}$$

$$\partial C_1^8 = 0 \tag{B.123}$$

$$\partial C_2^8 = 0 \tag{B.124}$$

$$\partial C_3^8 = -E_1 h_1 \frac{h^3}{12}\frac{\partial^2}{\partial x^2} \tag{B.125}$$

$$\partial C_4^8 = 0 \tag{B.126}$$

$$\partial C_5^8 = 0 \tag{B.127}$$

REFERENCES

[1] Allen, H. G., "Sandwich Construction Today and Tomorrow," Proceedings of the First International Conference on Sandwich Constructions, Stockholm, Sweden, 1989.

[2] Chai, H., and C. D. Babcock, "Two Dimensional Modeling of Compressive Failure in Delaminated Laminates," Journal of Composite Materials, Vol.19, pp. 67-97, 1985.

[3] NageshBabu, G. L. and S. Hanagud, "Delaminations in Smart Composite Structures—A Parametric Study on Vibration," Proceedings of AIAA/ASME/ASCE/AHS/ASC 31st Structures, Structural Dynamics and Materials Conference, AIAA, Long Beach, pp.2417-2426, 1990.

[4] McConnel, V. P., "Composites Render Sailboat Aeronautical," Advanced Composites, Vol. 16, pp.69-74, Sept./Oct., 1988.

[5] Nagai, T. and S. L. Chuang, "Review of Structural Response Aspects of Slamming," Journal of Ship Research, Vol. 21, pp.182-191, 1977.

[6] Adam, R. D., P. Cawley, C. J. Pye and B. J. Stone, "A Vibration Technique for Non-Destructive Assessing the Integrity of Structures," Journal of Mechanical Engineering Science, Vol.20, pp.93-100, 1978.

[7] Cawley, P. and R. D. Adam, "A Vibration Technique for Non-Destructive Testing of Fiber Composite Structures," Journal Composite Materials, Vol.13, pp.161-175, 1979.

[8] Dibenetto, A. T. J. V. Gauchel, R. L. Thomas and J. W. Barlow, "Non-Destructive Determination of Fatigue Crack Damage Using Vibration Tests," Journal of Materials, Vol.7, pp.211-215, 1972.

[9] Yang, J. C. S., "Detection and Identification of Structural Damage from Dynamic Response Measurement," ASME, The 4th International Symposium on Offshore Mechanics and Artic Engineering, Dallas, TX, February 1985.

[10] Gibson, R. F., "Dynamic Mechanical Behavior of Fiber-Reinforced Composites: Measurement and Analysis," Journal of Composite Materials, Vol.10, pp.325-332, 1976.

[11] Baliscrema, L., A. Castellani and I. Peroni, "Modal Tests on Composite Material Structures Application in Damage Detection,", Proceedings of the 3rd International Modal Analysis Conference, Orlando, FL, pp.708-716, 1985.

[12] Adam, R. D., D. Walton, J. E. Flitcroft and D. Short, "Vibration Testing as a Non-Destructive Test Tool for Composite Materials," Composite Reliability, ASTM STP 580, American Society for Testing and Materials, p.159-175, 1975.

[13] Chamis, C. C., J. H. Sinclair and R. F. Lark, "Dynamic Response of Damaged Angle Plied Fiber Composites," Presented to Modern Developments in Composite Materials and Structures, ASME Winter Meeting, New York, 1979.

[14] Cawley, P. and R. D. Adams, "The Location of the Defects in Structures from Measurements of Natural Frequencies," Journal of Strain Analysis, Vol.14, pp.49-56, 1979.

[15] Liang, R. Y., J. Hu and F. Choy, "Theoretical Study of Crack-Induced Eigenfrequency Changes on Beam Structures," Journal of Engineering Mechanics, Vol.118, pp.384-396, 1992.

[16] Grady, J. E. and C. T. Sun, "An Experimental Study of Dynamic Delamination in Graphite/Epoxy Laminates," Report No. CML 84-2, Composite Material Laboratory, Purdue University, 1984.

[17] Tracy, J. J., D. J. Dimas and G. C. Pardoen, "The Effect of Impact Damage on the Dynamic Properties of Laminated Composite Plates," Proceedings of the Fifth International Conference on Composite Materials, San Diego, CA, June 1985.

[18] Jones, R. and A. Goldman, "Evaluation of a Vibration Technique for Detection of Barely-Visible Impact-Damage in Composites," Department of Defense Aeronautical Research Laboratories, Commonwealth of Australia, Report No. ARL-STRUC-TECH-MEMO-370, December 1983.

[19] Kulkarni, S. V., R. B. Pipes, R. L. Ramakumar and W.R. Scott, "The Analytical, Experimental and Nondestructive Evaluation of the Criticality of an Interlaminar Defect in a Composite Laminate," ICCM-2, Proceedings of the 2nd International Conference on Composite Materials, pp.259-276, Toronto, Canda, 1978.

[20] Reddy, A. D., L. W. Rehfield and R. S. Haag, "Influence of Prescribed Delaminations on Stiffness-Controlled Behavior of Composite Laminates," Effects of Defects in Composite Materials, ASTM STP 836, American Society for Testing and Materials, pp.71-80, 1984.

[21] Tracy, J. J. and G. C. Pardoen, "Effect of Delamination on the Natural Frequencies of Composite Laminates," Journal of Composite Materials, Vol.23, pp.1201-1215, 1989.

[22] Leissa, A. W., "Advances in Vibration, Buckling and Postbuckling Studies on Composite Plate and Shell Panels," Proceedings of First International Conference on Composite Structures, Edited by I. M. Marshall, pp.312-334, Stockholm, Sweden, 1981.

[23] Bert, C. W., "Research on Dynamic Behavior of Composite and Sandwich Plates," Shock and Vibration Digest, Vol.17, pp.3-15, Nov. 1985.

[24] Reddy, J. N., "A Review of the Literature on Finite-Element Modelling of Laminated Composite Plates and Shells," Shock and Vibration Digest, Vol.15, pp.124-138, 1983.

[25] Reddy, J. N., "A Review of the Literature on Finite-Element Modelling of Laminated Composite Plates," Shock and Vibration Digest, Vol.17, pp.3-8, 1985.

[26] Benison, A. S. and J. Mayers, "General Instability and Face Wrinkling of Sandwich Plates: Unified Theory and Applications," AIAA Journal, Vol.5, pp.729-739, 1967.

[27] Allen, H. G., *Analysis and Design of Structural Sandwich Panels*, Pergamon Press, London, 1969.

[28] Plantema, F. J., *Sandwich Construction,* John Wiely and Sons., New York, 1966.

[29] *Mechanical Properties of Hexcel Honeycomb Materials*, TSB120, Hexcel Corporation, Dublin, CA, 1982.

[30] Ojalvo, I. U., "Departures from Classical Beam Theory in Laminated, Sandwich, and Short Beams," AIAA Journal, Vol.15, pp.1581-1591, 1977.

[31] Ogorkiewicz, R. M. and A. A. M. Sayigh, "Deflection of Carbon Fiber/Acrylic Foam Sandwich Beams," Composites, Vol.4, pp.254-257, Nov. 1973.

[32] Weissman-Berman, D., G. L. Petrie and M-H Wang, "Flexural Response of Foam-Cored FRP Sandwich Panels," Proceedings of Annual Meeting of the Society of Naval Architects and Marine Engineers, No.2, pp.1-16, 1988.

[33] Kant, T. and B. S. Manjunath, "Refined Theories for Composite and Sandwich Beams with C^0 Finite Elements," Computers and Structures, Vol.33, pp.755-764, 1989.

[34] Vaswani, J., N., T. Asnani and B. C. Nakra, "Vibration and Damping Analysis of Curved Sandwich Beams with a Viscoelastic Core," Composite Structures, Vol.10, pp.231-245, 1988.

[35] Senthilnathan, N. R., S. P. Lim, K. H. Lee, and S. T. Chow, "Vibration of Laminated Orthotropic Plates Using a Simplified High-Order Deformation Theory," Composite Structures, Vol.10, pp. 211-229, 1988.

[36] Ko, C. L., "Dynamic Analysis for Free Vibrations of Rotating Sandwich Tapered Beam," AIAA Journal, Vol.27, pp.1425-1433, 1989.

[37] Lu, C. and C. Libove, "Beamlike Harmonic Vibration of Variable-Thickness Sandwich Plates," AIAA Journal. Vol. 29, pp.299-305, 1989.

[38] Bai, J. M. and C. T. Sun, "Nonlinear Flexural Vibration of Sandwich Plates Subjected to In-Plane Forces," Proceedings of the Second International Conference on Sandwich Constructions, pp.203-218, Gainesville, FL, 1992.

[39] Reddy, J. N., *Energy and Variational Methods in Applied Mechanics*, John Wiley and Sons, Inc., New York, 1984.

[40] Reddy, J. N., "A Review of Refined Theories of Laminated Composite Plate," The Shock and Vibration Digest, Vol.22, No.7, pp.231-242, 1993.

[41] Ross, D., E. E. Ungar and E. M. Kerwin, Jr., "Damping of Plate Flexural Vibrations by Means of Viscoelastic Laminate," Structural Damping, ASME, New York, pp.49-88, 1959.

[42] R. A. DiTaranto, "Theory of Vibratory Bending for Elastic and Viscoelastic Layered Finite Length Beams," ASME Journal of Applied Mechanics, Vol.87, pp.881-886, 1965.

[43] Mead, D. J. and S. Markus, "The Forced Vibration of a Three-Layer, Damped Sandwich Beam with Arbitrary Boundary Conditions," Journal of Sound and Vibration, Vol.10, pp.163-175, 1969.

[44] Lu, Y. P. and B. E. Douglas, "On the Forced Vibrations of Three-Layer Damped Sandwich Beams," Journal of Sound and Vibration, Vol. 32, pp.13-516, 1974.

[45] Yan, M. J. and E. H. Dowell, "Governing Equations for Vibrating Constrained-Layer damping of Sandwich Beams and Plates," ASME Journal of Applied Mechanics, Vol.94, pp.1041-1047, 1972.

[46] Rao, Y. V. K. and B. C. Nakra, "Vibrations of Unsymmetrical Sandwich Beams and Plates with Viscoelastic Cores," Journal of Sound and Vibration, Vol.34, pp. 309-326, 1974.

[47] Hwu, C. and J. S. Hu, "Buckling and Postbuckling of Delaminated Composite Sandwich Beams," AIAA Journal, Vol.30, pp.1901-1909, July, 1992.

[48] Carlsson, L. A., L. S. Sendlein and S. L. Merry, "Characterization of Face Sheet/Core Shear Fracture of Composite Sandwich Beams," Journal of Composite Materials, Vol.25, pp.101-112, 1991.

[49] Schryver, D., "Boat Test No. 451; Gulfstar 55 Yacht," Boating, Vol. 12, pp.37-42, 1987.

[50] Fazio, P., R. Hussein and K. H. Ha, "Sandwich Beam-columns with Interlayer Slips," Journal of Engineering Mechanics, ASCE, Vol.108, pp.354-366, 1982.

[51] Hussein, R., "Sandwich Plates with Interlayer Slip," Journal of Engineering Mechanics, ASCE, Vol.110, pp.493-506, 1984.

[52] Kim, C. G. and C. S. Hong, "Viscoelastic Sandwich Plates with Crossply Faces," Journal of Structural Engineering, ASCE, Vol.114, pp.150-164, 1988.

[53] Kapania, R. K. and S. Raciti, "Nonlinear Vibrations of Unsymmetrically Laminated Beams," AIAA Journal, Vol.27, pp.201-211, 1989.

[54] Kapania, R. K. and S. Raciti, "Recent Advances in Analysis of Laminated Beams and Plates, Part II: Vibrations and Wave Propagation," AIAA Journal, Vol.27, pp.935-946, 1989.

[55] Reddy, J. N. and T. Kuppusamy, "Natural Vibrations of Laminated Anisotropic Plates," Journal of Sound and Vibration, Vol.94, pp.63-69, May 1984.

[56] Bhimaraddi, A. and L. K. Stephens, "A High order Theory for Free Vibrations of Orthotropic, Homogeneous, and Laminated Rectangular Plates," Journal of Applied Mechanics, Vol.51, pp.195-198, March 1984.

[57] Stein, M. and D. C. Jegley, "Effects of Transverse Shearing on Cylindrical Bending, Vibration, and Buckling of Laminated Plates," AIAA Paper 85-0744, April 1985.

[58] Simitses, G. J., S. N. Sallam and W. L. Yin, "Effect of Delamination of Axially Loaded Homogeneous Laminated Plates," AIAA Journal, Vol.23, pp.1437-1445, 1985.

[59] Yin, W. L., S. N. Sallam and G. J. Simitses, "Ultimate Axial Load Capacity of a Delaminated Beam-Plate," AIAA Journal, Vol.24, pp.123-128, 1986.

[60] Chai, H., C. D. Babcock and W. G. Knauss, "One Dimensional Modeling of Failure in Laminated Plates by Delamination Buckling," International Journal of Solid & Structures, Vol.17, pp.1069-1083, 1981.

[61] Chow, C. L. and Nagan, K. M., "Method of Fracture Toughness Evaluation of Adhesive Joints," Journal of Strain Analysis, Vol.15, pp.97-101, 1980.

[62] Whitcomb, J. D., "Finite Element Analysis of Instability Related Delamination Growth," Journal of Composite Materials, Vol. 15, pp.403-426, 1981.

[63] Yin, W. L. and J. T. S. Wang, "The Energy Release Rate in the Growth of a One-Dimensional Delamination," Journal of Applied Mechanics, Vol.51, pp.939-941, 1984.

[64] Yin, W. L., "Energy Balance and the Speed of Crack Growth in a Buckled Strip Delamination," Proceedings of AIAA/ASME/ASCE/AHS/ASC 28th Structures, Structural Dynamics and Materials Conference, AIAA, New York, pp.748-765, 1987.

[65] Chen, H. P. and W. L. Yin, "Dynamic Analysis of Delamination Growth in a Compressed Laminate," Computational Mechanics'88 Theory and Applications, Vol.1, Springer-Verlag, Berlin, 1988.

[66] Chen, H. P. and H. Ngo, "Dynamic Analysis of Delamination Growth," Proceedings of AIAA/ASME/ASCE/AHS/ASC 30th Structures, Structural Dynamics and Materials Conference, AIAA, Washington, DC, pp.1264-1272, 1989.

[67] Barbero, E. J. and J. N. Reddy, "Modeling of Delamination in Composite Laminates Using a Layer-Wise Plate Theory," International Journal of Solids and Structures, Vol.28, pp.373-388, 1991.

[68] Lee, J., Z. Gürdal and O. H. Griffin, "A Layer-Wise Approach for the Bifurcation Problem in Laminated Composites with Delaminations," AIAA Journal, Vol.31, pp.331-338, 1993.

[69] Suemasu, H., "Effects of Multiple Delaminations on Compressive Buckling of Composite Panels," Journal of Composite Materials, Vol.27, pp.1172-1192, 1993.

[70] Suemasu, H., "Postbuckling Behaviors of Composite Panels with Multiple Delaminations," Journal of Composite Materials, Vol.27, pp.1077-1096, 1993.

[71] Kultu, Z. and F. Chang, "Modeling Compression Failure of Laminated Composites Containing Multiple Through-the-Width Delaminations," Journal of Composite Materials, Vol.26, pp.350-387, 1992.

[72] Peck, S. O. and G. S. Springer, "The Behavior of Delaminations in Composite Plates—Analytical and Experimental Results," Journal of Composites, Vol.25, pp.907-929, 1991.

[73] Kulkarni, S. V. and D. Fredericks, "Frequency as a Parameter in Delamination Problem," Journal of Composite Materials, Vol.5, pp.112-119, 1971.

[74] Ramkumar, R. L., S. V. Kulkarni and R. B. Pipes, "Free Vibration Frequencies of a Delaminated Beam," Proceedings of 34th Annual Technical Conference, Reinforced Plastics/Composite Institute, The Society of the Plastics Industry, Section 22-E, pp.1-5, 1979.

[75] Wang, J. T. S., Y. Y. Liu and J. A. Gibby, "Vibration of Split Beams," Journal of Sound and Vibration, Vol.84, pp.491-502, 1982.

[76] Mujumdar, P. M. and S. Suryanarayan, "Flexural Vibrations of Beams with Delamination," Journal of Sound and Vibration, Vol.125, pp.441-461, 1988.

[77] Yin, W. L. and K. Jane, "Vibration of a Delaminated Beam-Plate Relative to Buckled State," Proceedings of AIAA/ASME/ASCE/AHS/ASC 29th Structures, Structural Dynamics and Materials Conference, AIAA, Williamsburg, VA, 1988.

[78] Shen, M.-H. H. and J. E. Grady, "Free Vibrations of Delaminated Beams," Proceedings of AIAA/ASME/ASCE/AHS/ASC 32th Structures, Structural Dynamics and Materials Conference, AIAA, Baltimore, MD, pp.3017-3025, 1991.

[79] Chen, H. P. and P. J. Goggin, "Free Vibration of A Compressed Delaminated Plate," Proceedings of AIAA/ASME/ASCE/AHS/ASC 33th Structures, Structural Dynamics and Materials Conference, AIAA, Dallas, TX, pp.1830-1840, 1992.

[80] Minich, M. D. and C. C. Chamis, "Analytical Displacements and Vibrations of Cantilevered Unsymmetric Fiber Composite Laminates," NASA TMX-F1699, 1975.

[81] Jensen, D. W. and E. F. Crawley, "Frequency Determination Techniques for Cantileverd Plates with Bending-Torsion Coupling," AIAA Journal, Vol.22, pp.415-420, 1984.

[82] Weissharr, T. A., "Vibration Tailoring of Advanced Composite Lifting Surfaces," Journal of Aircraft, Vol.22, pp.141-147, 1985.

[83] Tracy, J. J. and G. C. Pardoen, "Effect of Delamination on the Natural Frequencies of Composite Laminates," Journal of Composite Materials, Vol. 23, pp.1201-1215, 1989.

[84] Shiau, Le-Chung, "Flutter of Composite Laminated Beam Plates with Delamination," AIAA Journal, Vol.30, pp.2504-2511, 1992.

[85] Dym, C. L. and I. H. Shames, *Solid Mechanics: A Variational Approach*, McGraw-Hill, New York, 1973.

[86] Snowdon, J. C., *Vibration and Shock in Damped Mechanical Sysytem*, John Wiely and Sons, Inc., New York, NY, 1968.

[87] Nicolau, A.,"A Development Environment for Scientific Parallel Programs," Applied Mathematics and Computations, Vol.20, pp.175-183, 1986.

[88] Leighton, F. T., *Introduction to Parallel Algorithms and Architectures: Arrays, Trees, Hypercubes*, Morgan Kaufmann Publishers, Inc., San Mateo, CA, 1992.

[89] Gannon, D., D. Atapatta, M. H. Lee and B. Shei, "A software tool for Building Supercomputer Applications," ASME AMD-96, New York, 1991.

[90] Rodrigue, G., "Some Ideas for Decomposing the Domain of Elliptic Partial Differential Equations in the Schwarz Process", Communications in Applied Numerical Methods, Vol.2, pp.245-249, 1986.

BIOGRAPHICAL SKETCH

Jiamin Bai was born on April 23, 1961, in Shanghai, People's Republic of China. He received his B. S. degree in mechanical engineering from the Shanghai Jiaotong University in China in July 1983. In March 1986, he received a Master of Science in Engineering from the same University. Then he joined the faculty in the Department of Engineering Mechanics of Shanghai Jiaotong University, where he was hired as a lecturer. In August 1990, he was admitted to the graduate program at the University of Florida. He received his Ph.D. from the University of Florida in December 1994.

I certify that I have read this study and that in my opinion it conforms to acceptable standards of scholarly presentation and is fully adequate, in scope and quality, as a dissertation for the degree of the Doctor of Philosophy.

C. T. Sun

Chang-Tsan Sun, Chairman
Professor of Aerospace Engineering,
Mechanics and Engineering Science

I certify that I have read this study and that in my opinion it conforms to acceptable standards of scholarly presentation and is fully adequate, in scope and quality, as a dissertation for the degree of the Doctor of Philosophy.

B Sankar

Bhavani V. Sankar
Associate Professor of Aerospace
Engineering, Mechanics and Engineering
Science

I certify that I have read this study and that in my opinion it conforms to acceptable standards of scholarly presentation and is fully adequate, in scope and quality, as a dissertation for the degree of the Doctor of Philosophy.

Deborah Weissman-Berman

Deborah Weissman-Berman
Associate Scientist of Aerospace
Engineering, Mechanics and Engineering
Science

I certify that I have read this study and that in my opinion it conforms to acceptable standards of scholarly presentation and is fully adequate, in scope and quality, as a dissertation for the degree of the Doctor of Philosophy.

Ibrahim K. Ebcioglu

Ibrahim K. Ebcioglu
Professor of Aerospace Engineering,
Mechanics and Engineering Science

I certify that I have read this study and that in my opinion it conforms to acceptable standards of scholarly presentation and is fully adequate, in scope and quality, as a dissertation for the degree of the Doctor of Philosophy.

Sharma Chakravarthy
Associate Professor of Computer and
Information Science

The dissertation was submitted to the Graduate Faculty of the College of Engineering and to the Graduate School and was accepted as partial fulfillment of the requirements for the degree of Doctor of Philosophy.

December 1994

Winfred M. Phillips
Dean, College of Engineering

Karen A. Holbrook
Dean, Graduate School